Bayesian Markov Switching Tensor Regression for Time-varying Networks*

Monica Billio[†1], Roberto Casarin[‡1], Matteo Iacopini[§1,2]

[1]Ca' Foscari University of Venice
[2]Université Paris 1 - Panthéon-Sorbonne

30th January 2018

Abstract

We propose a new Bayesian Markov switching regression model for multi-dimensional arrays (tensors) of binary time series. We assume a zero-inflated logit dynamics with time-varying parameters and apply it to multi-layer temporal networks. The original contribution is threefold. First, in order to avoid over-fitting we propose a parsimonious parametrization of the model, based on a low-rank decomposition of the tensor of regression coefficients. Second, the parameters of the tensor model are driven by a hidden Markov chain, thus allowing for structural changes. The regimes are identified through prior constraints on the mixing probability of the zero-inflated model. Finally, we model the jointly dynamics of the network and of a set of variables of interest. We follow a Bayesian approach to inference, exploiting the Pólya-Gamma data augmentation scheme for logit models in order to provide an efficient Gibbs sampler for posterior approximation. We show the effectiveness of the sampler on simulated datasets of medium-big sizes, finally we apply the methodology to a real dataset of financial networks.

*We thank the conference, workshop and seminar participants at: "11th CFENetwork" in London, 2017, "8th ESOBE" in Maastricht, 2017, "1st Italian-French Statistics Seminar" in Venice, 2017, "41st AMASES" in Cagliari, 2017 and "1st EcoSta" in Hong Kong, 2017. Iacopini's research is supported by the "Bando Vinci 2016" grant by the Université Franco-Italienne. This research used the SCSCF multiprocessor cluster system at Ca' Foscari University of Venice.

[†]E-mail: billio@unive.it
[‡]E-mail: r.casarin@unive.it
[§]E-mail: matteo.iacopini@unive.it

1 Introduction

The analysis of large sets of binary data is a central issue in many applied fields such as biostatistics (e.g. Schildcrout and Heagerty (2005), Wilbur et al. (2002)), image processing (e.g. Yue et al. (2012)), machine learning (e.g. Banerjee et al. (2008), Koh et al. (2007)), medicine (e.g. Christakis and Fowler (2008)), text analysis (e.g. Taddy (2013), Turney (2002)) and theoretical and applied statistics (e.g. Ravikumar et al. (2010), Sherman et al. (2006), Visaya et al. (2015)). Without loss of generality, in this paper we focus on binary series representing time-evolving networks.

From the outbreak of the financial crisis of 2007 there has been an increasing interest in financial network analysis. The fundamental questions on the role of agents' connections, the dynamic process of link formation and destruction, the diffusion process within the economic and/or financial system of external and internal shocks have attracted an increasing interest from the scientific community (e.g., Billio et al. (2012) and Diebold and Yılmaz (2014)).

Despite the wide economic and financial literature exploiting networks in theoretical models (e.g. Acemoglu et al. (2012), Di Giovanni et al. (2014), Chaney (2014), Mele (2017), Graham (2017)), the econometric analysis of networks and of their dynamical properties is at its infancy and many research questions are still striving for an answer. This paper contributes at filling this gap addressing some important questions in building statistical models for network data.

The first issue concerns measuring the impact of a given set of covariates on the dynamic process of link formation. We propose a parsimonious model that can be successfully used to this aim, building on a novel research domain on tensor calculus in statistics. This new literature (see, e.g. Kolda and Bader (2009), Cichocki et al. (2015) and Cichocki et al. (2016) for a review) proposes a generalisation of matrix calculus to higher dimensional arrays, called tensors. The main advantage in using tensors is the possibility of dealing with the complexity of novel data structures which are becoming increasingly available, such as networks, multilayer networks, three-way tables, spatial panels with multiple series observed for each unit (e.g., municipalities, regions, countries). The use of tensors prevents the reshaping and manipulation of the data, thus allowing to preserve the intrinsic structure. Another advantage of tensors stems from their numerous decompositions and approximations, which provide a representation of the model in a lower-dimensional space (see (Hackbusch, 2012, ch.7-8)). In this paper we exploit the PARAFAC decomposition for reducing the number of parameters to estimate, thus making inference on network models feasible.

Another issue regards the time stability of the dependence structure between variables. For example, Billio et al. (2012), Billio et al. (2015), Ahelegbey et al. (2016a), Ahelegbey et al. (2016b) and Bianchi et al. (2016) showed empirically that the network structure of the financial system has experienced a rather long period of stability in the early 2000s and a significantly increasing connectivity before the outbreak of the financial crisis. Starting from these stylized facts, we provide a new Markov switching model for structural changes of the network topology. After the seminal paper of Hamilton (1989), the existing Markov switching models at the core of the Bayesian econometrics literature consider VAR models (e.g., Sims and Zha (2006), Sims et al. (2008)), factor models (e.g., Kaufmann (2000), Kim and Nelson (1998)) or dynamic panels (e.g., Kaufmann (2015), Kaufmann (2010)) and have been extended allowing for stochastic volatility (Smith (2002), Chib et al. (2002)), ARCH and GARCH effects (e.g., see Hamilton and Susmel (1994), Haas et al. (2004), Klaassen (2002) and Dueker (1997), among the others) and stochastic correlation (Casarin et al. (2018)). We contribute to this literature by applying Markov switching dynamics to tensor-valued data.

Motivated by the observation that financial networks are generally sparse, with sudden abrupt changes in the level of sparsity across time, we define a framework which allows us to tackle

the issue of time-varying sparsity. To accomplish this task, we compose the proposed Markov switching dynamics with a zero-inflated logit model. In this sense, we contribute to the network literature on modelling edges' probabilities (e.g., Durante and Dunson (2014) and Wang et al. (2017)), by considering a time series of networks with multiple layers and varying sparsity patterns.

Finally, another relevant question concerns the study of the joint evolution of a network and a set of economic variables of interest. To the best of our knowledge, there is no previous work providing a satisfactory econometric framework to solve this problem. Within the literature on joint modelling discrete and continuous variables Dueker (2005) used the latent variable interpretation of the binary regression and built a VAR model for unobserved continuous-valued variables and quantitative observables. Instead, Taddy (2010) assumes the continuous variable follows a dynamic linear model and the discrete outcome follows a Poisson process with intensity driven by the continuous one. Our contribution to this literature consists in a new joint model for binary tensors and real-valued vectors.

The model we propose is presented in Section 2. We go through the details of the Bayesian inferential procedure in Sections 3-4 while in Section 5 we study the performance of the MCMC procedure on synthetic datasets. Finally, we apply the methodology to a real dataset and discuss the results in Section 6 and draw the conclusions in Section 7.

2 A Markov switching model for networks

A relevant object in our modelling framework is a a D-order tensor, that is a D-dimensional array, element of the tensor product of D vector spaces, each one endowed with a coordinate system. See (Hackbusch, 2012, ch.3) for an introduction to algebraic tensor spaces. A tensor can be though of as the multidimensional extension of a matrix (which is a 2-order tensor), where each dimension is called mode. Other objects of interest are the slice of a tensor, that is a matrix obtained by fixing all but two of the indices of the multidimensional array, and the tube, or fiber, that is a vector resulting from keeping fixed all indices but one. Matrix operations and results from linear algebra can be generalized to tensors (see Hackbusch (2012) or Kroonenberg (2008)). Here we define only the mode-n product between a tensor and a vector and refer the reader to Appendix A for further details. For a D-order tensor $\mathcal{X} \in \mathbb{R}^{d_1 \times \ldots \times d_D}$ and a vector $\mathbf{v} \in \mathbb{R}^{d_n}$, the mode-$n$ product between them is a $(D-1)$-order tensor $\mathcal{Y} \in \mathbb{R}^{d_1 \times \ldots \times d_{n-1} \times d_{n+1} \times \ldots \times d_D}$ whose entries are defined by:

$$\mathcal{Y}_{(i_1,\ldots,i_{n-1},i_{n+1},\ldots,i_D)} = (\mathcal{X} \times_n \mathbf{v})_{(i_1,\ldots,i_{n-1},i_{n+1},\ldots,i_D)} = \sum_{i_n=1}^{d_n} \mathcal{X}_{i_1,\ldots,i_n,\ldots,i_D} \mathbf{v}_{i_n} \,. \tag{1}$$

Let $\{\mathcal{X}_t\}_{t=1}^T$ and $\{\mathcal{X}_t^*\}_{t=1}^T$ be two sequences of binary and real 3-order tensors of size $I \times J \times K$, respectively. In our multilayer network application, $\mathcal{X}_t$ is an adjacency tensor and each of its frontal slices, $\mathbf{X}_{k,t}$, represents the adjacency matrix of k-th layer. See Boccaletti et al. (2014) and Kivelä et al. (2014) for an introduction to multilayer networks. Let $\{\mathbf{y}_t\}_{t=1}^T$ be a sequence of real-valued vectors $\mathbf{y}_t = (y_{t,1}, \ldots, y_{t,M})'$ representing a set of relevant economic or financial indicators. Our model consists of two systems of equations whose parameters switch over time according to a hidden Markov chain process.

The first set of equations pertains the model for the temporal network. One of the most recurrent features of observed networks is edge sparsity, which in random graph theory is defined to be the case in which the number of edges of a graph grows about linearly with the number of nodes (see (Diestel, 2012, ch.7)). For a finite graph size, we consider a network to be sparse when the fraction of edges over the square of nodes, or total degree density, is below 10%. Moreover,

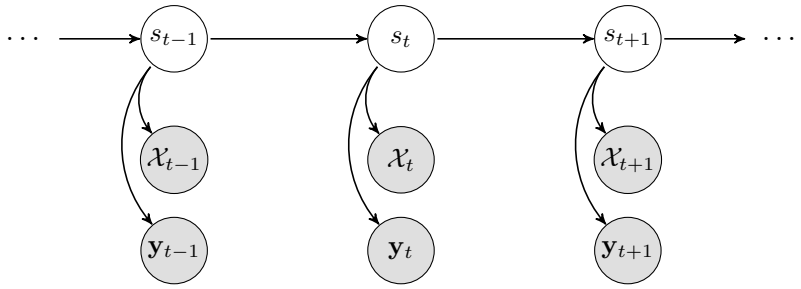

Figure 1: Directed acyclic graph (DAG) of the model in eq. (8a)-(8c). Gray circles represent observable variables and white circles latent variables. Directed arrows indicate the direction of causality.

the sparsity pattern of many real networks is not time homogeneous. To describe its dynamics we assume that the probability of observing an edge in each layer of the network is a mixture of a Dirac mass at 0 and a Bernoulli distribution, where both the mixing probability and the probability of success are time-varying. Consequently, each entry $x_{ijk,t}$ of the tensor $\mathcal{X}_t$ (that is, each edge of the corresponding network) is distributed as a zero-inflated logit:

$$x_{ijk,t}|\rho(t), \mathbf{g}_{ijk}(t) \sim \rho(t)\delta_{\{0\}}(x_{ijk,t}) + (1-\rho(t))\mathcal{B}ern\left(x_{ijk,t}\middle|\frac{\exp\{\mathbf{z}'_{ijk,t}\mathbf{g}_{ijk}(t)\}}{1+\exp\{\mathbf{z}'_{ijk,t}\mathbf{g}_{ijk}(t)\}}\right). \tag{2}$$

Notice that this model admits an alternative representation as:

$$x_{ijk,t}|\rho(t), \mathbf{g}_{ijk}(t) \sim \rho(t)\delta_{\{0\}}(x_{ijk,t}) + (1-\rho(t))\delta_{\{d_{ijk,t}\}}(x_{ijk,t}) \tag{3}$$

$$d_{ijk,t} = \mathbb{1}_{\mathbb{R}_+}(x^*_{ijk,t}) \tag{4}$$

$$x^*_{ijk,t} = \mathbf{z}'_{ijk,t}\mathbf{g}_{ijk}(t) + \varepsilon_{ijk,t} \qquad \varepsilon_{ijk,t} \overset{iid}{\sim} \text{Logistic}(0,1)\,. \tag{5}$$

where $\mathbf{z}_{ijk,t} \in \mathbb{R}^Q$ is a vector of edge-specific covariates and $\mathbf{g}_{ijk}(t) \in \mathbb{R}^Q$ is a time-varying edge-specific vector of parameters. This specification allows to classify the zeros (i.e. absence of edge) into "structural" and "random", conditionally on arising from the atomic mass, or due to the randomness described in eqs. (4)-(5), respectively. The parameter $\rho(t)$ is thus the time-varying probability of observing a structural zero. In the following, without loss of generality, we focus on the case of common set of covariates, that is $\mathbf{z}_{ijk,t} = \mathbf{z}_t$, for $t = 1, \dots, T$.

The second set of equations regards the vector of economic variables and is given by:

$$y_{m,t} = \mu_{m,t} + \varpi_{m,t} \qquad \varpi_{m,t} \sim \mathcal{N}(0, \sigma^2_{m,t})\,, \tag{6}$$

for $m = 1, \dots, M$ and $t = 1, \dots, T$. In vector form, we denote the mean vector and the covariance matrix by $\boldsymbol{\mu}(t)$ and $\boldsymbol{\Sigma}(t)$, respectively.

The specification of the model is completed with the assumption that the time variation of the parameters $\boldsymbol{\mu}(t)$, $\boldsymbol{\Sigma}(t)$, $\rho(t)$, $\mathbf{g}_{ijk}(t)$ are driven by a hidden homogeneous Markov chain $\{s_t\}_{t=1}^T$ with discrete, finite state space $\{1, \dots, L\}$, that is $\boldsymbol{\mu}(t) = \boldsymbol{\mu}_{s_t}$, $\boldsymbol{\Sigma}(t) = \boldsymbol{\Sigma}_{s_t}$, $\rho(t) = \rho_{s_t}$ and $\mathbf{g}_{ijk}(t) = \mathbf{g}_{ijk,s_t}$. The transition matrix of the chain $\{s_t\}_t$ is assumed to be time-invariant and denoted by $\boldsymbol{\Xi} = (\boldsymbol{\xi}_1, \dots, \boldsymbol{\xi}_L)'$, where each $\boldsymbol{\xi}_l = (\xi_{l,1}, \dots, \xi_{l,L})'$ is a probability vector and the transition probability from state i to state j is $\mathbb{P}(\{s_t = j\}|\{s_{t-1} = i\}) = \xi_{i,j}$, $i, j = 1, \dots, L$.

The causal structure of the model is given in Fig. 1, whereas the description of the systems follows.

In order to give a compact representation of the general model, define $\mathbb{X}^d = \{\mathcal{X} \in \mathbb{R}^{i_1 \times \dots \times i_d}\}$ the set of real-valued d-order tensors of size $(i_1 \times \dots \times i_d)$ and $\mathbb{X}^d_{0,1} = \{\mathcal{X}^{\in}\mathbb{R}^{i_1 \times \dots \times i_d} : \mathcal{X}_{i_1,\dots,i_d} \in$

$\{0,1\}\} \subset \mathbb{X}^d$ the set of adjacency tensors of size $(i_1 \times \ldots \times i_d)$. Define a linear operator between these two sets by $\Psi : \mathbb{X}^d \to \mathbb{X}_{0,1}^d$ such that $\mathcal{X}^* \mapsto \Psi(\mathcal{X}^*) \in \{0,1\}^{i_1 \times \ldots \times i_d}$. Denote the indicator function for the set A by $\mathbb{1}_A(x)$, which takes value 1 if $x \in A$ and 0 otherwise, and let $\mathbb{R}_+$ be the positive real half-line. For a matrix $\mathbf{X}_{k,t}^* \in \mathcal{X}^{I,J}$ it is possible to write the first equation of the model in matrix form by $\Psi(\mathbf{X}_{k,t}^*) = (\mathbb{1}_{\mathbb{R}_+}(x_{ijk,t}^*))_{i,j}$, for each slice k of $\mathcal{X}_t^*$. Eq. (5) postulates that each edge x_{ijk} admits an individual set of coefficients $\mathbf{g}_{ijk}(t)$. By collecting all these vectors along the indices i, j, k, we can rewrite eq. (5) in compact form by means of a fourth-order tensor $\mathcal{G}(t) \in \mathbb{R}^{I \times J \times K \times Q}$, thus obtaining:

$$\mathcal{X}_t^* = \mathcal{G}(t) \times_4 \mathbf{z}_t + \mathcal{E}_t \,, \tag{7}$$

where $\mathcal{E}_t \in \mathbb{R}^{I \times J \times K}$ is a third-order tensor with entries $\varepsilon_{ijk,t} \sim \text{Logistic}(0,1)$ and $\times_n$ stands for the mode-n product between a tensor and a vector previously introduced.

The statistical framework we propose for a time series $\{\mathcal{X}_t, \mathbf{y}_t\}_{t=1}^T$ is given by the following system of equations:

$$\begin{cases} \mathcal{X}_t = \mathcal{B}(t) \odot \Psi(\mathcal{X}_t^*) & b_{ijk}(t) \overset{iid}{\sim} \mathcal{B}ern(1-\rho(t)) \quad (8a) \\ \mathcal{X}_t^* = \mathcal{G}(t) \times_4 \mathbf{z}_t + \mathcal{E}_t & \quad (8b) \\ \mathbf{y}_t = \boldsymbol{\mu}(t) + \boldsymbol{\varpi}_t & \boldsymbol{\varpi}_t \overset{iid}{\sim} \mathcal{N}_M(\mathbf{0}, \boldsymbol{\Sigma}(t)) \quad (8c) \end{cases}$$

where $\mathcal{B}(t)$ is a tensor of the same size of $\mathcal{X}_t$ whose entries are independent and identically distributed (iid) Bernoulli random variables with probability of success $1 - \rho(t)$ and $\odot$ stands for the element-by-element Hadamard product (see (Magnus and Neudecker, 1999, ch.3)).

This model can be represented as a SUR (see Zellner (1962)) and also admits an interpretation as a factor model. To this aim, let $\otimes$ denote the Kronecker product (see (Magnus and Neudecker, 1999, ch.3)) and define $\mathbf{z}_t = (1, \tilde{\mathbf{z}}_t)'$, where $\tilde{\mathbf{z}}_t$ denotes the covariates and $\boldsymbol{\Sigma}^{1/2}$ is a matrix satisfying $\boldsymbol{\Sigma}^{1/2}\boldsymbol{\Sigma}^{1/2} = \boldsymbol{\Sigma}$. In addition, let $\{\tilde{\mathbf{u}}_t\}_t$ be a martingale difference process and $\overline{\boldsymbol{\xi}}_t = (\mathbb{1}_{\{1\}}(s_t), \ldots, \mathbb{1}_{\{L\}}(s_t))'$. Then we obtain:

$$\begin{cases} \mathcal{X}_t = \mathcal{B}(t) \odot \Psi(\mathcal{X}_t^*) & b_{ijk}(t) \overset{iid}{\sim} \mathcal{B}ern(1-\rho(t)) \\ \mathcal{X}_t^* = \mathcal{G} \times_4 (\overline{\boldsymbol{\xi}}_t \otimes \mathbf{z}_t)' + \mathcal{E}_t = \mathcal{G} \times_4 (\overline{\boldsymbol{\xi}}_t, \overline{\boldsymbol{\xi}}_t \otimes \tilde{\mathbf{z}}_t)' + \mathcal{E}_t & \varepsilon_{ijk,t} \overset{iid}{\sim} \text{Logistic}(0,1) \\ \mathbf{y}_t = (\overline{\boldsymbol{\xi}}_t \otimes \boldsymbol{\mu}) + (\overline{\boldsymbol{\xi}}_t \otimes \boldsymbol{\Sigma}^{1/2})\boldsymbol{\varpi}_t^* & \boldsymbol{\varpi}_t^* \overset{iid}{\sim} \mathcal{N}_M(\mathbf{0}_M, \mathbf{I}_M) \\ \overline{\boldsymbol{\xi}}_{t+1} = \boldsymbol{\Xi}\overline{\boldsymbol{\xi}}_t + \tilde{\mathbf{u}}_t & \mathbb{E}[\tilde{\mathbf{u}}_t | \tilde{\mathbf{u}}_{t-1}] = 0 \end{cases} \tag{9}$$

3 Bayesian Inference

To derive the likelihood function of the model in eqs. (8a) to (8c) and develop an efficient inferential process, it is useful to start from eq. (2), which describes the statistical model for the likelihood of each edge as a a zero-inflated logit model. Starting from the seminal work of Lambert (1992), who proposed a modelling framework for count data with a great proportion of zeros, zero-inflated models have been applied to settings where the response variable is not integer-valued. Binary responses have been considered by Harris and Zhao (2007), who dealt with an ordered probit model. This is the closest approach to ours, though the specification in eq. (2) substantially differs in two aspects. First, we use of a logistic link function, which is known to have slightly fatter tails than the cumulative normal distribution used in probit models. Second, differently from the majority of the literature which assumes a constant mixing probability, the parameter $\rho(t)$ is evolving according to a latent process.

From eq. (2) we derive the probability of observing or not an edge, respectively, as:

$$\mathbb{P}(x_{ijk,t}=1|\rho(t),\mathbf{g}_{ijk}(t)) = (1-\rho(t))\frac{\exp\{\mathbf{z}_t'\mathbf{g}_{ijk}(t)\}}{1+\exp\{\mathbf{z}_t'\mathbf{g}_{ijk}(t)\}} \tag{10a}$$

$$\mathbb{P}(x_{ijk,t}=0|\rho(t),\mathbf{g}_{ijk}(t)) = \rho(t)+(1-\rho(t))\left(1-\frac{\exp\{\mathbf{z}_t'\mathbf{g}_{ijk}(t)\}}{1+\exp\{\mathbf{z}_t'\mathbf{g}_{ijk}(t)\}}\right). \tag{10b}$$

This allows us to exploit different types of tensor representations (see Kolda and Bader (2009) for a review), in particular for the sake of parsimony, we assume a PARAFAC decomposition with rank R (assumed fixed and known) for the tensor $\mathcal{G}(t)$:

$$\mathcal{G}(t) = \sum_{r=1}^{R} \boldsymbol{\gamma}_1^{(r)}(t)\circ\boldsymbol{\gamma}_2^{(r)}(t)\circ\boldsymbol{\gamma}_3^{(r)}(t)\circ\boldsymbol{\gamma}_4^{(r)}(t)\,, \tag{11}$$

where for each value of the state s_t the vectors $\boldsymbol{\gamma}_h^{(r)}(t)=\boldsymbol{\gamma}_{h,s_t}^{(r)}$, $h\in\{1,2,3,4\}$, $r=1,\dots,R$, are the marginals of the PARAFAC decomposition and have length I, J, K and Q, respectively. By the same argument, we denote $\mathcal{G}(t)=\mathcal{G}_{s_t}$ and $\mathbf{g}_{ijk}(t)=\mathbf{g}_{ijk,s_t}$. This specification permits us to achieve two distinct but fundamental goals: (i) parsimony of the model, since for each value of the state s_t the dimension of the parametric space is reduced from $IJKQ$ to $R(I+J+K+Q)$ parameters; (ii) sparsity of the tensor coefficient, through a suitable choice of the prior distribution for the marginals.

We are given a sample $\{\mathcal{X}_t,\mathbf{y}_t\}_{t=1}^T$ and adopt the notation: $\boldsymbol{\mathcal{X}}=\{\mathbf{X}_t\}_{t=1}^T$, $\mathbf{y}=\{\mathbf{y}_t\}_{t=1}^T$, $\mathbf{s}=\{\mathbf{s}_t\}_{t=0}^T$, $\mathcal{D}=\{\mathcal{D}_t\}_{t=1}^T$ and $\boldsymbol{\Omega}=\{\boldsymbol{\Omega}_t\}_{t=1}^T$. Define $\mathcal{T}_l=\{t:s_t=l\}$ and $T_l=\#\mathcal{T}_l$, for each regime $l=1,2$. Then, in order to write down the analytic form of the complete data likelihood, we introduce the latent variables $\{s_t\}_{t=1}^T$, taking values $s_t=l$, $l\in\{1,2\}$ and evolving according to a discrete Markov chain with transition matrix $\boldsymbol{\Xi}\in\mathbb{R}^{L\times L}$. Finally, denote the whole set of parameters by $\boldsymbol{\theta}$.

The inference is carried out following the Bayesian paradigm and exploiting a data augmentation strategy (Tanner and Wong (1987)). The Pólya-Gamma scheme for models with binomial likelihood proposed by Polson et al. (2013) has been proven to outperform existing schemes for Bayesian inference in logistic regression models in terms of computational speed and higher effective sample size. Furthermore, given a normal prior of the vector of parameters, a Pólya-Gamma prior on latent variables leads to a conjugate posteriors: the full conditional for the parameter vector is normal while that of the latent variable follows a Pólya-Gamma. This allows to use a Gibbs sampler instead of a Metropolis-Hastings algorithm, thus avoiding the need to choose and adequately tune the proposal distribution. Among recent uses of this data augmentation scheme, Wang et al. (2017) used it in a similar framework for network-response regression model, while Holsclaw et al. (2017) exploited it in a time-inhomogeneous hidden Markov model.

The complete data likelihood for $\boldsymbol{\mathcal{X}}$ is given by:

$$\begin{aligned}
&L(\boldsymbol{\mathcal{X}},\mathbf{y},\mathcal{D},\boldsymbol{\Omega},\mathbf{s}|\boldsymbol{\theta}) = \\
&= \prod_{l=1}^{L}\prod_{t\in\mathcal{T}_l}\prod_{i=1}^{I}\prod_{j=1}^{J}\prod_{k=1}^{K}\rho_l^{d_{ijk,t}}\cdot\delta_{\{0\}}(x_{ijk,t})^{d_{ijk,t}}\cdot\left(\frac{1-\rho_l}{2}\right)^{1-d_{ijk,t}}\cdot\exp\left\{-\frac{\omega_{ijk,t}}{2}(\mathbf{z}_t'\mathbf{g}_{ijk,l})^2+\kappa_{ijk,t}(\mathbf{z}_t'\mathbf{g}_{ijk,l})\right\} \\
&\cdot\prod_{l=1}^{L}\prod_{t\in\mathcal{T}_l}(2\pi)^{-m/2}\left|\boldsymbol{\Sigma}_l\right|^{-1/2}\exp\left\{-\frac{1}{2}(\mathbf{y}_t-\boldsymbol{\mu}_l)'\boldsymbol{\Sigma}_l^{-1}(\mathbf{y}_t-\boldsymbol{\mu}_l)\right\} \\
&\cdot\left[\prod_{t=1}^{T}\prod_{i=1}^{I}\prod_{j=1}^{J}\prod_{k=1}^{K}p(\omega_{ijk,t})\right]\cdot\left[\prod_{g=1}^{L}\prod_{l=1}^{L}\xi_{g,l}^{N_{gl}(\mathbf{s})}\right]\cdot p(s_0|\boldsymbol{\Xi})\,,
\end{aligned} \tag{12}$$

where $d_{ij,t}$ is a latent allocation variable and $\omega_{ij,t}$ is a Pólya-Gamma latent variable. See Appendix C for the details of the data augmentation strategy and the derivation of the complete data likelihood.

A well known identification issue for mixture models is the label switching problem (see, for example, Celeux (1998)), which stems from the fact that the likelihood function is invariant to relabelling of the mixture components. This may represent a problem for Bayesian inference, especially when the unobserved components are not well separated, since the associated labels may wrongly change across iterations. Several proposals have been made for solving this identification issue (see Frühwirth-Schnatter (2006) for a review). The permutation sampler proposed by Frühwirth-Schnatter (2001) can be applied under the assumption of exchangeability of the posterior distribution, which is satisfied when the prior distribution for the transition probabilities of the hidden Markov chain is symmetric. Alternatively, there are situations when the particular application provides meaningful restrictions on the value of some parameters. These restrictions generally stem from theoretical results, or interpretation of the different regimes, which is the reason why they are widely used in macroeconomics and finance.

Following this second approach, we can use as identification constraint for the regimes the mixing probability of the zero-inflated logit in eq. (3). This can be interpreted as the likelihood of a "structural" absent edge, therefore by sorting the regimes in decreasing order, from "sparse" to "dense", we impose: $\rho_1 > \rho_2 > \ldots > \rho_L$.

As regards the prior distributions for the parameters of interest, we choose the following specifications. Denote $\boldsymbol{\iota}_n$ the n-dimensional vector of ones. We assume an independent prior on $\boldsymbol{\gamma}_{h,l}^{(r)}$ for each regime $l = 1, \ldots, L$, thus representing the *a priori* ignorance of the different value of these parameters for varying l. In particular, for each $r = 1, \ldots, R$, each $h = 1, \ldots, 4$ and each $l = 1, \ldots, L$ we specify the global-local shrinkage prior:

$$\pi(\boldsymbol{\gamma}_{h,l}^{(r)} | \overline{\boldsymbol{\zeta}}_{h,l}^{r}, \tau, \phi_r, w_{h,r,l}) \sim \mathcal{N}_{n_h}(\overline{\boldsymbol{\zeta}}_{h,l}^{r},\ \tau\phi_r w_{h,r,l} \mathbf{I}_{n_h}) \tag{13}$$

where $\mathbf{n} = (I, J, Q)'$ is a vector containing the length of each vector $\boldsymbol{\gamma}_{h,l}^{(r)}$ and the prior mean is set to $\overline{\boldsymbol{\zeta}}_{h,l}^{r} = 0$ for each $h = 1, \ldots, 4$, $l = 1, \ldots, L$, $r = 1, \ldots, R$. The parameter τ represents the global component of the variance, common to all marginals, ϕ_r is level component (specific for each $r = 1, \ldots, R$) and $w_{h,r}$ is the local component. The choice of a global-local shrinkage prior, as opposed to a spike-and-slab distribution, is motivated by the reduced computational complexity and the capacity to handle high-dimesnional settings.

In addition, for allowing greater flexibility, we assume the following hyper-priors for the variance components[1]:

$$\pi(\tau) \sim \mathcal{G}a(\overline{a}^{\tau}, \overline{b}^{\tau}) \tag{14}$$

$$\pi(\boldsymbol{\phi}) \sim \mathcal{D}ir(\overline{\boldsymbol{\alpha}}) \qquad \overline{\boldsymbol{\alpha}} = \overline{\alpha}\boldsymbol{\iota}_R \tag{15}$$

$$\pi(w_{h,r,l} | \lambda_l) \sim \mathcal{E}xp(\lambda_l^2/2) \qquad \forall\, h, r, l \tag{16}$$

$$\pi(\lambda_l) \sim \mathcal{G}a(\overline{a}_l^{\lambda}, \overline{b}_l^{\lambda}) \qquad \forall\, l\,. \tag{17}$$

The further level of hierarchy for the local components $w_{h,r,l}$ is added with the aim of favouring information sharing across local components of the variance (indices h, r) within a

[1] We use the shape-rate formulation for the gamma distribution, that is for $\alpha > 0, \beta > 0$:

$$x \sim \mathcal{G}a(\alpha, \beta) \iff f(x) = \frac{\beta^{\alpha}}{\Gamma(\alpha)} x^{\alpha-1} e^{-\beta x} \quad x \in (0, +\infty)\,.$$

given regime l. This hierarchical prior induces the following marginal prior on the vector $\mathbf{w}_l = (w_{1,1,l}, \ldots, w_{4,R,l})'$:

$$\begin{aligned}\pi(\mathbf{w}_l) &= \int_{\mathbb{R}_+} \prod_{r=1}^{R} \prod_{h=1}^{4} \pi(w_{h,r,l}|\lambda_l)\pi(\lambda_l)\,\mathrm{d}\lambda_l \\ &= \int_{\mathbb{R}_+} \frac{(\overline{b}_l^{\lambda})^{\overline{a}_l^{\lambda}}}{2\Gamma(\overline{a}_l^{\lambda})} \lambda_l^{\overline{a}_l^{\lambda}+8R-1} \exp\left\{-\overline{b}_l^{\lambda}\lambda_l - \left(\sum_{r=1}^{R}\sum_{h=1}^{4} w_{h,r,l}\right)\frac{\lambda_l^2}{2}\right\}\mathrm{d}\lambda_l\,. \end{aligned} \tag{18}$$

The marginal prior for a generic entry $w_{h,r,l}$ is a compound gamma distribution[2], that is $p(w_{h,r,l}) \sim \mathrm{CoGa}(1, \overline{a}_l^{\lambda}, 1, \overline{b}_l^{\lambda})$, with $\overline{a}_l^{\lambda} > -1$. In the univariate case (i.e $H = 1$, $R = 1$ and $L = 1$), we obtain a generalized Pareto distribution[3] $\pi(w) = gP(0, a_\lambda, b_\lambda/a_\lambda)$.

The specification of an exponential distribution for the local component of the variance of the $\boldsymbol{\gamma}_{h,l}^{(r)}$ yields a Laplace distribution for each component of the vectors once the $w_{h,r,l}$ is integrated out, that is $\boldsymbol{\gamma}_{h,l,i}^{(r)}|\lambda_l, \tau, \phi_r \sim \mathrm{Laplace}(\mathbf{0}, \lambda_l/\sqrt{\tau\phi_r})$ for all $i = 1, \ldots, n_h$. The marginal distribution of each entry, integrating all remaining random components, is instead a generalized Pareto distribution.

In probit and logit models it is not possible to identify the coefficients of the latent regression equation as well as the variance of the noise (e.g., see Wooldridge (2010)). As a consequence, we make the usual identifying restriction by imposing unitary variance for each $\epsilon_{ijk,t}$.

The mixing probability of the observation model is assumed beta distributed:

$$\pi(\rho_l) \sim \mathcal{B}e(\overline{a}_l^{\rho}, \overline{b}_l^{\rho}) \qquad \forall\, l = 1, \ldots, L\,. \tag{22}$$

Concerning the parameters of the second equation (vector $\mathbf{y}_t \in \mathbb{R}^m$), we assume the priors:

$$\pi(\boldsymbol{\mu}_l) \sim \mathcal{N}_M(\overline{\boldsymbol{\mu}}_l, \overline{\boldsymbol{\Upsilon}}_l) \quad \forall\, l = 1, \ldots, L \tag{23}$$

$$\pi(\boldsymbol{\Sigma}_l) \sim \mathcal{IW}_M(\overline{\nu}_l, \overline{\boldsymbol{\Psi}}_l) \quad \forall\, l = 1, \ldots, L\,. \tag{24}$$

Finally, each row of the transition matrix of the Markov chain process $\mathbf{s}_t$ is assumed to be *a priori* distributed according to a Dirichlet distribution:

$$\pi(\boldsymbol{\xi}_{l,:}) \sim \mathcal{D}ir(\overline{\mathbf{c}}_{l,:}) \quad \forall\, l = 1, \ldots, L\,. \tag{25}$$

[2]Alternatively, following (Johnson et al., 1995, p.248), this is called generalized beta prime distribution or generalized beta distribution of the second kind $\mathcal{B}e_2(\alpha, \beta, p, q)$, whose probability density function (with $B(\alpha, \beta)$ being the usual beta function) is given by:

$$p(x|\alpha, \beta, p, q) = \frac{1}{qB(\alpha, \beta)} p \left(\frac{x}{q}\right)^{\alpha p - 1} \left[1 + \left(\frac{x}{q}\right)^{p}\right]^{-(\alpha+\beta)} \qquad x \in \mathbb{R}_+,\ \alpha, \beta, p, q \in \mathbb{R}_+\,. \tag{19}$$

In our case, the probability density function is defined by a mixture of two gamma distributions (see also Dubey (1970)):

$$p(x|\alpha, \beta, 1, q) = \int_0^{\infty} \mathcal{G}a(x|\alpha, p)\mathcal{G}a(p|\beta, q)\,\mathrm{d}p = \frac{q^{\beta} x^{\alpha-1}(q+x)^{\alpha+\beta}}{B(\alpha, \beta)} \qquad x \in \mathbb{R}_+,\ \alpha, \beta, q \in \mathbb{R}_+\,. \tag{20}$$

In our case, the parametrisation is $(1, a_\lambda, 1, b_\lambda)$. This special case is also called a $\mathrm{Lomax}(a, b)$ distribution with parameters (a_λ, b_λ).

[3]The probability density function of the generalized Pareto distribution is:

$$p(x|\mu, \xi, \sigma) = \frac{1}{\sigma}\left(1 + \frac{(x-\mu)}{\xi\sigma}\right)^{-(\xi+1)} \qquad x \in \mathbb{R}_+,\ \mu, \xi \in \mathbb{R},\ \sigma \in \mathbb{R}_+\,. \tag{21}$$

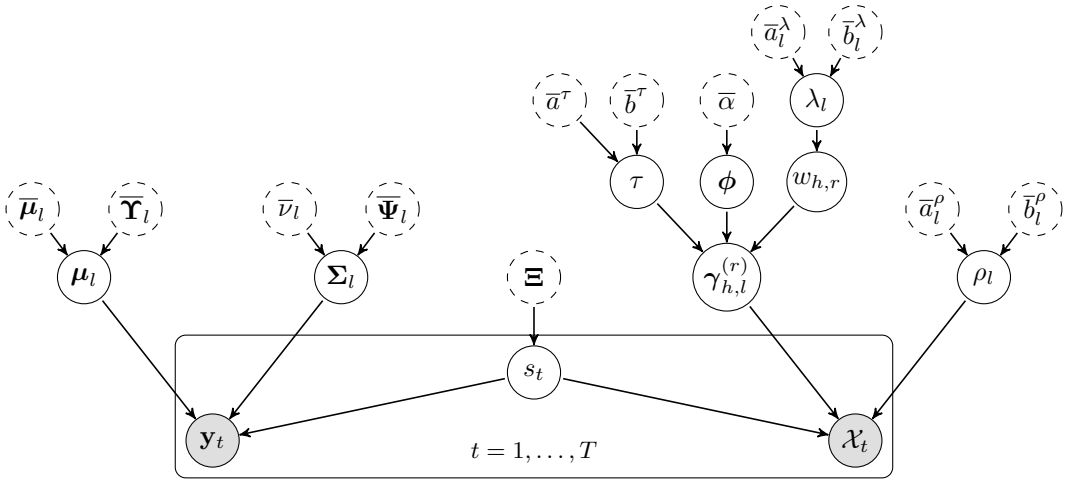

Figure 2: DAG of the model in eq. (8a)-(8c) and prior structure in eq. (13)-(25). Gray circles denote observable variables, white circles with continuous border indicate parameters, white circles with dashed border indicate fixed hyper-parameters.

The overall structure of the hierarchical prior distribution is represented graphically by means of the directed acyclic graph (DAG) in Fig. 2.

4 Posterior Approximation

For explanatory purposes, in this section we focus on single layer graphs (i.e. $k = 1$), which is a special case of the model in eqs. (8a)-(8c). In Appendix D we present the computational details for the general case with multi-layer network observations (i.e. $K > 1$).

For reducing the burden of the notation, we define $\mathcal{G} = \{\mathcal{G}_l\}_{l=1}^L$, $\boldsymbol{\mu} = \{\boldsymbol{\mu}_l\}_{l=1}^L$, $\boldsymbol{\Sigma} = \{\boldsymbol{\Sigma}_l\}_{l=1}^L$ and $\boldsymbol{\rho} = \{\rho_l\}_{l=1}^L$. Moreover, denote by $\mathbf{W} \in \mathbb{R}^{3\times R\times L}$ the matrix whose elements $(w_{h,r_l})_{h,r,l}$ are the components of the marginal-specific variance. Combining the complete data likelihood with the prior distributions yields a posterior sampling scheme consisting of four blocks (see Appendix D for the derivation of the posterior full conditional distributions).

In the first block (I) the sampler draws the latent variables from the full conditional distribution:

$$p(\mathbf{s}, \mathcal{D}, \boldsymbol{\Omega} | \boldsymbol{\mathcal{X}}, \mathbf{y}, \mathcal{G}, \boldsymbol{\mu}, \boldsymbol{\Sigma}, \boldsymbol{\Xi}, \boldsymbol{\rho}) = p(\mathbf{s} | \boldsymbol{\mathcal{X}}, \mathbf{y}, \mathcal{G}, \boldsymbol{\mu}, \boldsymbol{\Sigma}, \boldsymbol{\Xi}, \boldsymbol{\rho}) \tag{26}$$

$$\cdot \prod_{ijt} p(\omega_{ij,t} | x_{ij,t}, s_t, \mathcal{G}_{s_t}) p(d_{ij,t} | x_{ij,t}, s_t, \mathcal{G}_{s_t}, \rho_{s_t}) \,. \tag{27}$$

Samples of $\mathbf{s}$ are obtained via the multi-move Forward-Filtering-Backward-Sampler (see Frühwirth-Schnatter (2006)). The latent variables $\omega_{ij,t}$ are sampled independently for each $i = 1, \ldots, I$, $j = 1, \ldots, J$ and $t = 1, \ldots, T$ from:

$$p(\omega_{ij,t} | x_{ij,t}, s_t, \mathcal{G}_{s_t}) \propto PG(1, \mathbf{z}_t' \mathbf{g}_{ijk,s_t}) \,, \tag{28}$$

The latent variables $\omega_{ij,t}$ are sampled in block for each t. This is done by sampling $\mathbf{u}_t = \text{vec}\,(\boldsymbol{\Omega}_t)$ from the vectorised version of the PG random number generator, then reshaping $\boldsymbol{\Omega}_t = \text{vecr}(\mathbf{u}_t)$. The latent variables $d_{ij,t}$ are sampled independently for each $i = 1, \ldots, I$, $j = 1, \ldots, J$ and $t = 1, \ldots, T$ from:

$$p(d_{ij,t} = 1 | x_{ij,t}, s_t, \mathcal{G}_{s_t}, \rho_{s_t}) \propto \rho_{s_t} \delta_{\{0\}}(x_{ij,t}) \tag{29a}$$

$$p(d_{ij,t}=0|x_{ij,t},s_t,\mathcal{G}_{s_t},\rho_{s_t}) \propto (1-\rho_{s_t})\frac{\exp\{(\mathbf{z}_l'\mathbf{g}_{ijk,s_t})x_{ij,t}\}}{1+\exp\{\mathbf{z}_t'\mathbf{g}_{ijk,s_t}\}}\,. \tag{29b}$$

Block (II) regards the hyper-parameters which control the variance of the PARAFAC marginals, and have full conditional distribution:

$$p(\tau,\boldsymbol{\phi},\mathbf{W}|\{\boldsymbol{\gamma}_{h,l}^{(r)}\}_{h,l,r}) = p(\boldsymbol{\phi}|\{\boldsymbol{\gamma}_{h,l}^{(r)}\}_{h,l,r},\mathbf{W})p(\tau|\{\boldsymbol{\gamma}_{h,l}^{(r)}\}_{h,l,r},\mathbf{W},\boldsymbol{\phi})p(\mathbf{W}|\{\boldsymbol{\gamma}_{h,l}^{(r)}\}_{h,l,r},\boldsymbol{\phi},\tau)\,. \tag{30}$$

The auxiliary variables ψ_r are sampled independently for $r=1,\dots,R$ from:

$$p(\psi_r|\{\boldsymbol{\gamma}_{h,1}^{(r)}\}_{h,l},\mathbf{w}_r) \propto \text{GiG}\left(2\overline{b}^{\tau},\sum_{h=1}^{3}\sum_{l=1}^{L}\frac{\boldsymbol{\gamma}_{h,l}^{(r)'}\boldsymbol{\gamma}_{h,l}^{(r)}}{w_{h,r}},\overline{\alpha}-n\right) \tag{31}$$

then, for each $r=1,\dots,R$ define:

$$\phi_r = \frac{\psi_r}{\sum_{v=1}^{R}\psi_v}\,. \tag{32}$$

The parameters $\boldsymbol{\phi}$ are sampled in a separate block since they all enter the full conditionals of $w_{h,r,l}$ and $\boldsymbol{\gamma}_{h,l}^{(r)}$. The global variance parameter τ is drawn from:

$$p(\tau|\{\boldsymbol{\gamma}_{h,l}^{(r)}\}_{h,l,r},\mathbf{W},\boldsymbol{\phi}) \propto \text{GiG}\left(2\overline{b}^{\tau},\sum_{r=1}^{R}\sum_{h=1}^{3}\sum_{l=1}^{L}\frac{\boldsymbol{\gamma}_{h,l}^{(r)'}\boldsymbol{\gamma}_{h,l}^{(r)}}{\phi_r w_{h,r}},(\overline{\alpha}-n)R\right)\,. \tag{33}$$

The local variance parameters $w_{h,r,l}$ are independently drawn for each $h=1,2,3$, $r=1,\dots,R$ and $l=1,\dots,L$ from:

$$p(w_{h,r,l}|\boldsymbol{\gamma}_{h,l}^{(r)},\phi_r,\tau,\lambda_l) \propto \text{GiG}\left(\lambda_l^2,\frac{\boldsymbol{\gamma}_{h,l}^{(r)'}\boldsymbol{\gamma}_{h,l}^{(r)}}{\tau\phi_r},1-\frac{n_h}{2}\right)\,. \tag{34}$$

Finally, denoting $\mathbf{w}_l$ the collection of all $w_{h,r,l}$ for a given l, the parameters λ_l are independently drawn for each $l=1,\dots,L$ from:

$$p(\lambda_l|\mathbf{w}_l) \propto \lambda_l^{\overline{a}_l^{\lambda}+6R-1}\cdot\exp\left\{-\lambda_l\overline{b}_l^{\lambda}\right\}\cdot\left\{-\frac{\lambda_l^2}{2}\sum_{r=1}^{R}\sum_{h=1}^{3}w_{h,r,l}\right\}\,. \tag{35}$$

The third block (III) concerns the marginals of the PARAFAC decomposition for the tensors $\mathcal{G}_l$ for every $l=1,\dots,L$. The vectors $\boldsymbol{\gamma}_{h,l}^{(r)}$ are sampled independently for all $h=1,2,3$ and every $r=1,\dots,R$ from:

$$p(\boldsymbol{\gamma}_{h,l}^{(r)}|\mathcal{X},\mathbf{W},\boldsymbol{\phi},\tau,\mathbf{s},\mathcal{D},\boldsymbol{\Omega}) \propto \mathcal{N}_{n_h}\left(\tilde{\boldsymbol{\zeta}}_{h,l}^{r},\tilde{\boldsymbol{\Lambda}}_{h,l}^{r}\right)\,. \tag{36}$$

Finally, in block (IV) are drawn the mixing probability, the transition matrix and the main parameters of the second equation. The mixing probability is sampled for every $l=1,\dots,L$ from:

$$p(\rho_l|\mathcal{D},\mathbf{s}) \propto \mathcal{B}e(\tilde{a}_l,\tilde{b}_l)\,. \tag{37}$$

Each row of the transition matrix is independently drawn for every $l=1,\dots,L$ from:

$$p(\boldsymbol{\xi}_{l,:}) \propto \mathcal{D}ir(\tilde{\mathbf{c}})\,. \tag{38}$$

The mean and covariance matrix of the second equation are sampled independently for every $l = 1, \ldots, L$, respectively from:

$$p(\boldsymbol{\mu}_l | \mathbf{y}, \mathbf{s}, \boldsymbol{\Sigma}_l) \propto \mathcal{N}_M(\tilde{\boldsymbol{\mu}}_l, \tilde{\boldsymbol{\Upsilon}}_l) \tag{39}$$

and:

$$p(\boldsymbol{\Sigma}_l | \mathbf{y}, \mathbf{s}, \boldsymbol{\mu}_l) \propto \mathcal{IW}_M(\tilde{\nu}_l, \tilde{\boldsymbol{\Psi}}_l)\,. \tag{40}$$

Blocks (I) and (II) are Rao-Blackwellized Gibbs steps: in block (I) we have marginalised over both $(\mathcal{D}, \boldsymbol{\Omega})$ in the full joint conditional distribution of the state $\mathbf{s}$ and $\mathcal{D}$ (together with $\boldsymbol{\rho}$) in the full conditional of $\boldsymbol{\Omega}$, while in (II) we have integrated out τ from the full conditional of $\boldsymbol{\phi}$ (see sec. D.2). Blocks (III) and (IV) are standard Gibbs steps, concerned with sampling from the full conditional (eventually exploiting conditional independence relations).

5 Simulation Results

We consider three simulation settings for the model in eqs. (8a)-(8c) corresponding to different sizes I and J, with $I = J$, of the adjacency matrix $\mathbf{X}_t$. The other parameters indicated below are kept fixed across settings. The three synthetic datasets used to check the efficiency of the proposed Gibbs sampler share the same hyperparameters' values, but differ in the size of the adjacency matrices. We consider:

(I) $I = J = 100$, with $Q = 3$ common covariates and $M = 2$ exogenous variables;

(II) $I = J = 150$, with $Q = 3$ common covariates and $M = 2$ exogenous variables;

(III) $I = J = 200$, with $Q = 3$ common covariates and $M = 2$ exogenous variables.

We generated a sample of size $T = 60$ and at each time step we simulate a square matrix $\mathbf{X}_t$, a vector $\mathbf{y}_t$ of length $m = 2$ and a set of $Q = 3$ covariates $\mathbf{z}_t$. The covariates have been generated from a stationary Gaussian VAR(1) process with entries of the coefficient matrix i.i.d. from a truncated standard normal distribution. We considered two regimes (i.e. $L = 2$) and generated the trajectory of the Markov chain $\{s_t\}_{t=1}^T$ setting:

$$\boldsymbol{\Xi} = \begin{bmatrix} 0.8 & 0.2 \\ 0.3 & 0.7 \end{bmatrix} \quad p(s_0) = \begin{bmatrix} 0.7 \\ 0.3 \end{bmatrix}. \tag{41}$$

For each regime $l = 1, 2$, we generated the marginals of the PARAFAC decomposition (rank $R = 5$) of the tensor $\mathcal{G}_l$, the mixing probability in the first equation and the mean and covariance in the second equation of the model according to:

$$\begin{aligned}
&\rho_1 = 0.8 && \rho_2 = 0.2 \\
&\boldsymbol{\gamma}_{h,1}^{(r)} \overset{iid}{\sim} \mathcal{N}_{n_h}(\mathbf{0}_{n_h}, \mathbf{I}_{n_h}) \;\; \forall\, h, r && \boldsymbol{\gamma}_{h,2}^{(r)} \overset{iid}{\sim} \mathcal{N}_{n_h}(\boldsymbol{\iota}_{n_h}, \mathbf{I}_{n_h}) \;\; \forall\, h, r \\
&\boldsymbol{\mu}_1 = [2, 2]' && \boldsymbol{\mu}_2 = [-2, -2]' \\
&\boldsymbol{\Sigma}_1 = \begin{bmatrix} 2 & 0.5 \\ 0.5 & 2 \end{bmatrix} && \boldsymbol{\Sigma}_2 = \begin{bmatrix} 4 & 1 \\ 1 & 4 \end{bmatrix}
\end{aligned} \tag{42}$$

We initialised the marginals of the PARAFAC decomposition of the tensor of coefficients $\mathcal{G}_l$ at the output of the Simulated Annealing algorithm (see (Robert and Casella, 2004, pp. 163-173)) and we kept the same value for each $l = 1, \ldots, L$. The other parameters $(\boldsymbol{\rho}, \mathbf{W}, \boldsymbol{\phi}, \tau, \boldsymbol{\Xi}, \boldsymbol{\mu}, \boldsymbol{\Sigma})$

have been initialised by sampling from their prior. Finally, we have chosen the following values for the hyperparameters:

$$\begin{array}{llll} \overline{\alpha} = 0.5 & \overline{b}_\tau = 2 & \overline{\lambda} = 4 & \boldsymbol{\zeta}^r_{h,l} = \mathbf{0}_{n_h} \;\; \forall\, h, l, r \\ \overline{a}_1 = 5 & \overline{b}_1 = 2 & \overline{a}_2 = 2 & \overline{b}_2 = 5 \\ \overline{\boldsymbol{\mu}}_1 = \mathbf{0}_m & \overline{\boldsymbol{\mu}}_2 = \mathbf{0}_m & \overline{\boldsymbol{\Upsilon}}_1 = \mathbf{I}_m & \overline{\boldsymbol{\Upsilon}}_2 = \mathbf{I}_m \\ \overline{\nu}_1 = m & \overline{\nu}_2 = m & \overline{\boldsymbol{\Psi}}_1 = \mathbf{I}_m & \overline{\boldsymbol{\Psi}}_2 = \mathbf{I}_m \\ \overline{\mathbf{c}}_1 = [8, 4] & \overline{\mathbf{c}}_2 = [4, 8] & & \end{array} \tag{43}$$

For each simulation setting, we evaluate the mean square error of the estimated coefficient tensor:

$$MSE = \frac{1}{2}(MSE_1 + MSE_2) = \frac{1}{2IJK}\left(\left\|\mathcal{G}_1^* - \hat{\mathcal{G}}_1\right\|_2^2 + \left\|\mathcal{G}_2^* - \hat{\mathcal{G}}_2\right\|_2^2\right), \tag{44}$$

where $\|\cdot\|_2$ is the Frobenious norm for tensors, i.e.:

$$\left\|\mathcal{G}_\ell^* - \hat{\mathcal{G}}_\ell\right\|_2^2 = \sum_{i=1}^{I}\sum_{j=1}^{J}\sum_{k=1}^{K}(g^*_{ijk,\ell} - \hat{g}_{ijk,\ell})^2\,. \tag{45}$$

All simulations have been performed using MATLAB r2016b with the aid of the Tensor Toolbox v.2.6[4].

Figs. 3(a)-3(c)-3(e) report the trace plots of the error, for each of the three simulations, respectively, while Figs. 3(b)-3(d)-3(f) plot the corresponding autocorrelation functions. All these graphs show that the estimated total error series rapidly stabilises around a small value, meaning that the sampler is able to recover the true value of the tensor parameter. Furthermore, from the analysis of Figs. 3(b)-3(d)-3(f) we can say that the autocorrelation of the posterior draws of the total error vanishes after three lags, thus representing a first indicator of the efficiency of the sampler. We remind to Appendix F for further details and plots about the performance of the sampler in each simulated example.

[4]Available at: `http://www.sandia.gov/~tgkolda/TensorToolbox/index-2.6.html`

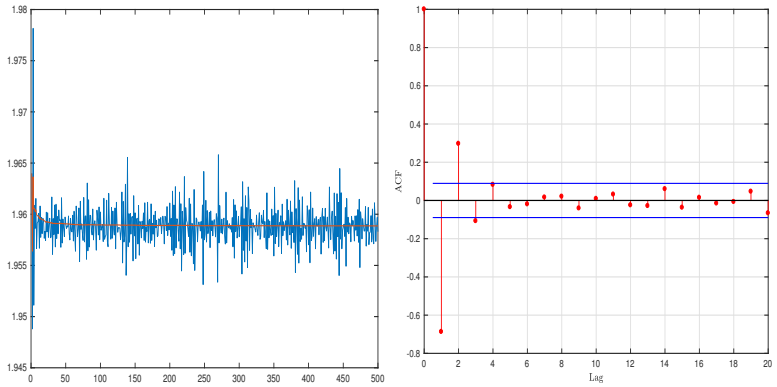

(a) Simulation (I): trace plot. (b) Simulation (I): ACF.

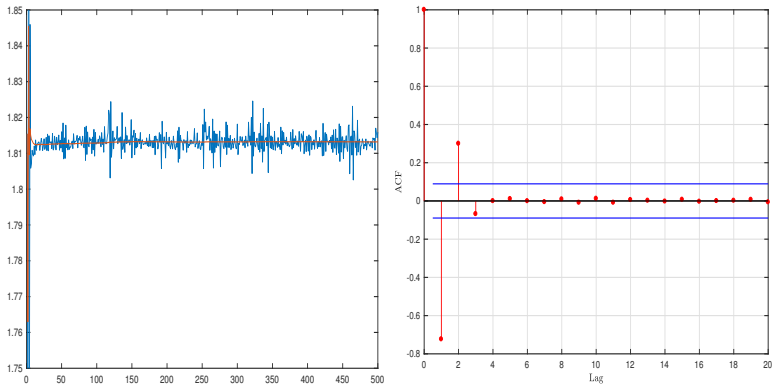

(c) Simulation (II): trace plot. (d) Simulation (II): ACF.

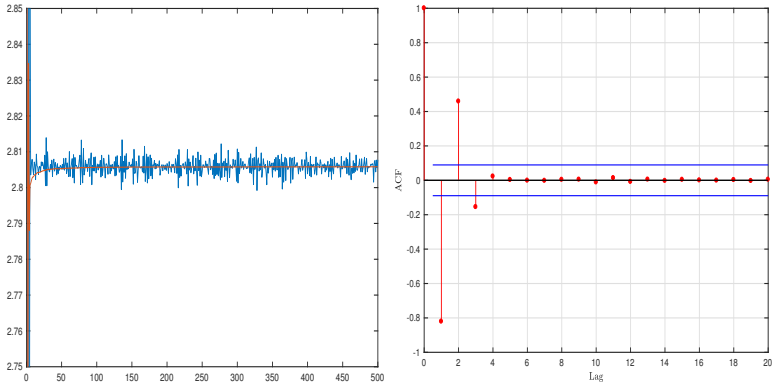

(e) Simulation (III): trace plot. (f) Simulation (III): ACF.

Figure 3: *Left:* Trace plots (blue line) with superimposed progressive mean (orange line) of the total error in estimating the tensor of regression coefficients, for each simulation. *Right:* corresponding autocorrelation function, for each simulation.

Table (1) reports the effective sample size (ESS) in the formulation provided by Gelman et al. (2014):

$$ESS = \frac{N}{1 + 2\sum_{l=1}^{\infty} \hat{\varrho}_l}, \tag{46}$$

where $\hat{\varrho}_l$ is the sample autocorrelation function at lag l and N is the sample size (i.e., the length of the simulation). For computational reasons, the infinite sum is truncated at $L = \min\{l : \hat{\varrho}_l <$

Simulation	ESS	ACF(1)	ACF(5)
I	250	...	...
II	245	...	...
III	248	...	...

Table 1: Convergence diagnostic statistics for the total error, for each simulated case. ESS is rounded to the smallest integer.

$10^{-4}\}$. The ESS is interpreted as an efficiency index: it represents the number of simulated draws that can be interpreted as iid draws from the posterior distribution (in fact, in presence of exact iid sampling schemes we have $ESS = N$). The results in Tab. (1) show that in all three simulation settings the effective sample size is about half of the length of the simulation.

6 Applications

6.1 Data description

We apply the proposed methodology to the well known dataset of financial networks of Billio et al. (2012), Ahelegbey et al. (2016b), Ahelegbey et al. (2016b), Bianchi et al. (2016). The dataset consists of $T = 110$ monthly binary, directed networks estimated via the Granger causality approach, where the nodes are European financial institutions. Other methods for extracting the network structure from data can be used, as this is not relevant for our econometric framework, which applies to any sequence of binary tensors.

The original dataset is composed by the daily closing price series at a daily frequency from 29th December 1995 to 16th January 2013 of all the European financial institutions active and dead in order to cope with survivorship bias. It covers a total of 770 European financial firms which are traded in 10 European financial markets (core and peripheral). The pairwise Granger causalities are estimated on daily returns using a rolling window approach with a length for each window of 252 observations (approximately 1 year). We obtain a total of 4197 adjacency matrices during the period from 8th January 1997 to 16th January 2013.

Then, we define a binary adjacency matrix for each month by setting an entry to 1 only if the corresponding Granger-causality link existed for the whole month (i.e. for each trading day of the corresponding month), and setting the entry to 0 otherwise. Since the panel is unbalanced due to entry and exit of financial institutions from the sample over time, we consider a subsample of length $T = 110$ months (from December 2003 to January 2013) made of 61 financial institutions.

We can visualize a sequence of adjacency matrices representing a time series of networks in several ways. Fig. 4(a) shows a stacked representation of a subsample composed by six adjacency matrices, while Fig. 4(b) plots a 3-dimensional array representation of the same data. In the first case, all matrices are stacked horizontally. Instead, the 3-dimensional representation plots each matrix in front of the other, as frontal slices of an array. It is possible to interpret the two plots as equivalent representations of a third-order tensor: in this case, Fig. 4(a) shows the matricised form (along mode 1) of the tensor, while Fig. 4(b) plots its frontal slices. Finally, Fig. 5 plots the graph associated to two of these adjcency matrices. Though this representation allows for visualising the topology of a network, it is impractical for giving a compact representation of the whole time series of networks. Thus, we provide in Fig. 6 the stacked representation of the whole network sequence. Each row plots twelve time-consecutive adjacency matrices, starting from the top-left corner.

The most striking features emerging from Fig. 6 are the time-varying degree distribution and

the temporal clustering of sparse and dense networks.

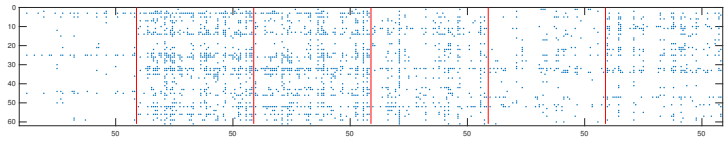

(a) Stacked representation.

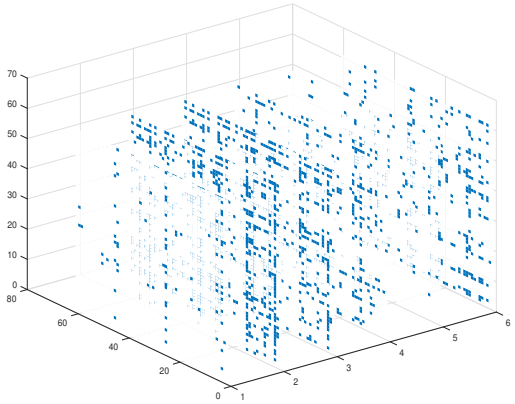

(b) 3D representation.

Figure 4: Stacked (a) and 3-dimensional (b) representations of a subsample of adjacency matrices (months $t = 65, 69, 73, 77, 81, 85$). Blue dots are existing edges, white dots are absent edges. A red line is used to separate each matrix (or tensor slice).

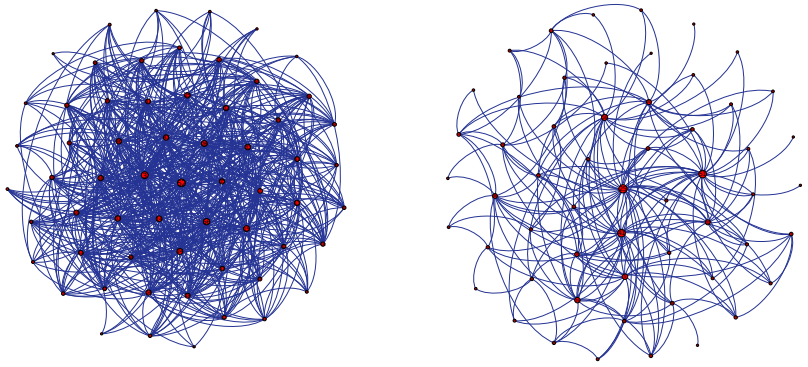

Figure 5: Graphical representation of networks at time $t = 69$ (dense case) and $t = 77$ (sparse case), respectively. The size of the each node is proportional to its total degree. Edges are clockwise directed.

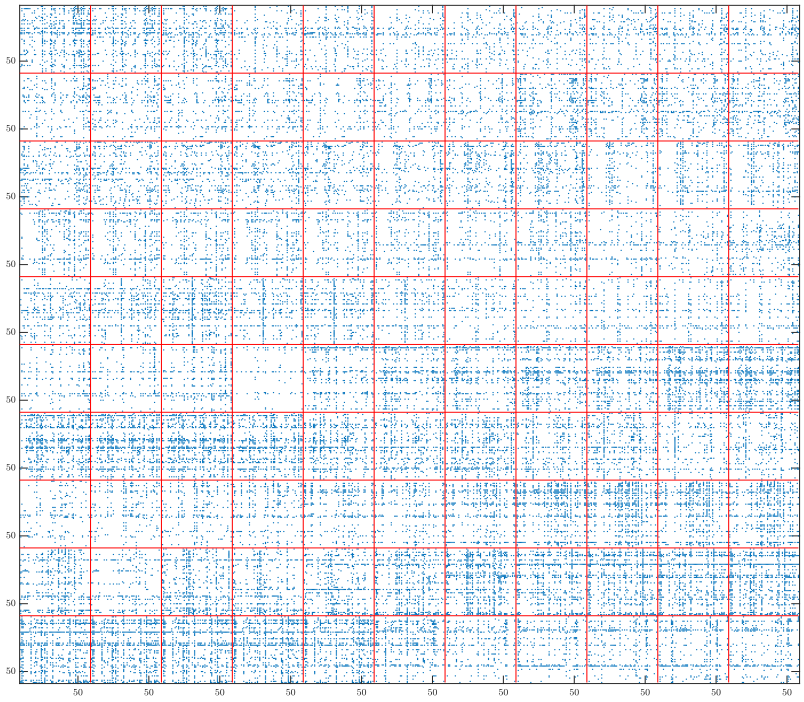

Figure 6: Full network dataset, with $I = J = 61$ nodes and sample size of $T = 110$ months. In each red box there is an adjacency matrix, starting from top-left at time $t = 1$, the first row contains matrices from time $t = 1$ to $t = 11$, the second row from $t = 12$ to $t = 22$ and so on. Blue dots are existing edges, white dots are absent edges. Red lines are used to delimit the matrices. Labels on the horizontal and vertical axes stand for the corresponding node of the network.

The set of covariates $\mathbf{z}_t$ used to explain each edge's probability includes a constant term and:

- the network total degree (dtd), defined as the total number of edges in the network at time $t = 1, \ldots, T$;
- the monthly change of the VSTOXX index (DVX), which is the volatility index for the STOXX50 (and may considered the counterpart of the VIX for Europe);
- the monthly log-returns on the STOXX50 index (STX), taken as a European equivalent to the US S&P500 index;
- the credit spread (crs), defined as the difference between BAA and AAA indices provided by Moody's;
- the term spread (trs), defined as the difference between the 10-year returns of reference Government bonds and the 6-months EURIBOR;
- the momentum factor (mom).

All covariates have been standardised and included with one lag of delay, except DVX which is contemporaneous to the response, following the standard practice in volatility modelling (e.g., see, Corsi et al. (2013), Delpini and Bormetti (2015) Majewski et al. (2015)).

6.2 Results

We estimated a stripped-down version of the general model presented in Section (2) consisting only of eq. (8a). We run the Gibbs sampler for $N = 10000$ iterations, after having initialised the latent state variables $\{\mathbf{s}_t\}_t$ according to suitable network statistics and the marginals of the tensor decomposition in both regimes (see Supplementary material for further details). We estimate the model with tensor rank $R = 5$ and discuss the main empirical findings (the analysis has been performed also for $R = 8$, obtaining similar results).

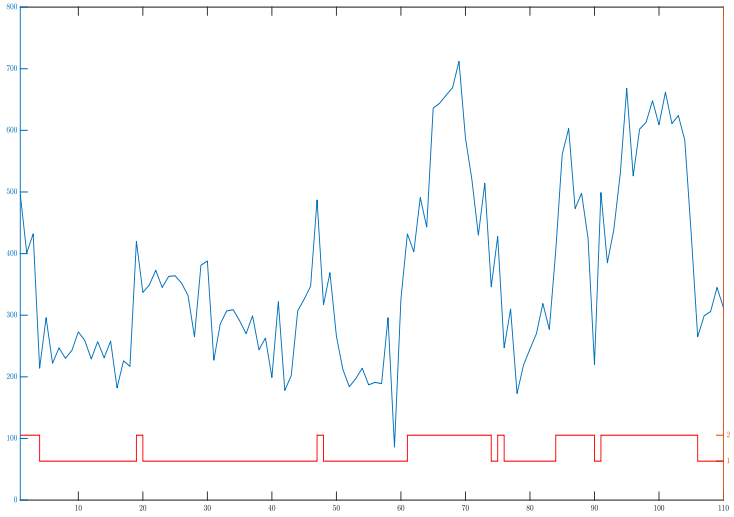

Figure 7: Total degree of the observed network time series (blue) against the estimated hidden Markov chain (red).

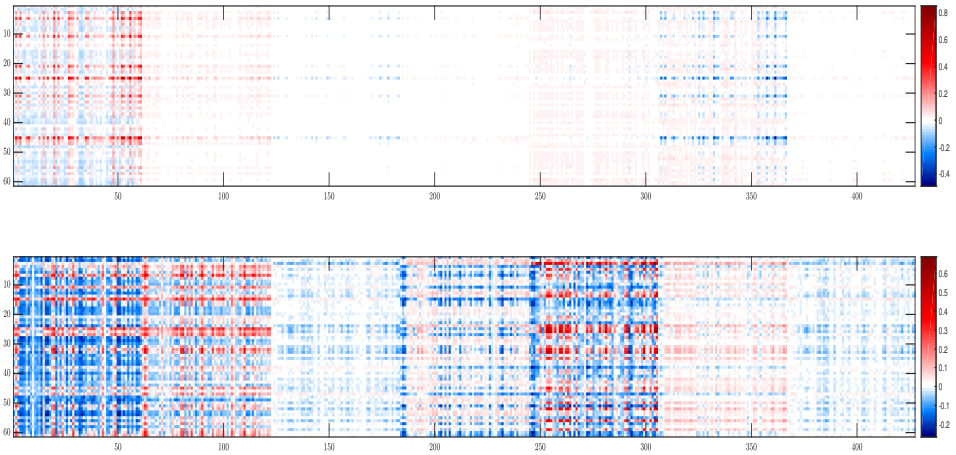

Figure 8: Posterior mean of tensor of coefficients, in matricised form, in the first (*top*) and second (*bottom*) state of the Markov switching process. For all the slices of each tensor we used the same color scale. Red, blue and white colors indicates positive, negative and zero values of the coefficients, respectively.

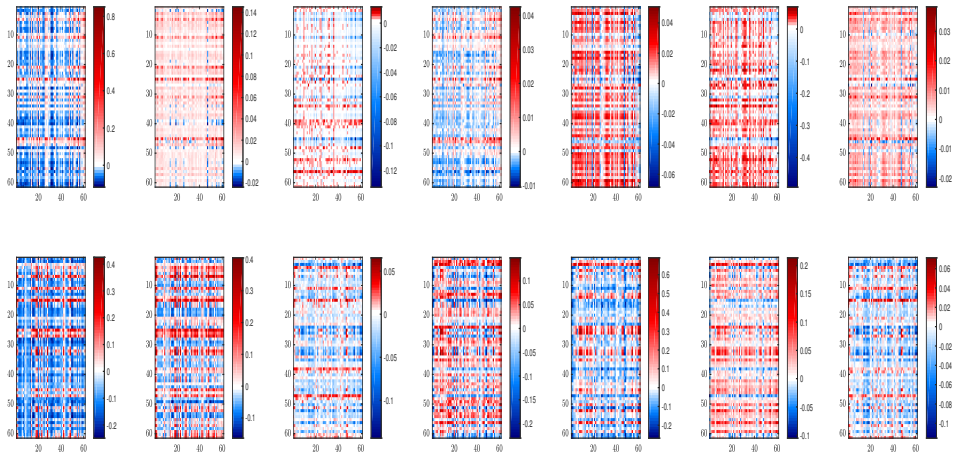

Figure 9: Posterior mean of tensor of coefficients, in matricised form, in the first (*top*) and second (*bottom*) state of the Markov switching process. For each slice of each tensor we used a different color scale. Red, blue and white colors indicates positive, negative and zero values of the coefficients, respectively.

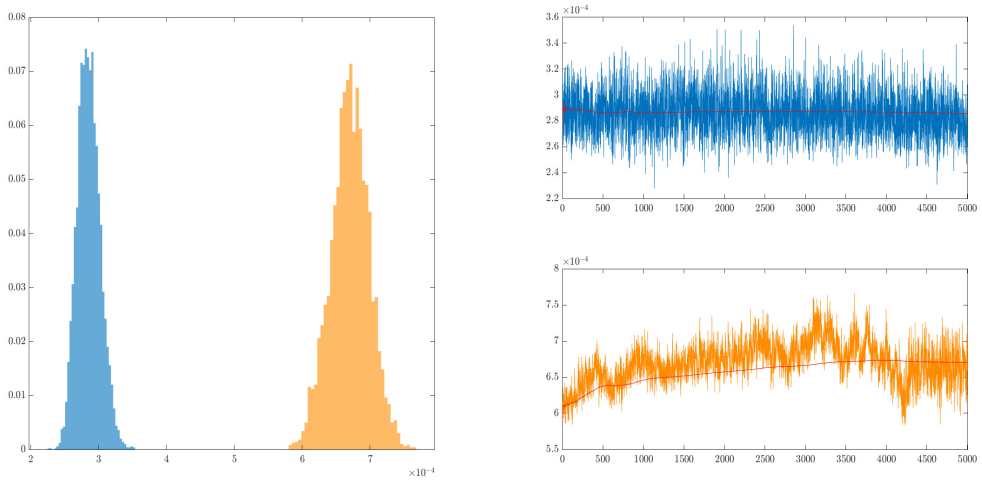

Figure 10: Posterior distribution (*left* plot) and MCMC output (*right* plots) of the quadratic norm of the tensor of coefficients, in regime 1 (*blue*) and regime 2 (*orange*).

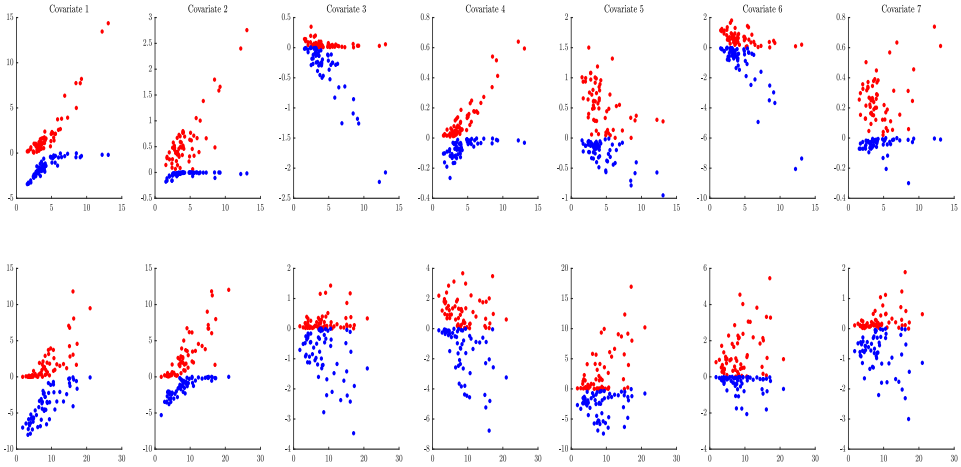

Figure 11: Scatterplots of total node degree averaged over networks within regime (*x-axis*) versus the sum of positive (*y-axis*, *red*) and the sum of negative (*y-axis*, *blue*) entries of each slice of the coefficient tensor, in regime 1 (*top*) and regime 2 (*bottom*). Coefficients corresponding to incoming edges' probability.

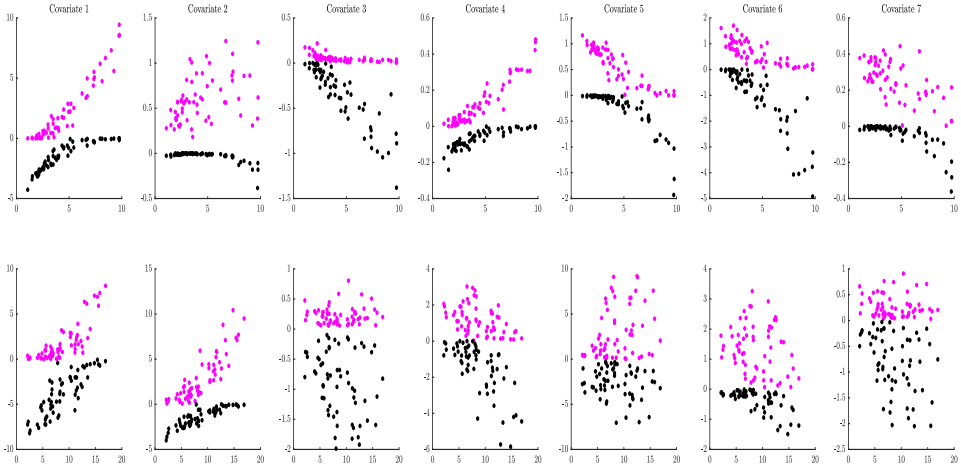

Figure 12: Scatterplots of total node degree averaged over networks within regime (*x-axis*) versus the sum of positive (*y-axis*, *magenta*) and the sum of negative (*y-axis*, *black*) entries of each slice of the coefficient tensor, in regime 1 (*top*) and regime 2 (*bottom*). Coefficients corresponding to outgoing edges' probability.

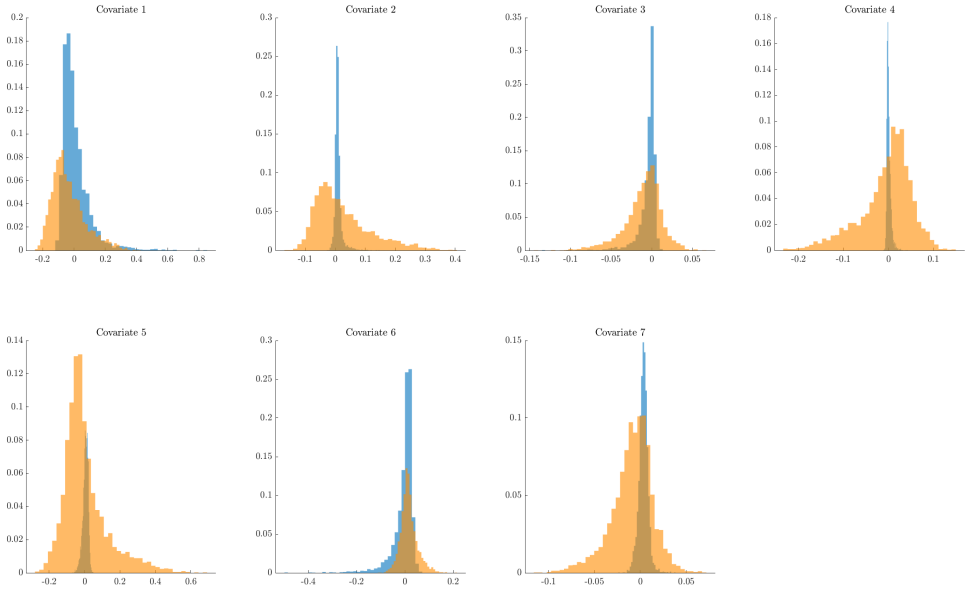

Figure 13: Distribution of the entries of each slice (different plots) of the estimated coefficient tensor, in regime 1 (*blue*) and regime 2 (*orange*).

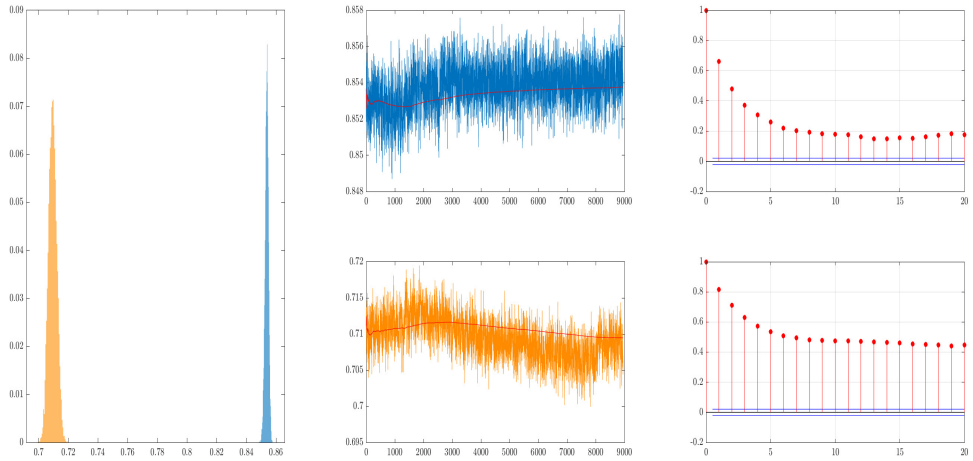

Figure 14: Posterior distribution (*left* plot), MCMC output (*middle* plots) and autocorrelation functions (*right* plots) of the mixing coefficient ρ_l in the two regimes. Regime 1 in blue and in top panels, regime 2 in orange and in bottom panels.

The estimated hidden Markov chain is plotted in Fig. 7 together with the total degree of the observed network time series, using label 1 for the sparse regime and label 2 for the dense regime. The algorithm associates to the dense state in periods when the total degree of the network is remarkably above the average.

There is substantial heterogeneity in the effect of covariates across edges, within the same regime, as reported in Figs. 8-9. Here, the estimated tensor is plotted in matricized form along mode 1 (using two different color scales in the two figures): on the vertical axis we have 61 nodes, while on the horizontal there are $61 \cdot 7$ nodes (the number of covariates including the

constant), corresponding to 7 matrices, one for each covariate, horizontally stacked. The entry (i, j) of matrix in position k reports the coefficient of the k-th covariate on the probability of observing the edge (i, j). Thus, within the same regime we observe a significant variation of both the sign and the magnitude of the effect of a covariate on the probability of observing an edge. In words, there is not a single covariate able to explain (and predict) an edge's probability by itself, but several indicators are required. Moreover, a model with pooled time series fails to capture such heterogeneity. The posterior mean is 1.56 in regime 1 and 4.63 in regime 2, but in both cases it is not significantly different from zero, that is, it lies inside a 95% credible interval around zero (see Fig. 46 in Appendix G). This is in contrast with our model, where the fraction of tensor entries statistically different from zero is 12% and 36% in regime 1 and 2, respectively. Thus, we conclude that a pooled model is not suited for describing the heterogeneous effects of the various covariates on the different edges, whereas our model is able to capture them.

We find substantial evidence in favour of major changes of the effects that the covariates exert on the edges' probability in the two regimes. By comparing the two matricized tensors in Fig. 8 we note that both the sign and the magnitude of the coefficients differ in the two states. The interpretation is that, according to the regime, the probability of observing a link between two nodes is driven by a different set of variables but also the qualitative influence (i.e. the sign of the coefficient) of the same regressor varies. For example, on average, the credit spread seems to exert a positive effect on the probability of observing an edge in the sparse regime, while its effect in the dense regime has higher magnitude and acts in the opposite direction.

Fig. 11 reports, for each regime and covariate, the scatterplot of the total degree of each node (horizontal axis), averaged within regime, against the sum of all negative and positive coefficients' values for the probability of observing an incoming edge. Similarly, Fig. 12 shows the same plot considering the effects on the probability of observing an outcoming edge. Together, these plots allow to detect the existence of a relation between the overall positive and negative magnitude of the effects of the covariates on the probability of observing an edge, conditionally on the total degree of the node to which the link is attached. The results show that for several covariates such an association exists: on average, more central nodes (i.e. those with higher total degree) tend to have higher probability of establishing an edge, either incoming or outgoing. This is due to the upward sloping shape of the scatterplot. It is remarkable to notice that for different covariates, such as the momentum factor, there is a different relation for negative and positive effects: for increasingly central nodes, both sums tend to more extreme values. Moreover, by comparing the results in Figs. 11-12 we see that the results are similar if we look either at incoming or outgoing edges. Finally, between regimes there seems to be no change except for the strength of the relation, which appears stronger in the second one (corresponding to the dense state of the network).

In Fig. 13 we plot the distribution of the entries of each slice (over the edges), for every regime, for a more qualitative analysis of the change of the coefficients' values between regimes. There is a different dispersion in the cross-sectional distribution of the coefficients' estimates. In particular, all distributions appear more concentrated around zero in the sparse state, while in the dense regime the mean value is different (and varies according to the covariate) and all distributions show fatter tails than in sparse state.

As a summary statistic, Fig. 10 reports the distribution and the trace plots of the quadratic norm of the tensor coefficients in each regime. The two distributions are well separated, with the norm in the first regimes concentrated around smaller values than in the second regime. This implies that, on average, in the sparse state there is a higher probability that the zeros (i.e. absence of edges) are due to the structural component (that is, the Dirac mass in eq. (3)), moreover the probability of success of the Bernoulli distribution is smaller than in the dense regime.

Finally, Fig. 14 shows the posterior distributions of the regime-dependent probabilities of observing a structural zero, in the two regimes. The distributions are well separated, with posterior means around 0.85 and 0.71 in the sparse and dense state, respectively.

Additional plots regarding the hyper-parameters of the model are shown in Appendix G.

7 Conclusions

We presented an econometric framework for modelling of a time series of binary tensors, which we interpret as representing multi-layer networks. We proposed a parsimonious parametrization based on the PARAFAC decomposition of the parameter tensor. Moreover, the parameters of the model can switch between multiple regimes, thus allowing to capture the time-varying topology of financial networks and economic indicators. We specified a zero-inflated logit model for the probability of each entry of the observed tensor, which permits to capture the varying sparsity patterns of the observed time series. The proposed framework is also able to jointly model a temporal sequence of binary arrays and a vector of economic variables.

We followed the Bayesian paradigm in the inferential process and developed a Gibbs sampler via multiple data augmentation steps for estimating the parameters of interest. The performance of the algorithm has been tested on simulated datasets with networks of different sizes, ranging from medium (i.e. 100 nodes) to big (i.e. 200 nodes). The results of the estimation procedure are encouraging in all simulations.

Finally, we estimated a stripped-down version the model on a real dataset of networks between European financial institutions. The results suggest the existence of two different regimes associated to the degree density of the network. Moreover, in each regime the most degree central nodes tend to be more sensitive to the effect of covariates (either positive or negative) on their probability to link to other nodes. Overall, the probability of forming an edge is not depending on a single covariate, but a combination of several financial indicators is needed to explain and predict it. Finally, nature of the absent edges is estimated to be different, with the sparse regime having a high probability of structural zeros, as compared to the dense regime.

Acknowledgements

This research has benefited from the use of the Scientific Computation System of Ca' Foscari University of Venice (SCSCF) for the computational for the implementation of the inferential procedure.

References

Acemoglu, D., V. M. Carvalho, A. Ozdaglar, and A. Tahbaz-Salehi (2012): "The network origins of aggregate fluctuations," *Econometrica*, 80, 1977–2016.

Ahelegbey, D. F., M. Billio, and R. Casarin (2016a): "Bayesian graphical models for structural vector autoregressive processes," *Journal of Applied Econometrics*, 31, 357–386.

——— (2016b): "Sparse Graphical Vector Autoregression: A Bayesian Approach," *Annals of Economics and Statistics/Annales d'Économie et de Statistique*, 333–361.

Banerjee, O., L. E. Ghaoui, and A. d'Aspremont (2008): "Model selection through sparse maximum likelihood estimation for multivariate gaussian or binary data," *Journal of Machine learning research*, 9, 485–516.

Bianchi, D., M. Billio, R. Casarin, and M. Guidolin (2016): "Modeling Systemic Risk with Markov Switching Graphical SUR Models," *Available at SSRN: https://ssrn.com/abstract=2537986*.

Billio, M., M. Caporin, R. Panzica, and L. Pelizzon (2015): "Network connectivity and systematic risk," Tech. rep., European Financial Management Association.

Billio, M., M. Getmansky, A. W. Lo, and L. Pelizzon (2012): "Econometric measures of Connectedness and Systemic Risk in the Finance and Insurance Sectors," *Journal of Financial Economics*, 104, 535–559.

Boccaletti, S., G. Bianconi, R. Criado, C. I. Del Genio, J. Gómez-Gardenes, M. Romance, I. Sendina-Nadal, Z. Wang, and M. Zanin (2014): "The Structure and Dynamics of Multilayer Networks," *Physics Reports*, 544, 1–122.

Carroll, J. D. and J.-J. Chang (1970): "Analysis of Individual Differences in multidimensional Scaling via an N-way Generalization of "Eckart-Young" Decomposition," *Psychometrica*, 35, 283–319.

Casarin, R., D. Sartore, and M. Tronzano (2018): "A Bayesian Markov-switching correlation model for contagion analysis on exchange rate markets," *Journal of Business & Economic Statistics*, 36, 101–114.

Celeux, G. (1998): "Bayesian inference for mixture: The label switching problem," in *Compstat*, Springer, 227–232.

Chaney, T. (2014): "The network structure of international trade," *The American economic review*, 104, 3600–3634.

Chib, S., F. Nardari, and N. Shephard (2002): "Markov Chain Monte Carlo methods for stochastic volatility models," *Journal of Econometrics*, 108, 281–316.

Christakis, N. A. and J. H. Fowler (2008): "The collective dynamics of smoking in a large social network," *New England journal of medicine*, 358, 2249–2258.

Cichocki, A., N. Lee, I. Oseledets, A. Phan, Q. Zhao, and D. Mandic (2016): "Low-Rank Tensor Networks for Dimensionality Reduction and Large-Scale Optimization Problems: Perspectives and Challenges PART 1," *arXiv preprint arXiv:1609.00893*.

Cichocki, A., D. Mandic, L. De Lathauwer, G. Zhou, Q. Zhao, C. Caiafa, and H. A. Phan (2015): "Tensor Decompositions for Signal Processing Applications: From two-way to Multiway Component Analysis," *IEEE Signal Processing Magazine*, 32, 145–163.

Cichocki, A., R. Zdunek, A. H. Phan, and S.-i. Amari (2009): *Nonnegative matrix and tensor factorizations: applications to exploratory multi-way data analysis and blind source separation*, John Wiley & Sons.

Corsi, F., N. Fusari, and D. La Vecchia (2013): "Realizing smiles: Options pricing with realized volatility," *Journal of Financial Economics*, 107, 284–304.

Delpini, D. and G. Bormetti (2015): "Stochastic volatility with heterogeneous time scales," *Quantitative Finance*, 15, 1597–1608.

Di Giovanni, J., A. A. Levchenko, and I. Méjean (2014): "Firms, destinations, and aggregate fluctuations," *Econometrica*, 82, 1303–1340.

Diebold, F. X. and K. Yilmaz (2014): "On the network topology of variance decompositions: Measuring the connectedness of financial firms," *Journal of Econometrics*, 182, 119–134.

Diestel, R. (2012): *Graph Theory*, vol. 173 of *Graduate Texts in Mathematics*, Springer.

Dubey, S. D. (1970): "Compound gamma, beta and F distributions," *Metrika*, 16, 27–31.

Dueker, M. J. (1997): "Markov switching in GARCH processes and mean-reverting stock-market volatility," *Journal of Business & Economic Statistics*, 15, 26–34.

——— (2005): "Dynamic forecasts of qualitative variables: a Qual VAR model of US recessions," *Journal of Business & Economic Statistics*, 23, 96–104.

Durante, D. and D. B. Dunson (2014): "Bayesian Logistic Gaussian Process Models for Dynamic Networks," *Proceedings of the 17th International Conference on Artificial Intelligence and Statistics (AISTATS)*, 33.

Frühwirth-Schnatter, S. (2001): "Markov Chain Monte Carlo estimation of classical and dynamic switching and mixture models," *Journal of the American Statistical Association*, 96, 194–209.

——— (2006): *Finite Mixture and Markov Switching Models*, Springer.

Gelman, A., J. B. Carlin, H. S. Stern, D. B. Dunson, A. Vehtari, and D. B. Rubin (2014): *Bayesian data analysis*, vol. 2, CRC Press.

Graham, B. S. (2017): "An econometric model of network formation with degree heterogeneity," *Econometrica*, 85, 1033–1063.

Guhaniyogi, R., S. Qamar, and D. B. Dunson (2017): "Bayesian Tensor Regression," *Journal of Machine Learning Research*, 18, 1–31.

Haas, M., S. Mittnik, and M. S. Paolella (2004): "A new approach to Markov-switching GARCH models," *Journal of Financial Econometrics*, 2, 493–530.

Hackbusch, W. (2012): *Tensor Spaces and Numerical Tensor Calculus*, Springer Science & Business Media.

Hamilton, J. D. (1989): "A new approach to the economic analysis of nonstationary time series and the business cycle," *Econometrica*, 57, 357–384.

Hamilton, J. D. and R. Susmel (1994): "Autoregressive conditional heteroskedasticity and changes in regime," *Journal of Econometrics*, 64, 307–333.

Harris, M. N. and X. Zhao (2007): "A zero-inflated ordered probit model, with an application to modelling tobacco consumption," *Journal of Econometrics*, 141, 1073–1099.

Harshman, R. A. (1970): "Foundations of the PARAFAC Procedure: Models and Conditions for an "Explanatory" Multi-modal Factor Analysis," *UCLA Working Papers in Phonetics, 16, 1- 84.*

Holsclaw, T., A. M. Greene, A. W. Robertson, and P. Smyth (2017): "Bayesian Non-Homogeneous Markov Models via Pólya-Gamma Data Augmentation with Applications to Rainfall Modeling," *arXiv preprint arXiv:1701.02856.*

Johnson, N. L., S. Kotz, and N. Balakrishnan (1995): *Continuous univariate distributions*, vol. 2 of *Wiley series in Probability and Mathematical Statistics: Applied Probability and Statistics*, Wiley, New York.

Kaufmann, S. (2000): "Measuring business cycles with a dynamic Markov switching factor model: An assessment using Bayesian simulation methods," *The Econometrics Journal*, 3, 39–65.

——— (2010): "Dating and forecasting turning points by Bayesian clustering with dynamic structure: A suggestion with an application to Austrian data," *Journal of Applied Econometrics*, 25, 309–344.

——— (2015): "K-state switching models with time-varying transition distributions—Does loan growth signal stronger effects of variables on inflation?" *Journal of Econometrics*, 187, 82–94.

Kiers, H. A. (2000): "Towards a Standardized Notation and Terminology in Multiway Analysis," *Journal of Chameometrics*, 14, 105–122.

Kim, C.-J. and C. R. Nelson (1998): "Business cycle turning points, a new coincident index, and tests of duration dependence based on a dynamic factor model with regime switching," *Review of Economics and Statistics*, 80, 188–201.

Kivelä, M., A. Arenas, M. Barthelemy, J. P. Gleeson, Y. Moreno, and M. A. Porter (2014): "Multilayer networks," *Journal of Complex Networks*, 2, 203–271.

Klaassen, F. (2002): "Improving GARCH volatility forecasts with regime-switching GARCH," in *Advances in Markov-Switching Models*, Springer, 223–254.

Koh, K., S.-J. Kim, and S. Boyd (2007): "An interior-point method for large-scale l1-regularized logistic regression," *Journal of Machine learning research*, 8, 1519–1555.

Kolda, T. G. and B. W. Bader (2009): "Tensor Decompositions and Applications," *SIAM Review*, 51, 455–500.

Kroonenberg, P. M. (2008): *Applied multiway data analysis*, John Wiley & Sons.

Lambert, D. (1992): "Zero-inflated Poisson regression, with an application to defects in manufacturing," *Technometrics*, 34, 1–14.

Lee, N. and A. Cichocki (2016): "Fundamental Tensor Operations for Large-Scale Data Analysis in Tensor Train Formats," *arXiv preprint arXiv:1405.7786*.

Magnus, J. R. and H. Neudecker (1999): *Matrix Differential Calculus with Applications in Statistics and Econometrics*, Wiley, New York.

Majewski, A. A., G. Bormetti, and F. Corsi (2015): "Smile from the past: A general option pricing framework with multiple volatility and leverage components," *Journal of Econometrics*, 187, 521–531.

Mele, A. (2017): "A structural model of Dense Network Formation," *Econometrica*, 85, 825–850.

Neal, R. M. (2011): "MCMC using Hamiltonian dynamics," in *Handbook of Markov Chain Monte Carlo*, ed. by S. Brooks, A. Gelman, J. L. Galin, and X.-L. Meng, Chapman & Hall /CRC, chap. 5.

Polson, N. G., J. G. Scott, and J. Windle (2013): "Bayesian Inference for Logistic Models using Pólya–Gamma Latent Variables," *Journal of the American Statistical Association*, 108, 1339–1349.

Ravikumar, P., M. J. Wainwright, J. D. Lafferty, et al. (2010): "High-dimensional Ising model selection using l1-regularized logistic regression," *The Annals of Statistics*, 38, 1287–1319.

Robert, C. P. and G. Casella (2004): *Monte Carlo Statistical Methods*, Springer.

Schildcrout, J. S. and P. J. Heagerty (2005): "Regression analysis of longitudinal binary data with time-dependent environmental covariates: bias and efficiency," *Biostatistics*, 6, 633–652.

Sherman, M., T. V. Apanasovich, and R. J. Carroll (2006): "On estimation in binary autologistic spatial models," *Journal of Statistical Computation and Simulation*, 76, 167–179.

Sims, C. A., D. F. Waggoner, and T. Zha (2008): "Methods for inference in large multiple-equation Markov-switching models," *Journal of Econometrics*, 146, 255–274.

Sims, C. A. and T. Zha (2006): "Were there regime switches in US monetary policy?" *The American Economic Review*, 96, 54–81.

Smith, D. R. (2002): "Markov-switching and stochastic volatility diffusion models of short-term interest rates," *Journal of Business & Economic Statistics*, 20, 183–197.

Springer, M. and W. Thompson (1970): "The distribution of products of beta, gamma and Gaussian random variables," *SIAM Journal on Applied Mathematics*, 18, 721–737.

Taddy, M. (2013): "Multinomial inverse regression for text analysis," *Journal of the American Statistical Association*, 108, 755–770.

Taddy, M. A. (2010): "Autoregressive mixture models for dynamic spatial Poisson processes: Application to tracking intensity of violent crime," *Journal of the American Statistical Association*, 105, 1403–1417.

Tanner, M. A. and W. H. Wong (1987): "The calculation of posterior distributions by data augmentation," *Journal of the American Statistical Association*, 82, 528–540.

Turney, P. D. (2002): "Thumbs up or thumbs down? Semantic orientation applied to unsupervised classification of reviews," in *Proceedings of the 40th annual meeting on association for computational linguistics*, Association for Computational Linguistics, 417–424.

Van Dyk, D. A. and T. Park (2008): "Partially collapsed Gibbs samplers: Theory and methods," *Journal of the American Statistical Association*, 103, 790–796.

Visaya, M. V., D. Sherwell, B. Sartorius, and F. Cromieres (2015): "Analysis of Binary Multivariate Longitudinal Data via 2-Dimensional Orbits: An Application to the Agincourt Health and Socio-Demographic Surveillance System in South Africa," *PloS one*, 10, e0123812.

Wang, L., D. Durante, R. E. Jung, and D. B. Dunson (2017): "Bayesian network–response regression," *Bioinformatics*, 33, 1859–1866.

Wilbur, J., J. Ghosh, C. Nakatsu, S. Brouder, and R. Doerge (2002): "Variable Selection in High-Dimensional Multivariate Binary Data with Application to the Analysis of Microbial Community DNA Fingerprints," *Biometrics*, 58, 378–386.

Wooldridge, J. M. (2010): *Econometric analysis of cross section and panel data*, MIT press.

Yue, Y. R., M. A. Lindquist, and J. M. Loh (2012): "Meya-analysis of functional neuroimaging data using Bayesian nonparametric binary regression," *The Annals of Applied Statistics*, 697–718.

Zellner, A. (1962): "An efficient method of estimating seemingly unrelated regressions and tests for aggregation bias," *Journal of the American Statistical Association*, 57, 348–368.

A Tensor calculus and decompositions

In this section we introduce some notation for multilinear arrays (i.e. tensors) and some basic operations defined on them: the operations on tensors and between tensors and lower-dimensional objects (such as matrices and vectors) and the representation results for tensors (or tensor decomposition/approximation). A noteworthy introduction to tensors and corresponding operations is in Lee and Cichocki (2016), while a remarkable reference for tensor decomposition methods is Kolda and Bader (2009). Throughout the paper, we use the following notation: matrices are represented by boldface uppercase letters, vectors by boldface lowercase letters, scalars by lowercase letters and, finally, calligraphic letters denote tensors, if not differently specified.

A multidimensional array is an object which generalises the concept of matrix. It may have an arbitrary number of dimensions (or modes), whose number is the *order* of the tensor. Consequently, a matrix is a second order tensor. By convention, we denote a whole column (or row) of a matrix by the symbol ":" and the same is used for tensors, where this symbol denotes that we are considering the corresponding whole dimension. The mode-k fiber of a tensor is a generalization of the concept of row/column in the matrix case: it is the vector obtained along the dimension k by fixing all the other dimensions. Differently from the bi-dimensional case, however, with higher order arrays it is possible to identify also slices (i.e. bi-dimensional fibers of matrices) or generalizations of them, by fixing all but two or more dimensions (or modes) of the tensor. For example, the mode-k fiber of the tensor $\mathcal{X}$ is denoted by:

$$\mathcal{X}_{(i_1,\ldots,i_{k-1},:,:,i_{k+2},\ldots,i_D)} \qquad \forall\, k \in \{1,\ldots,D\}\,. \tag{A.1}$$

The operation of transforming a D-array $\mathcal{X}$ into a matrix is called matricization. The *mode-n matricization*, denoted by $\mathbf{X}_{(n)}$, consists in re-arranging all the mode-n fibers to be the columns of a matrix, which will have size $\mathbf{X}_{(n)} \in \mathbb{R}^{d_n \times \bar{d}_{(-n)}}$ with $\bar{d}_{(-n)} = \Pi_{i \neq n} d_i$. For detailed examples, see Kolda and Bader (2009). Analogously to the matrix version, the *vectorization* of a tensor consists in stacking all the elements in a unique vector of dimension $\bar{d} = \Pi_i d_i$. Notice that, the ordering of the elements is not important as long as it is consistent across the calculations.

Many product operations have been defined for tensors, but here we constrain ourselves to the operator used in this work and we point to Lee and Cichocki (2016) for a summary of other operators. The *mode−n product* between a tensor $\mathcal{X}$ and a vector $\mathbf{v} \in \mathbb{R}^{d_n}$ can be interpreted as the standard Euclidean inner product between the vector and each mode-n fiber of the tensor. Consequently, this operator suppresses one dimension of the tensor and results in a lower order tensor. It is defined, element-wise, by:

$$\mathcal{Y}_{(i_1,\ldots,i_{n-1},i_{n+1},\ldots,i_D)} = (\mathcal{X} \times_n \mathbf{v})_{(i_1,\ldots,i_{n-1},i_{n+1},\ldots,i_D)} = \sum_{i_n}^{d_n} \mathcal{X}_{i_1,\ldots,i_D} \mathbf{v}_{i_n}, \tag{A.2}$$

with $\mathcal{Y} \in \mathbb{R}^{d_1 \times \ldots, d_{n-i}, d_{n+1}, \ldots \times d_D}$. Notice that this product is not commutative, since the order of the elements in the multiplication is relevant.

Finally, let $\mathcal{Y} \in \mathbb{R}^{d_1^Y \times \ldots \times d_M^Y}$ and $\mathcal{X} \in \mathbb{R}^{d_1^X \times \ldots \times d_N^X}$. The *outer product* $\circ$ of two tensors[5] is the tensor $\mathcal{Z} \in \mathbb{R}^{d_1^Y \times \ldots \times d_M^Y \times d_1^X \times \ldots \times d_N^X}$ whose entries are:

$$\mathcal{Z}_{i_1,\ldots,i_M,j_1,\ldots,j_N} = (\mathcal{Y} \circ \mathcal{X})_{i_1,\ldots,i_M,j_1,\ldots,j_N} = \mathcal{Y}_{i_1,\ldots,i_M} \mathcal{X}_{j_1,\ldots,j_N}. \tag{A.3}$$

For example, the outer product of two vectors is a matrix, while the outer product of two matrices is a tensor of order 4. As a special case, the outer product of two column vectors $\mathbf{a}$, $\mathbf{b}$ can be equivalently represented by means of the Kronocker product $\otimes$:

$$\mathbf{a} \circ \mathbf{b} = \mathbf{b} \otimes \mathbf{a} = \mathbf{a} \cdot \mathbf{b}'. \tag{A.4}$$

We now define two tensor representations, or decompositions, which are useful in two respects: (i) the algebraic objects that form the decomposition are generally low dimensional and more easily tractable than the tensor; (ii) they can be used to provide a good approximation of the original array. Also, let us denote with R^* be the rank of tensor $\mathcal{X}$, the abstraction of the notion of matrix rank.

The Tucker decomposition can be thought of as a higher-order generalization of Principal Component Analysis (PCA): a tensor $\mathcal{X} \in \mathbb{R}^{d_1 \times \ldots \times d_D}$ is decomposed into (more precisely, it is approximated by) the product (along the corresponding mode) of a "core" tensor $\mathcal{Y} \in \mathbb{R}^{y_1 \times \ldots \times y_D}$ and D factor matrices $A^{(l)} \in \mathbb{R}^{d_l \times y_l}$, $1 \leq l \leq D$. Following the notation in Kolda and Bader (2009):

$$\mathcal{X} = \mathcal{Y} \times_1 A^{(1)} \times_2 A^{(2)} \times_3 \ldots \times_D A^{(D)} = \sum_{i_1=1}^{y_1} \sum_{i_2=1}^{y_2} \ldots \sum_{i_D=1}^{y_D} y_{i_1,i_2,\ldots,i_D} \mathbf{a}_{i_1}^{(1)} \circ \mathbf{a}_{i_2}^{(2)} \circ \ldots \circ \mathbf{a}_{i_D}^{(D)}. \tag{A.5}$$

Here $\mathbf{a}_{i_l}^{(l)} \in \mathbb{R}^{g_l \times 1}$ is the l-th column of the matrix $A^{(l)}$. As a result, each entry of the tensor is obtained as:

$$\mathcal{X}_{j_1,\ldots,j_D} = \sum_{i_1=1}^{y_1} \sum_{i_2=1}^{y_2} \ldots \sum_{i_D=1}^{y_D} y_{i_1,i_2,\ldots,i_D} a_{i_1,j_1}^{(1)} a_{i_2,j_2}^{(2)} \ldots a_{i_D,j_D}^{(D)} \quad 1 \leq j_l \leq d_l,\ 1 \leq l \leq D. \tag{A.6}$$

A special case of the Tucker decomposition is obtained when the core tensor collapses to a scalar and the factor matrices reduce to a single column vector each one is called PARAFAC(R)[6]. More precisely, the PARAFAC(R) decomposition allows to represent a D-order tensor $\mathcal{X} \in \mathbb{R}^{d_1 \times \ldots \times d_D}$ as the sum of R rank one tensors, that is, of outer products (denoted by $\circ$) of vectors (also called marginals in this case)[7]:

$$\mathcal{X} = \sum_{r=1}^{R} \mathcal{X}_r = \sum_{r=1}^{R} \mathbf{x}_1^{(r)} \circ \ldots \circ \mathbf{x}_D^{(r)}, \tag{A.7}$$

with $\mathbf{x}_j^{(r)} \in \mathbb{R}^{d_j}\ \forall j = 1, \ldots, D$. For a tensor of arbitrary order, the determination of the rank is a $NP-$hard problem (Kolda and Bader (2009)), as a consequence, in applied works, one generally

[5]This operator still applies to vectors and matrices, as they are special cases of tensors of order 1 and 2, respectively.

[6]See Harshman (1970). Some authors (e.g., Carroll and Chang (1970) and Kiers (2000)) use the term CO-DECOMP or CP instead of PARAFAC.

[7]An alternative representation may be used, if all the vectors $\mathbf{x}_j^r$ are normalized to have unitary length. In this case the weight of each component r is captured by the $r-th$ component of the vector $\boldsymbol{\lambda} \in \mathbb{R}^R$:

$$\mathcal{X} = \sum_{r=1}^{R} \lambda_r \left(\mathbf{x}_1^{(r)} \circ \ldots \circ \mathbf{x}_D^{(r)} \right)$$

.

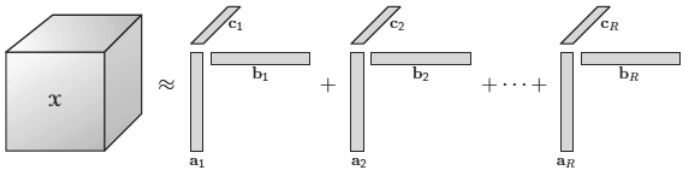

Figure 15: PARAFAC decomposition of $\mathcal{X} \in \mathbb{R}^{d_1 \times d_2 \times d_3}$, with $\mathbf{a}_r \in \mathbb{R}^{d_1}$, $\mathbf{b}_r \in \mathbb{R}^{d_2}$ and $\mathbf{c}_r \in \mathbb{R}^{d_3}$, $1 \leq r \leq R$. Figure from Kolda and Bader (2009).

fixes R, uses a PARAFAC(R) approximation, and then run a sensitivity analysis of the results with respect to R. The higher the value of R, the better is the approximation. Alternatively, whenever it is possible to define a measure for the approximation accuracy one may define a grid of values $\{R_i\}_{i=1}^{\bar{R}}$ at which evaluate the accuracy, then choose the value of the grid which yields the best approximation.

B Prior distribution on tensor entries

The assumed hierarchical prior distribution on the marginals of the PARAFAC(R) decomposition assumed for the tensor of coefficients in each regime induces a prior distribution on each single entry of the tensor which is not normal. Fig. 16-18 show the empirical distribution of two randomly chosen entries of a tensor $\mathcal{Y} \in \mathbb{R}^{100 \times 100 \times 3}$ whose PARAFAC decomposition is assumed with $R = 5$ and $R = 10$, respectively. Compared to the standard normal distribution and the standard Laplace distribution[8] the prior distribution induced on the single entries of the tensor is still symmetric, but has heavier tails.

[8]The probability density function of the Laplace distribution with mean μ and variance $2b^2$ is given by:

$$f(x|\mu, b) = \frac{1}{2b} \exp\left\{-\frac{|x-\mu|}{2b}\right\} \qquad x \in \mathbb{R},\ \mu \in \mathbb{R},\ b > 0$$

and has kurtosis equal to 6.

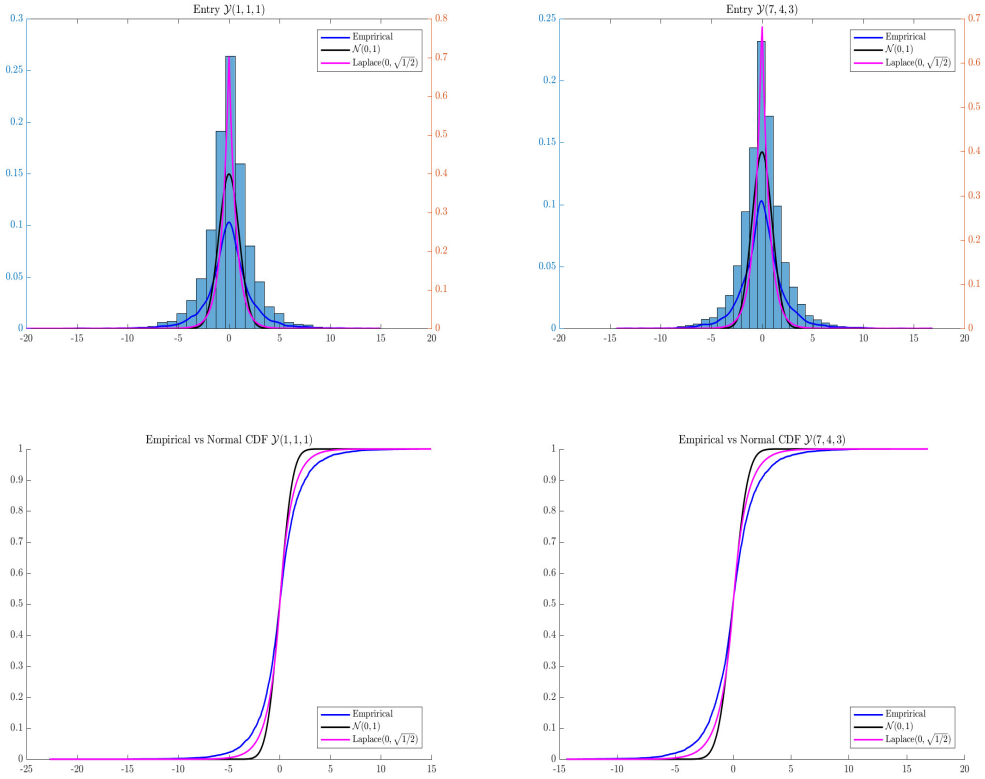

Figure 16: Monte Carlo approximation of prior distribution (with $R = 5$) of an element of the tensor (histogram and dark blue line) against the standard Normal distribution (black) and the standard Laplace distribution (magenta).

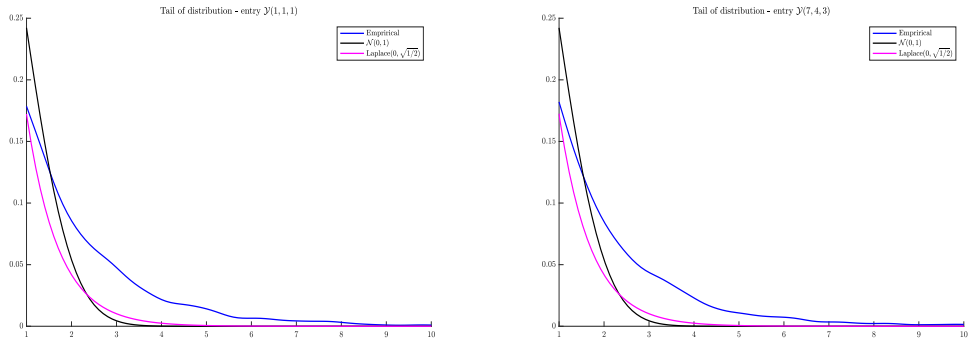

Figure 17: Monte Carlo approximation of the right tail of the prior distribution (with $R = 5$) of an element of the tensor (histogram and dark blue line) against the standard Normal distribution (black) and the standard Laplace distribution (magenta).

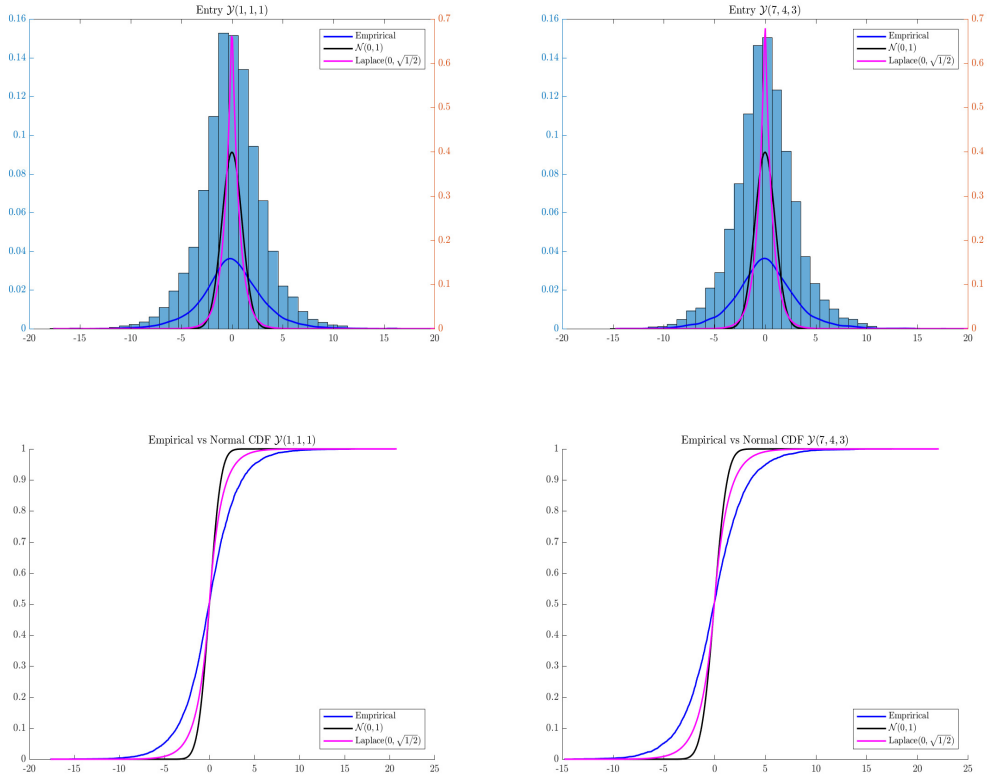

Figure 18: Monte Carlo approximation of prior distribution (with $R = 10$) of an element of the tensor (histogram and dark blue line) against the standard Normal distribution (black) and the standard Laplace distribution (magenta).

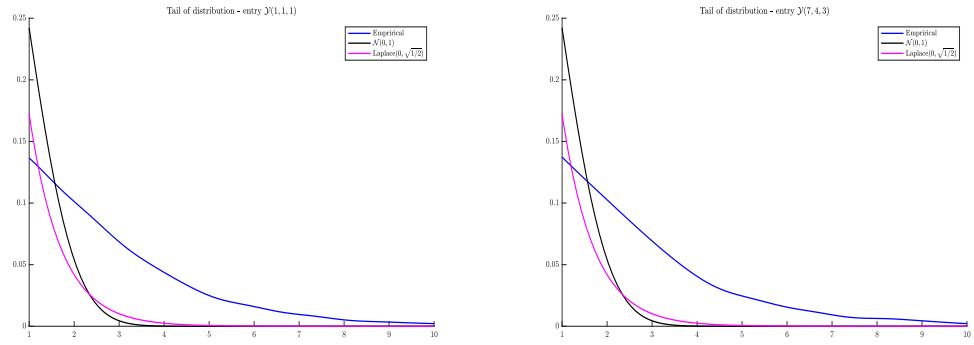

Figure 19: Monte Carlo approximation of the right tail of the prior distribution (with $R = 10$) of an element of the tensor (histogram and dark blue line) against the standard Normal distribution (black) and the standard Laplace distribution (magenta).

The analytical formula for the prior distribution of the generic entry $g_{ijkp,l}$ of the fourth-order tensor $\mathcal{G}_l \in \mathbb{R}^{I\times J\times K\times P}$ can be obtained from the PARAFAC(R) decomposition in eq. (A.7) and

the hierarchical prior on the marginals in eq. (13), (14), (15), (16):

$$\pi(g_{ijkp,l}) = \int_{\mathbb{R}_+} \int_{\mathcal{S}^R} \int_{(\mathbb{R}_+ \times \mathbb{R}_+)^{4R}} \pi(g_{ijkp,l}|\tau, \boldsymbol{\phi}, \mathbf{w}) \pi(\tau) \pi(\boldsymbol{\phi}) \pi(\mathbf{w}) \, \mathrm{d}\tau \, \mathrm{d}\boldsymbol{\phi} \, \mathrm{d}\mathbf{w} \,, \tag{B.1}$$

where $\mathcal{S}^R$ is the standard R-simplex. The entry $g_{ijkp,l}$ can be expressed in terms of the tensor marginals $\{\boldsymbol{\gamma}_{h,l}^{(r)}\}_{hrl}$ as follows:

$$g_{ijkp,l} = \sum_{r=1}^{R} \gamma_{1,i,l}^{(r)} \cdot \gamma_{2,j,l}^{(r)} \cdot \gamma_{3,k,l}^{(r)} \cdot \gamma_{4,p,l}^{(r)} \,. \tag{B.2}$$

By exploiting the conditional independence relations in the hierarchical prior of the marginals in eq. (13), we can thus rewrite the conditional distribution $\pi(g_{ijkp,l}|\tau, \boldsymbol{\phi}, \mathbf{w})$ in eq. (B.1) as:

$$\pi(g_{ijkp,l}|\tau, \boldsymbol{\phi}, \mathbf{w}) = \mathbb{P}\left(\sum_{r=1}^{R} \gamma_{1,i,l}^{(r)} \cdot \gamma_{2,j,l}^{(r)} \cdot \gamma_{3,k,l}^{(r)} \cdot \gamma_{4,p,l}^{(r)} \right) \,, \tag{B.3}$$

which is the distribution of a finite sum of independent, univariate normal distributions, centred in zero, but with individual-specific variance. The distribution of each of these products has been characterised by Springer and Thompson (1970), who proved the following theorem.

Theorem B.1 (4 in Springer and Thompson (1970))**.** *The probability density function of the product $z = \prod_{j=1}^{J} x_j$ of J independent Normal random variables $x_j \sim \mathcal{N}(0, \sigma_j^2)$, $j = 1, \ldots, J$, is a Meijer G-function multiplied by a normalising constant H:*

$$p(z|\{\sigma_j^2\}_{j=1}^J) = H \cdot G_{J,0}^{J,0}\left(z^2 \cdot \prod_{j=1}^{J} \frac{1}{2\sigma_j} \Big| \mathbf{0} \right) \,, \tag{B.4}$$

where

$$H = \left[(2\pi)^{J/2} \cdot \prod_{j=1}^{J} \sigma_j \right]^{-1} \tag{B.5}$$

and $G_{p,q}^{m,n}(\cdot|\cdot)$ is a Meijer G-function (with $c \in \mathbb{R}$ and $s \in \mathbb{C}$):

$$G_{p,q}^{m,n}\left(z \Big| \begin{matrix} a_1, \ldots, a_p \\ b_1, \ldots, b_q \end{matrix} \right) = \frac{1}{2\pi i} \int_{c-i\infty}^{c+i\infty} z^{-s} \frac{\prod_{j=1}^{m} \Gamma(s + b_j) \cdot \prod_{j=1}^{n} \Gamma(1 - a_j - s)}{\prod_{j=n+1}^{p} \Gamma(s + a_j) \cdot \prod_{j=m+1}^{q} \Gamma(1 - b_j - s)} \, \mathrm{d}s \,. \tag{B.6}$$

The integral is taken over a vertical line in the complex plane. Notice that in the special case $J = 2$ we have $z \sim c_1 P_1 - c_2 P_2$, with $P_1, P_2 \sim \chi_1^2$ and $c_1 = \mathbb{V}(x_1 + x_2)/4$, $c_2 = \mathbb{V}(x_1 - x_2)/4$.

C Data augmentation

The likelihood function is:

$$L(\boldsymbol{\mathcal{X}}, \mathbf{y}|\boldsymbol{\theta}) = \sum_{s_1, \ldots, s_T} \prod_{t=1}^{T} p(\mathcal{X}_t, \mathbf{y}_t|s_t, \boldsymbol{\theta}) p(s_t|s_{t-1}) \,, \tag{C.1}$$

where the index $l \in \{1, \ldots, L\}$ represents the regime. Through the introduction of a latent variables $\mathbf{s} = \{s_t\}_{t=0}^T$, we obtain the data augmented likelihood:

$$L(\boldsymbol{\mathcal{X}}, \mathbf{y}, \mathbf{s}|\boldsymbol{\theta}) = \prod_{t=1}^{T} \prod_{l=1}^{L} \prod_{h=1}^{L} \left[p(\mathcal{X}_t, \mathbf{y}_t|s_t = l, \boldsymbol{\theta}) p(s_t = l|s_{t-1} = h, \boldsymbol{\Xi}) \right]^{\mathbb{1}(s_t = l)\mathbb{1}(s_{t-1} = h)} \,. \tag{C.2}$$

The conditional distribution of the observation given the latent variable and marginal distribution of s_t are given by, respectively:

$$p(\mathcal{X}_t, \mathbf{y}_t | s_t = l, \boldsymbol{\theta}) = f_l(\mathcal{X}_t, \mathbf{y}_t | \boldsymbol{\theta}_l) \tag{C.3}$$

$$p(s_t = l | s_{t-1} = h, \boldsymbol{\Xi}) = p_h \,. \tag{C.4}$$

Considering the observation model in eq. (2) and defining $\mathcal{T}_l = \{t : s_t = l\}$ for each $l = 1, \ldots, L$, we can rewrite eq. (C.2) as:

$$\begin{aligned}
L(\boldsymbol{\mathcal{X}}, \mathbf{y}, \mathbf{s} | \boldsymbol{\theta}) &= \prod_{t=1}^{T} \prod_{l=1}^{L} \left[p(\mathcal{X}_t | s_t = l, \boldsymbol{\theta}) p(\mathbf{y}_t | s_t = l, \boldsymbol{\theta}) \right]^{\mathbb{1}(s_t = l)} \prod_{h=1}^{L} \left[p(s_t = l | s_{t-1} = h, \boldsymbol{\Xi}) \right]^{\mathbb{1}(s_t = l)\mathbb{1}(s_{t-1} = h)} \\
&= \prod_{l=1}^{L} \prod_{t \in \mathcal{T}_l} \prod_{i=1}^{I} \prod_{j=1}^{J} \prod_{k=1}^{K} \left[(1 - \rho_l) \frac{\exp\{\mathbf{z}_t' \mathbf{g}_{ijk,l}\}}{1 + \exp\{\mathbf{z}_t' \mathbf{g}_{ijk,l}\}} \right]^{x_{ijk,t}} \left[\rho_l + (1 - \rho_l) \frac{1}{1 + \exp\{\mathbf{z}_t' \mathbf{g}_{ijk,l}\}} \right]^{1 - x_{ijk,t}} \\
&\cdot \prod_{l=1}^{L} \prod_{t \in \mathcal{T}_l} (2\pi)^{-m/2} \left| \Sigma_l \right|^{-1/2} \exp \left\{ -\frac{1}{2} (\mathbf{y}_t - \boldsymbol{\mu}_l)' \boldsymbol{\Sigma}_l^{-1} (\mathbf{y}_t - \boldsymbol{\mu}_l) \right\} \\
&\cdot \prod_{t=1}^{T} \prod_{l=1}^{L} \prod_{h=1}^{L} p_h^{\mathbb{1}(s_t = l)\mathbb{1}(s_{t-1} = h)} \,.
\end{aligned} \tag{C.5}$$

Since the function cannot be expressed as a series of products due to the sum in the rightmost term, we choose to further augment the data via the through the introduction of latent allocation variables $\mathcal{D} = \{\mathcal{D}_l\}_{l=1}^{L}$, with $\mathcal{D}_l = (d_{ijk,l})$ for $i = 1, \ldots, I$, $j = 1, \ldots, J$ and $k = 1, \ldots, K$. Finally, we perform another augmentation as in Polson et al. (2013), for dealing with the logistic part of the model. When the hidden chain is assumed to be first order Markov, with two possible states, that is $L = 2$, the complete data likelihood is given by:

$$\begin{aligned}
L(\boldsymbol{\mathcal{X}}, \mathbf{y}, \mathcal{D}, \boldsymbol{\Omega}, \mathbf{s} | \boldsymbol{\theta}) &= p(\boldsymbol{\mathcal{X}}, \mathcal{D}, \boldsymbol{\Omega} | \mathbf{s}, \boldsymbol{\theta}) p(\mathbf{y} | \mathbf{s}, \boldsymbol{\theta}) p(\mathbf{s} | \boldsymbol{\theta}) \\
&= \prod_{t=1}^{T} p(\mathcal{X}_t, \mathcal{D}_t, \boldsymbol{\Omega}_t | s_t, \boldsymbol{\theta}) p(\mathbf{y}_t | s_t, \boldsymbol{\theta}) p(s_t | \boldsymbol{\theta}) && \text{(C.6a)} \\
&= \left[\prod_{l=1}^{L} \prod_{t \in \mathcal{T}_l} \prod_{i=1}^{I} \prod_{j=i}^{J} \prod_{k=1}^{K} \underbrace{p(x_{ijk,t}, d_{ijk,t}, \omega_{ijk,t} | s_t = l, \rho_l, \mathcal{G}_l)}_{I} \right] && \text{(C.6b)} \\
&\cdot \left[\prod_{l=1}^{L} \prod_{t \in \mathcal{T}_l} \underbrace{p(\mathbf{y}_t | s_t = l, \boldsymbol{\mu}_l, \boldsymbol{\Sigma}_l)}_{II} \right] \cdot \left[\underbrace{p(\mathbf{s} | \boldsymbol{\Xi})}_{III} \right] && \text{(C.6c)}
\end{aligned}$$

where we have exploited the conditional independence of $\boldsymbol{\mathcal{X}}$ and $\mathbf{y}$ given the hidden chain $\mathbf{s}$. We start by analysing in detail the first term (I). The joint distribution of the observation $x_{ijk,t}$ and the latent variables $(d_{ijk,t}, \omega_{ijk,t})$ is obtained from the marginal distribution of the observation in two steps. First, we augment the model by introducing the latent allocation $d_{ijk,l} \in \{0, 1\}$ for $l = 1, 2$. Via this data augmentation step we are able to factorise the summation in eq. (2) for each regime $l = 1, 2$. In words, the allocation latent variable is used to identify the component of the mixture in eq. (2) from which the observation $x_{ijk,t}$ is drawn. Secondly, we use a further data augmentation step via the introduction of the latent variables $\omega_{ijk,t}$ following Polson et al. (2013), for dealing with the logistic part of the mixture.

By introducing the allocation variable $d_{ijk,t}$ in eq. (2), for each $i = 1, \ldots, I$, $j = 1, \ldots, J$, $k = 1, \ldots, K$ and $t = 1, \ldots, T$, we obtain:

$$p(x_{ijk,t} | d_{ijk,t}, s_t = l, \rho_l, \mathcal{G}_l)$$

$$
\begin{aligned}
&= \Big[\delta_{\{0\}}\Big]^{\mathbb{1}\{d_{ijk,t}=1\}} \cdot \big[\mathcal{B}ern(x_{ijk,t}|\eta_{ijk,t})\big]^{\mathbb{1}\{d_{ijk,t}=0\}} \\
&= \Big[\delta_{\{0\}}(x_{ijk,t})\Big]^{d_{ijk,t}} \cdot \left[\left(\frac{\exp\{\mathbf{z}_t'\mathbf{g}_{ijk,l}\}}{1+\exp\{\mathbf{z}_t'\mathbf{g}_{ijk,l}\}}\right)^{x_{ijk,t}} \left(1-\frac{\exp\{\mathbf{z}_t'\mathbf{g}_{ijk,l}\}}{1+\exp\{\mathbf{z}_t'\mathbf{g}_{ijk,l}\}}\right)^{1-x_{ijk,t}}\right]^{1-d_{ijk,t}} \\
&= \Big[\delta_{\{0\}}(x_{ijk,t})\Big]^{d_{ijk,t}} \cdot \frac{\big(\exp\{\mathbf{z}_t'\mathbf{g}_{ijk,l}\}\big)^{x_{ijk,t}(1-d_{ijk,t})}}{\big(1+\exp\{\mathbf{z}_t'\mathbf{g}_{ijk,l}\}\big)^{(1-d_{ijk,t})}} \,. \qquad \text{(C.7)}
\end{aligned}
$$

$$
\begin{aligned}
&p(x_{ijk,t}, d_{ijk,t}|s_t = l, \rho_l, \mathcal{G}_l) \\
&= \rho_l^{\mathbb{1}\{d_{ijk,t}=1\}} \cdot \Big[\delta_{\{0\}}(x_{ijk,t})\Big]^{\mathbb{1}\{d_{ijk,t}=1\}} \cdot (1-\rho_l)^{\mathbb{1}\{d_{ijk,t}=0\}} \cdot \big[\mathcal{B}ern(x_{ijk,t}|\eta_{ijk,t})\big]^{\mathbb{1}\{d_{ijk,t}=0\}} \\
&= \rho_l^{d_{ijk,t}} \cdot \Big[\delta_{\{0\}}(x_{ijk,t})\Big]^{d_{ijk,t}} \cdot (1-\rho_l)^{1-d_{ijk,t}} \cdot \frac{\big(\exp\{\mathbf{z}_t'\mathbf{g}_{ijk,l}\}\big)^{x_{ijk,t}(1-d_{ijk,t})}}{\big(1+\exp\{\mathbf{z}_t'\mathbf{g}_{ijk,l}\}\big)^{(1-d_{ijk,t})}} \,. \qquad \text{(C.8)}
\end{aligned}
$$

The marginal distribution of the allocation variable is:

$$
p(d_{ijk,t}|s_t) = \mathcal{B}ern(\rho_{s_t}) \,, \qquad \text{(C.9)}
$$

for $i = 1, \ldots, I$, $j = 1, \ldots, J$, $k = 1, \ldots, K$ and $t = 1, \ldots, T$.

By Theorem 1 in Polson et al. (2013), it is possible to decompose the ratio in the right hand side of eq. (C.8) as follows:

$$
\frac{\big(\exp\{\mathbf{z}_t'\mathbf{g}_{ijk,l}\}\big)^{x_{ijk,t}(1-d_{ijk,t})}}{\big(1+\exp\{\mathbf{z}_t'\mathbf{g}_{ijk,l}\}\big)^{(1-d_{ijk,t})}} = 2^{-(1-d_{ijk,t})} \int_0^\infty \exp\left\{-\frac{\omega_{ijk,t}}{2}(\mathbf{z}_t'\mathbf{g}_{ijk,l})^2 + \kappa_{ijk,t}(\mathbf{z}_t'\mathbf{g}_{ijk,l})\right\} p(\omega_{ijk,t})\mathrm{d}\omega_{ijk,t} \,, \qquad \text{(C.10)}
$$

where for every $l = 1, \ldots, L$, $i = 1, \ldots, I$, $j = 1, \ldots, J$, $k = 1, \ldots, K$ and $t = 1, \ldots, T$:

$$
\kappa_{ijk,t} = x_{ijk,t}(1-d_{ijk,t}) - \frac{1-d_{ijk,t}}{2} = (1-d_{ijk,t})\left(x_{ijk,t} - \frac{1}{2}\right) \,. \qquad \text{(C.11)}
$$

Therefore we get the following conditional and joint distributions, respectively:

$$
\begin{aligned}
&p(x_{ijk,t}, d_{ijk,t}|\omega_{ijk,t}, s_t = l, \rho_l, \mathcal{G}_l) = \\
&= \rho_l^{d_{ijk,t}} \cdot \left(0^{x_{ijk,t}} 1^{1-x_{ijk,t}}\right)^{d_{ij,t}} \cdot \left(\frac{1-\rho_l}{2}\right)^{1-d_{ijk,t}} \cdot \exp\left\{-\frac{\omega_{ijk,t}}{2}(\mathbf{z}_t'\mathbf{g}_{ijk,l})^2 + \kappa_{ijk,t}(\mathbf{z}_t'\mathbf{g}_{ijk,l})\right\} \,. \qquad \text{(C.12)}
\end{aligned}
$$

$$
\begin{aligned}
&p(x_{ijk,t}, d_{ijk,t}, \omega_{ijk,t}|s_t = l, \rho_l, \mathcal{G}_l) = \\
&= \rho_l^{d_{ijk,t}} \cdot \left(0^{x_{ijk,t}} 1^{1-x_{ijk,t}}\right)^{d_{ijk,t}} \cdot \left(\frac{1-\rho_l}{2}\right)^{1-d_{ijk,t}} \cdot \exp\left\{-\frac{\omega_{ijk,t}}{2}(\mathbf{z}_t'\mathbf{g}_{ijk,l})^2 + \kappa_{ijk,t}(\mathbf{z}_t'\mathbf{g}_{ijk,l})\right\} p(\omega_{ijk,t}) \,. \qquad \text{(C.13)}
\end{aligned}
$$

Finally, the marginal distribution of each latent variable $\omega_{ijk,t}$ from the data augmentation scheme follows a Pólya-Gamma distribution:

$$
\omega_{ijk,t} \sim PG(1, 0) \,. \qquad \text{(C.14)}
$$

A continuous random variable $x \in [0, +\infty)$ has a Pólya-Gamma distribution with parameters $b > 0$, $c \in \mathbb{R}$ if the following stochastic representation holds (where $\stackrel{D}{=}$ stands for equality in distribution):

$$x \sim PG(b, c) \quad \Longleftrightarrow \quad x \stackrel{D}{=} \frac{1}{2\pi^2} \sum_{k=1}^{\infty} \frac{g_k}{(k - 1/2)^2 + c^2/(4\pi^2)} \tag{C.15}$$

where $g_k \sim \mathcal{G}a(b, 1)$ are i.i.d. random variables. See Polson et al. (2013) for further details. The part (II) of eq. (C.6c) is the likelihood of a multivariate normal mean regression, hence:

$$p(\mathbf{y}_t | s_t = l, \boldsymbol{\theta}) = (2\pi)^{-m/2} \left|\boldsymbol{\Sigma}_l\right|^{-1/2} \exp\left\{-\frac{1}{2}(\mathbf{y}_t - \boldsymbol{\mu}_l)' \boldsymbol{\Sigma}_l^{-1} (\mathbf{y}_t - \boldsymbol{\mu}_l)\right\}. \tag{C.16}$$

The last term in eq. (C.6c), according to the assumption of first order time homogeneous Markov chain, factors as[9]:

$$p(s_t|\boldsymbol{\theta}) = p(s_0|\boldsymbol{\Xi}) \prod_{v=1}^{t} p(s_v|s_{v-1}, \boldsymbol{\Xi}) = p(s_0|\boldsymbol{\Xi}) \prod_{v=1}^{t} \xi_{s_{v-1}, s_v} = p(s_0|\boldsymbol{\Xi}) \prod_{g=1}^{L} \prod_{l=1}^{L} \xi_{g,l}^{N_{gl}(\mathbf{s}^t)} \tag{C.17}$$

where $\mathbf{s}^t = (s_0, \ldots, s_t)'$ and $N_{gl}(\mathbf{s}^t)$ is a function counting the number of transitions from state g to state l in the vector $\mathbf{s}^t$, that is (symbol # denotes the cardinality of a set): $N_{gl}(\mathbf{s}^t) = \#\{s_{t-1} = g, s_t = l\}$, $\forall\, g, l = 1, \ldots, L$. The complete data likelihood for $\mathcal{X}$ is thus obtained by plugging, for each $l = 1, \ldots, L$, eq. (C.13), eq. (C.16) and eq. (C.17) in eq. (C.6c):

$$\begin{aligned}
&L(\boldsymbol{\mathcal{X}}, \mathbf{y}, \mathcal{D}, \boldsymbol{\Omega}, \mathbf{s}|\boldsymbol{\theta}) = \\
&= \left[\prod_{l=1}^{L} \prod_{t \in \mathcal{T}_l} \prod_{i=1}^{I} \prod_{j=1}^{J} \prod_{k=1}^{K} \rho_l^{d_{ijk,t}} \cdot \delta_{\{0\}}(x_{ijk,t})^{d_{ij,t}} \cdot \left(\frac{1 - \rho_l}{2}\right)^{1 - d_{ijk,t}} \cdot \exp\left\{-\frac{\omega_{ijk,t}}{2} (\mathbf{z}_t' \mathbf{g}_{ijk,l})^2 + \kappa_{ijk,t} (\mathbf{z}_t' \mathbf{g}_{ijk,l})\right\}\right] \\
&\cdot \left[\prod_{l=1}^{L} \prod_{t \in \mathcal{T}_l} (2\pi)^{-m/2} \left|\boldsymbol{\Sigma}_l\right|^{-1/2} \exp\left\{-\frac{1}{2}(\mathbf{y}_t - \boldsymbol{\mu}_l)' \boldsymbol{\Sigma}_l^{-1} (\mathbf{y}_t - \boldsymbol{\mu}_l)\right\}\right] \\
&\cdot \left[\prod_{t=1}^{T} \prod_{i=1}^{I} \prod_{j=1}^{J} \prod_{k=1}^{K} p(\omega_{ijk,t})\right] \cdot \left[\prod_{g=1}^{L} \prod_{l=1}^{L} \xi_{g,l}^{N_{gl}(\mathbf{s})}\right] \cdot p(s_0|\boldsymbol{\Xi}) \,.
\end{aligned} \tag{C.18}$$

D Computational Details

D.1 Gibbs sampler

The structure of the partially collapsed Gibbs sampler (Van Dyk and Park (2008)) is as follows:

$$\begin{aligned}
&p(\mathbf{s}|\boldsymbol{\mathcal{X}}, \mathcal{G}, \boldsymbol{\rho}, \boldsymbol{\Xi}) \\
&p(\mathbf{D}|\mathbf{s}, \mathcal{G}, \boldsymbol{\rho}) \\
&p(\boldsymbol{\Omega}|\boldsymbol{\mathcal{X}}, \mathbf{s}, \mathcal{G}) \\
&p(\boldsymbol{\psi}|\mathcal{G}, \mathbf{W}) \\
&p(\tau|\mathcal{G}, \mathbf{W}, \boldsymbol{\phi}) \\
&p(w_{h,r,l}|\boldsymbol{\gamma}_{h,l}^{(r)}, \lambda_l, \boldsymbol{\phi}, \tau) \\
&p(\lambda_l|w_{1,1,l}, \ldots, w_{4,R,l})
\end{aligned}$$

[9] See (Frühwirth-Schnatter, 2006, ch.11) for more details.

$$
\begin{aligned}
&p(\boldsymbol{\gamma}_{1,l}^{(r)}|\boldsymbol{\gamma}_{-1,l}^{(r)}, \mathcal{G}_{-r,l}, \boldsymbol{\phi}, \tau, \mathbf{W}, \boldsymbol{\mathcal{X}}, \mathbf{s}) \\
&p(\boldsymbol{\gamma}_{2,l}^{(r)}|\boldsymbol{\gamma}_{-2,l}^{(r)}, \mathcal{G}_{-r,l}, \boldsymbol{\phi}, \tau, \mathbf{W}, \boldsymbol{\mathcal{X}}, \mathbf{s}) \\
&p(\boldsymbol{\gamma}_{3,l}^{(r)}|\boldsymbol{\gamma}_{-3,l}^{(r)}, \mathcal{G}_{-r,l}, \boldsymbol{\phi}, \tau, \mathbf{W}, \boldsymbol{\mathcal{X}}, \mathbf{s}) \\
&p(\boldsymbol{\gamma}_{4,l}^{(r)}|\boldsymbol{\gamma}_{-4,l}^{(r)}, \mathcal{G}_{-r,l}, \boldsymbol{\phi}, \tau, \mathbf{W}, \boldsymbol{\mathcal{X}}, \mathbf{s}) \\
&\quad p(\boldsymbol{\rho}|\mathbf{s}, \mathbf{D}) \\
&\quad p(\boldsymbol{\Xi}|\mathbf{s}) \\
&p(\boldsymbol{\mu}_l|\mathbf{y}, \mathbf{s}, \boldsymbol{\Sigma}_l) \sim \mathcal{N}_M(\tilde{\boldsymbol{\mu}}_l, \tilde{\boldsymbol{\Upsilon}}_l) \\
&p(\boldsymbol{\Sigma}_l|\mathbf{y}, \mathbf{s}, \boldsymbol{\mu}_l) \sim \mathcal{IW}_M(\tilde{\nu}_l, \tilde{\boldsymbol{\Psi}}_l)\,.
\end{aligned}
$$

Step 1. sample latent variables from

$$
p(\mathbf{s}, \mathbf{D}, \boldsymbol{\Omega}|\boldsymbol{\mathcal{X}}, \mathcal{G}, \boldsymbol{\rho}, \boldsymbol{\Xi}) = p(\mathbf{s}|\boldsymbol{\mathcal{X}}, \mathcal{G}, \boldsymbol{\rho}, \boldsymbol{\Xi}) \cdot p(\mathbf{D}|\mathbf{s}, \mathcal{G}, \boldsymbol{\rho}) \cdot p(\boldsymbol{\Omega}|\boldsymbol{\mathcal{X}}, \mathbf{s}, \mathcal{G})
$$

- $p(\mathbf{s}|\boldsymbol{\mathcal{X}}, \mathcal{G}, \boldsymbol{\rho}, \boldsymbol{\Xi})$ via FFBS (Frühwirth-Schnatter (2006))
- $p(d_{ijk,t}|s_t, \mathcal{G}_t, \rho_t) \sim \mathcal{B}ern(\tilde{p}_{d_{ijk,t}})$
- $p(\omega_{ijkv,t}|x_{ijk,t}, s_t, \mathcal{G}_t) \sim PG(1,\, \mathbf{z}_t'\mathbf{g}_{ijk,s_t})$

Step 2. sample variance hyperparameters from

$$
p(\boldsymbol{\phi}, \tau, W|\mathcal{G}) = \underbrace{p(\boldsymbol{\phi}|\mathcal{G}, \mathbf{W})}_{\text{collapse } \tau} \cdot p(\tau|\mathcal{G}, \boldsymbol{\phi}, \mathbf{W}) \cdot p(\mathbf{W}|\mathcal{G}, \boldsymbol{\lambda}, \boldsymbol{\phi}, \tau) p(\boldsymbol{\lambda}|\mathbf{W})
$$

- $p(\psi_r|\mathcal{G}^{(r)}, \mathbf{w}_r) \sim GiG\left(2\overline{b}^{\tau},\, \sum_{h=1}^{4}\sum_{l=1}^{L} \frac{\boldsymbol{\gamma}_{h,l}^{(r)\prime}\boldsymbol{\gamma}_{h,l}^{(r)}}{w_{h,r}},\, \overline{\alpha} - n\right)$ then $\phi_r = \psi_r / \sum_i \psi_i$
- $p(\tau|\mathcal{G}, \mathbf{W}, \boldsymbol{\phi}) \sim GiG\left(2\overline{b}^{\tau},\, \sum_{r=1}^{R}\sum_{h=1}^{4}\sum_{l=1}^{L} \frac{\boldsymbol{\gamma}_{h,l}^{(r)\prime}\boldsymbol{\gamma}_{h,l}^{(r)}}{\phi_r w_{h,r}},\, (\overline{\alpha} - n)R\right)$
- $p(w_{h,r,l}|\boldsymbol{\gamma}_{h,l}^{(r)}, \phi_r, \tau, \lambda_l) \sim \text{GiG}\left(\lambda_l^2,\, \frac{\boldsymbol{\gamma}_{h,l}^{(r)\prime}\boldsymbol{\gamma}_{h,l}^{(r)}}{\tau\phi_r},\, 1 - \frac{n_h}{2}\right)$
- $p(\lambda_l|\mathbf{w}_l) \propto \lambda_l^{\overline{a}_l^{\lambda}+8R-1} \exp\left\{-\lambda_l \overline{b}_l^{\lambda}\right\} \cdot \exp\left\{-\frac{\lambda_l^2}{2}\sum_{r=1}^{R}\sum_{h=1}^{4} w_{h,r,l}\right\}$

Step 3. sample tensor marginals from

$$
p\left(\mathcal{G}|\boldsymbol{\mathcal{X}}, \mathbf{s}, \boldsymbol{\phi}, \tau, \mathbf{W}\right) = \prod_{l=1}^{L} p\left(\{\boldsymbol{\gamma}_{1,l}^{(r)}, \boldsymbol{\gamma}_{2,l}^{(r)}, \boldsymbol{\gamma}_{3,l}^{(r)}, \boldsymbol{\gamma}_{4,l}^{(r)}\}_{r=1}^{R} \big| \boldsymbol{\mathcal{X}}, \mathbf{s}, \boldsymbol{\phi}, \tau, \mathbf{W}\right)
$$

- $p(\boldsymbol{\gamma}_{1,l}^{(r)}|\boldsymbol{\gamma}_{-1,l}^{(r)}, \mathcal{G}_{-r,l}, \boldsymbol{\phi}, \tau, \mathbf{W}, \boldsymbol{\mathcal{X}}, \mathbf{s}) \sim \mathcal{N}_{d_1}(\boldsymbol{\mu}_{\boldsymbol{\gamma}_{1,l}}, \Sigma_{\boldsymbol{\gamma}_{1,l}})$
- $p(\boldsymbol{\gamma}_{2,l}^{(r)}|\boldsymbol{\gamma}_{-2,l}^{(r)}, \mathcal{G}_{-r,l}, \boldsymbol{\phi}, \tau, \mathbf{W}, \boldsymbol{\mathcal{X}}, \mathbf{s}) \sim \mathcal{N}_{d_2}(\boldsymbol{\mu}_{\boldsymbol{\gamma}_{2,l}}, \Sigma_{\boldsymbol{\gamma}_{2,l}})$
- $p(\boldsymbol{\gamma}_{3,l}^{(r)}|\boldsymbol{\gamma}_{-3,l}^{(r)}, \mathcal{G}_{-r,l}, \boldsymbol{\phi}, \tau, \mathbf{W}, \boldsymbol{\mathcal{X}}, \mathbf{s}) \sim \mathcal{N}_{d_3}(\boldsymbol{\mu}_{\boldsymbol{\gamma}_{3,l}}, \Sigma_{\boldsymbol{\gamma}_{3,l}})$

– $p(\boldsymbol{\gamma}_{4,l}^{(r)}|\boldsymbol{\gamma}_{-4,l}^{(r)}, \mathcal{G}_{-r,l}, \boldsymbol{\phi}, \tau, \mathbf{W}, \boldsymbol{\mathcal{X}}, \mathbf{s}) \sim \mathcal{N}_{d_4}(\boldsymbol{\mu}_{\boldsymbol{\gamma}_{4,l}}, \Sigma_{\boldsymbol{\gamma}_{4,l}})$

Step 4. sample switching parameters and transition matrix from

$$p(\rho_l, \xi_{l,l}|\mathbf{s}, \mathbf{D}) = p(\rho_l|\mathbf{s}, \mathbf{D}) \cdot p(\xi_{l,l}|\mathbf{s})$$

– $p(\rho_l|\mathbf{s}, \mathbf{D}) \sim \mathcal{B}e(\tilde{a}_l, \tilde{b}_l)$
– $p(\boldsymbol{\xi}_{l,:}|\mathbf{s}) \sim \mathcal{D}ir(\tilde{\mathbf{c}})$

Step 5. sample the parameters of the second equation from

$$p(\boldsymbol{\mu}_l, \boldsymbol{\Sigma}_l|\mathbf{y}, \mathbf{s}) = p(\boldsymbol{\mu}_l|\mathbf{y}, \mathbf{s}, \boldsymbol{\Sigma}_l)p(\boldsymbol{\Sigma}_l|\mathbf{y}, \mathbf{s}, \boldsymbol{\mu}_l)$$

– $p(\boldsymbol{\mu}_l|\mathbf{y}, \mathbf{s}, \boldsymbol{\Sigma}_l) \sim \mathcal{N}_M(\tilde{\boldsymbol{\mu}}_l, \tilde{\boldsymbol{\Upsilon}}_l)$
– $p(\boldsymbol{\Sigma}_l|\mathbf{y}, \mathbf{s}, \boldsymbol{\mu}_l) \sim \mathcal{IW}_M(\tilde{\nu}_l, \tilde{\boldsymbol{\Psi}}_l)$

The derivation of the full conditional distribution is illustrated in the following subsections.

D.2 Full conditional distribution of ϕ_r

The full conditional of the common (over r) component of the variance of the marginals from the PARAFAC, for each $r = 1, \ldots, R$, can be obtained in closed form collapsing τ. This can be done by exploiting a result in Guhaniyogi et al. (2017), which states that the posterior full conditional of each ϕ_r can be obtained by normalising Generalised Inverse Gaussian distributed random variables ψ_r, where $\psi_r = \tau\phi_r$:

$$p(\phi_r|\mathcal{G}^{(r)}, \mathbf{w}_r) = \frac{\psi_r}{\sum_{i=1}^{R} \psi_i} \qquad \forall\, r \tag{D.1}$$

where for every $r = 1, \ldots, R$:

$$\psi_r \sim \text{GiG}\left(2\overline{b}^{\tau}, \sum_{h=1}^{4}\sum_{l=1}^{L} \frac{\boldsymbol{\gamma}_{h,l}^{(r)'}\boldsymbol{\gamma}_{h,l}^{(r)}}{w_{h,r,l}}, \overline{\alpha} - n\right). \tag{D.2}$$

In the previous notation, $GiG(\cdot)$ stands for the Generalized Inverse Gaussian distribution. The Generalized Inverse Gaussian probability density function with three parameters $a > 0$, $b > 0$, $p \in \mathbb{R}$, for the random variable $x \in (0, +\infty)$, is given by:

$$x \sim GiG(a, b, p) \;\Rightarrow\; p(x|a, b, p) = \frac{(a/b)^{p/2}}{2K_p(\sqrt{ab})} x^{p-1} \exp\left\{-\frac{1}{2}\left(ax + \frac{b}{x}\right)\right\} \tag{D.3}$$

with $K_p(\cdot)$ a modified Bessel function of the second type.
The computation necessary for obtaining this result are as follows:

$$p(\boldsymbol{\phi}|\mathcal{G}, \mathbf{W}) \propto p(\boldsymbol{\phi}) \int_0^{\infty} p(\mathcal{G}|\mathbf{W}, \boldsymbol{\phi}, \tau)p(\tau)\, \mathrm{d}\tau \tag{D.4a}$$

$$\propto \prod_{r=1}^{R} \phi_r^{\overline{\alpha}-1} \int_0^{\infty} \prod_{r=1}^{R}\prod_{h=1}^{4}\prod_{l=1}^{L} (\tau\phi_r w_{h,r,l}\mathbf{I}_{n_h})^{-1/2} \exp\left\{-\frac{1}{2}\boldsymbol{\gamma}_{h,l}^{(r)'}(\tau\phi_r w_{h,r,l}\mathbf{I}_{n_h})^{-1}\boldsymbol{\gamma}_{h,l}^{(r)}\right\}$$

$$\cdot\, \tau^{a_\tau - 1} \exp\left\{-\overline{b}^\tau \tau\right\} \,\mathrm{d}\tau \tag{D.4b}$$

$$= \int_0^\infty \prod_{r=1}^{R} \phi_r^{\overline{\alpha}-1} \prod_{h=1}^{4} (\tau \phi_r w_{h,r,l} \mathbf{I}_{n_h})^{-1} \exp\left\{-\frac{1}{2} \sum_{l=1}^{L} (\tau \phi_r w_{h,r,l})^{-1} \boldsymbol{\gamma}_{h,l}^{(r)'} \boldsymbol{\gamma}_{h,l}^{(r)}\right\}$$

$$\cdot\, \tau^{\overline{a}^\tau - 1} \exp\left\{-\overline{b}^\tau \tau\right\} \,\mathrm{d}\tau\,. \tag{D.4c}$$

We define $n = n_1 + n_2 + n_3 + n_4 = I + J + K + Q$ and exploit the property $\det(kA) = k^n \det(A)$, for a square matrix A of size n and a scalar k. Finally, we assume:

$$\overline{a}^\tau = \overline{\alpha} R \tag{D.5}$$

which is allowed since the hyperparameter $\overline{a}^\tau$ must be positive. We can thus obtain:

$$\propto \int_0^\infty \prod_{r=1}^{R} \phi_r^{\overline{\alpha}-1} \prod_{h=1}^{4} (\tau \phi_r w_{h,r,l} \mathbf{I}_{n_h})^{-1} \exp\left\{-\frac{1}{2} \sum_{l=1}^{L} (\tau \phi_r w_{h,r,l})^{-1} \boldsymbol{\gamma}_{h,l}^{(r)'} \boldsymbol{\gamma}_{h,l}^{(r)}\right\}$$

$$\cdot\, \tau^{\overline{a}^\tau - 1} \exp\left\{-\overline{b}^\tau \tau\right\} \,\mathrm{d}\tau \tag{D.6a}$$

$$\propto \int_0^\infty \prod_{r=1}^{R} (\tau \phi_r)^{\overline{\alpha}-1} (\tau \phi_r)^{-n} \exp\left\{-\frac{1}{2}\left[2\overline{b}^\tau \tau + \sum_{h=1}^{4} \sum_{l=1}^{L} (\tau \phi_r w_{h,r,l})^{-1} \boldsymbol{\gamma}_{h,l}^{(r)'} \boldsymbol{\gamma}_{h,l}^{(r)}\right]\right\} \mathrm{d}\tau \tag{D.6b}$$

$$= \int_0^\infty \left(\prod_{r=1}^{R} (\tau \phi_r)^{\overline{\alpha}-n-1}\right) \exp\left\{-\frac{1}{2} \sum_{r=1}^{R}\left[2\overline{b}^\tau \tau \phi_r + \frac{1}{\tau \phi_r} \sum_{h=1}^{4} \sum_{l=1}^{L} \frac{\boldsymbol{\gamma}_{h,l}^{(r)'} \boldsymbol{\gamma}_{h,l}^{(r)}}{w_{h,r,l}}\right]\right\} \mathrm{d}\tau \tag{D.6c}$$

where in the last line we used $\sum_{r=1}^{R} \phi_r = 1$. It can be seen that the integrand is the kernel of a GiG with respect to the random variable $\psi_r = \tau \phi_r$. Following Guhaniyogi et al. (2017), it is possible to sample from the posterior of ϕ_r, for each $r = 1, \ldots, R$ by first sampling ψ_r from a GiG with kernel given in eq. (D.6c), then normalising over r, as reported in eq. (D.2)-(D.1), respectively.

As an alternative, it is possible to sample from eq. (D.2) using a Hamiltonian Monte Carlo step (Neal (2011)).

D.3 Full conditional distribution of τ

The full conditional of the global component of the variance of the PARAFAC marginals is:

$$p(\tau | \mathcal{G}, \mathbf{W}, \boldsymbol{\phi}) \sim \mathrm{GiG}\left(2\overline{b}^\tau,\, \sum_{r=1}^{R} \sum_{h=1}^{4} \sum_{l=1}^{L} \frac{\boldsymbol{\gamma}_{h,l}^{(r)'} \boldsymbol{\gamma}_{h,l}^{(r)}}{\phi_r w_{h,r,l}},\, (\overline{\alpha} - n) R\right)\,, \tag{D.7}$$

The posterior full conditional distribution is derived from:

$$p(\tau | \mathcal{G}, \mathbf{W}, \boldsymbol{\phi}) \propto \pi(\tau) p(\mathcal{G} | \mathbf{W}, \boldsymbol{\phi}, \tau)$$

$$\propto \tau^{\overline{a}^\tau - 1} \exp\left\{-\overline{b}^\tau \tau\right\} \prod_{r=1}^{R} \prod_{h=1}^{4} \prod_{l=1}^{L} \left|\tau \phi_r w_{h,r,l} \mathbf{I}_{n_h}\right|^{-1/2} \exp\left\{-\frac{1}{2} \boldsymbol{\gamma}_{h,l}^{(r)'} (\tau \phi_r w_{h,r,l} \mathbf{I}_{n_h})^{-1} \boldsymbol{\gamma}_{h,l}^{(r)}\right\} \tag{D.8a}$$

$$\propto \tau^{\overline{a}^\tau - nR - 1} \exp\left\{-\frac{1}{2}\left[2\overline{b}^\tau \tau + \frac{1}{\tau} \sum_{r=1}^{R} \sum_{h=1}^{4} \sum_{l=1}^{L} \frac{\boldsymbol{\gamma}_{h,l}^{(r)'} \boldsymbol{\gamma}_{h,l}^{(r)}}{\phi_r w_{h,r,l}}\right]\right\}\,, \tag{D.8b}$$

which is the kernel of the GiG in eq. (D.7), once the constraint in eq. (D.5) has been taken into account.

It is possible to sample from eq. (D.7) using a Hamiltonian Monte Carlo step (Neal (2011)).

D.4 Full conditional distribution of $w_{h,r,l}$

The full conditional distribution of the local component of the variance of each PARAFAC marginal, for $h = 1, \dots, 4$, $r = 1, \dots, R$ and $l = 1, \dots, L$, is given by:

$$p(w_{h,r,l}|\boldsymbol{\gamma}_{h,l}^{(r)}, \phi_r, \tau, \lambda_l) \sim \text{GiG}\left(\lambda_l^2,\ \frac{\boldsymbol{\gamma}_{h,l}^{(r)'}\boldsymbol{\gamma}_{h,l}^{(r)}}{\tau\phi_r},\ 1 - \frac{n_h}{2}\right), \tag{D.9}$$

which follows from:

$$p(w_{h,r,l}|\boldsymbol{\gamma}_{h,l}^{(r)}, \phi_r, \tau, \lambda_l) \propto \pi(w_{h,r,l}|\lambda_l)p(\boldsymbol{\gamma}_{h,l}^{(r)}|w_{h,r,l}, \phi_r, \tau) \tag{D.10a}$$

$$\propto \exp\left\{-\frac{\lambda_l^2}{2}w_{h,r,l}\right\}\left|\tau\phi_r w_{h,r,l}\mathbf{I}_{n_h}\right|^{-1/2}\exp\left\{-\frac{1}{2}\boldsymbol{\gamma}_{h,l}^{(r)'}(\tau\phi_r w_{h,r,l}\mathbf{I}_{n_h})^{-1}\boldsymbol{\gamma}_{h,l}^{(r)}\right\} \tag{D.10b}$$

$$\propto \exp\left\{-\frac{\lambda_l^2}{2}w_{h,r,l}\right\}w_{h,r,l}^{-n_h/2}\exp\left\{-\frac{1}{2}\frac{\boldsymbol{\gamma}_{h,l}^{(r)'}\boldsymbol{\gamma}_{h,l}^{(r)}}{\tau\phi_r w_{h,r,l}}\right\} \tag{D.10c}$$

$$= w_{h,r,l}^{-n_h/2}\exp\left\{-\frac{1}{2}\left[\lambda_l^2 w_{h,r,l} + \frac{1}{w_{h,r,l}}\frac{\boldsymbol{\gamma}_{h,l}^{(r)'}\boldsymbol{\gamma}_{h,l}^{(r)}}{\tau\phi_r}\right]\right\}. \tag{D.10d}$$

It is possible to sample from eq. (D.9) using a Hamiltonian Monte Carlo step (Neal (2011)).

D.5 Full conditional distribution of λ_l

The full conditional distribution of λ_l, for $l = 1, \dots, L$, is given by:

$$p(\lambda_l|\mathbf{w}_l) \propto \lambda_l^{\overline{a}_l^\lambda + 8R - 1}\exp\left\{-\lambda_l\overline{b}_l^\lambda\right\}\cdot\exp\left\{-\frac{\lambda_l^2}{2}\sum_{r=1}^{R}\sum_{h=1}^{4}w_{h,r,l}\right\}. \tag{D.11}$$

It is obtained from:

$$p(\lambda_l|\mathbf{w}_l) \propto \pi(\lambda_l)p(\mathbf{w}_l|\lambda_l) \tag{D.12a}$$

$$\propto \lambda_l^{a_\lambda^l - 1}\exp\left\{-b_\lambda^l\lambda_l\right\}\prod_{r=1}^{R}\prod_{h=1}^{4}\frac{\lambda_l^2}{2}\exp\left\{-\frac{\lambda_l^2}{2}w_{h,r,l}\right\} \tag{D.12b}$$

$$\propto \lambda^{\overline{a}_l^\lambda + 8R - 1}\exp\left\{-\lambda_l\overline{b}_l^\lambda\right\}\cdot\exp\left\{-\frac{\lambda_l^2}{2}\sum_{r=1}^{R}\sum_{h=1}^{4}w_{h,r,l}\right\}. \tag{D.12c}$$

Since the second exponential is always smaller than one due to the positiveness of all the parameters $\lambda_l, w_{h,r,l}$, we can sample from this distribution by means of an accept/reject algorithm using as proposal density a Gamma distribution $\mathcal{G}a(\tilde{a}, \tilde{b})$ with parameters:

$$\tilde{a} = \overline{a}_l^\lambda + 8R \qquad \tilde{b} = \overline{b}_l^\lambda. \tag{D.13}$$

Since this sampling scheme has very low acceptance rate, it is possible to sample from eq. (D.11) using a Hamiltonian Monte Carlo step (Neal (2011)).

D.6 Full conditional distribution of $\boldsymbol{\gamma}_{h,l}^{(r)}$

For deriving the full conditional distribution of each PARAFAC marginal, $\boldsymbol{\gamma}_{h,l}^{(r)}$, of the tensor $\mathcal{G}_l$, $l = 1, \ldots, L$, we start by manipulating the complete data likelihood in eq. (12) with the aim of singling out $\boldsymbol{\gamma}_{h,l}^{(r)}$. From eq. (C.13), considering all the entries of $\mathcal{X}_t$ at a given $t \in \{1, \ldots, T\}$ and denoting with $\pi(\mathcal{G}_l)$ the prior distribution induced on $\mathcal{G}_l$ by the hierarchical prior on the PARAFAC marginals in eq. (13), the following proportionality relation holds:

$$
\begin{aligned}
p(\mathcal{G}_l|\mathcal{X}_t, \mathcal{D}_t, \boldsymbol{\Omega}_t, s_t = l, \rho_l) &\propto \prod_{i=1}^{I}\prod_{j=1}^{J}\prod_{k=1}^{K} \exp\left\{-\frac{\omega_{ijk,t}}{2}(\mathbf{z}_t'\mathbf{g}_{ijk,l})^2 + \kappa_{ijk,t}(\mathbf{z}_t'\mathbf{g}_{ijk,l})\right\} p(\omega_{ijk,t})\pi(\mathcal{G}_l) \\
&= \prod_{i=1}^{I}\prod_{j=1}^{J}\prod_{k=1}^{K} \exp\left\{-\frac{1}{2\omega_{ijk,t}^{-1}}\left[(\mathbf{z}_t'\mathbf{g}_{ijk,l})^2 - 2\frac{\kappa_{ijk,t}}{\omega_{ijk,t}}(\mathbf{z}_t'\mathbf{g}_{ijk,l})\right]\right\} p(\omega_{ijk,t})\pi(\mathcal{G}_l) \\
&= \prod_{i=1}^{I}\prod_{j=1}^{J}\prod_{k=1}^{K} \exp\left\{-\frac{1}{2\omega_{ijk,t}^{-1}}\left(\mathbf{z}_t'\mathbf{g}_{ijk,l} - \frac{\kappa_{ijk,t}}{\omega_{ijk,t}}\right)^2\right\} p(\omega_{ijk,t})\pi(\mathcal{G}_l).
\end{aligned}
\tag{D.14}
$$

Define $u_{ijk,t} = \kappa_{ijk,t}/\omega_{ijk,t}$, then we rewrite eq. (D.14) in more compact form as:

$$
\begin{aligned}
&p(\mathcal{G}_l|\mathcal{X}_t, \mathcal{D}_t, \boldsymbol{\Omega}_t, s_t = l, \rho_l) \propto \\
&\propto \exp\left\{-\frac{1}{2}\sum_{i=1}^{I}\sum_{j=1}^{J}\sum_{k=1}^{K}\frac{1}{\omega_{ijk,t}^{-1}}\left(\mathbf{z}_t'\mathbf{g}_{ijk,l} - u_{ijk,t}\right)^2\right\} \cdot \prod_{i=1}^{I}\prod_{j=1}^{J}\prod_{k=1}^{K} p(\omega_{ijk,t}) \cdot \pi(\mathcal{G}_l) \\
&= \exp\left\{-\frac{1}{2}\sum_{i=1}^{I}\left(\mathcal{G}_l \times_4 \mathbf{z}_t - \mathcal{U}_t\right)_i' \operatorname{diag}\left(\boldsymbol{\omega}_{i:,t}\right)\left(\mathcal{G}_l \times_4 \mathbf{z}_t - \mathcal{U}_t\right)_i\right\} \cdot \prod_{i=1}^{I}\prod_{j=1}^{J}\prod_{k=1}^{K} p(\omega_{ijk,t}) \cdot \pi(\mathcal{G}_l) \\
&= \exp\left\{-\frac{1}{2}\left(\operatorname{vec}\left(\mathcal{G}_l \times_4 \mathbf{z}_t\right) - \operatorname{vec}\left(\mathcal{U}_t\right)\right)' \operatorname{diag}\left(\operatorname{vec}\left(\boldsymbol{\Omega}_t\right)\right)\left(\operatorname{vec}\left(\mathcal{G}_l \times_4 \mathbf{z}_t\right) - \operatorname{vec}\left(\mathcal{U}_t\right)\right)\right\} \\
&\cdot \prod_{i=1}^{I}\prod_{j=1}^{J}\prod_{k=1}^{K} p(\omega_{ijk,t}) \cdot \pi(\mathcal{G}_l) \\
&= f\left(\mathcal{G}_l, \mathbf{z}_t, \mathcal{U}_t, \boldsymbol{\Omega}_t\right) \cdot \prod_{i=1}^{I}\prod_{j=1}^{J}\prod_{k=1}^{K} p(\omega_{ijk,t}) \cdot \pi(\mathcal{G}_l)\,,
\end{aligned}
\tag{D.15}
$$

where $f(\cdot)$ is a function which contains the kernel of a multivariate normal distribution with respect to the variable $\operatorname{vec}\left(\mathcal{G}_l \times_4 \mathbf{z}_t\right)$.

Given the proportionality relation conditional on the latent variable s_t, the last step in the manipulation of the likelihood function consists in rewriting the complete data likelihood. Thus, considering eq. (12) and (D.15) we obtain the proportionality relation:

$$
L(\boldsymbol{\mathcal{X}}, \mathcal{D}, \boldsymbol{\Omega}, \mathbf{s}|\boldsymbol{\theta}) = \prod_{l=1}^{L}\prod_{t\in\mathcal{T}_l} p(\mathcal{X}_t, \mathcal{D}_t, \boldsymbol{\Omega}_t, s_t|\boldsymbol{\theta}) \propto \prod_{l=1}^{L}\prod_{t\in\mathcal{T}_l} f\left(\mathcal{G}_{s_t}, \mathbf{z}_t, \mathcal{U}_t, \boldsymbol{\Omega}_t\right)\,. \tag{D.16}
$$

We are now ready to compute the full conditional distributions of each vector $\boldsymbol{\gamma}_{h,l}^{(r)}$, $h = 1, \ldots, 4$, $l = 1, \ldots, L$ and $r = 1, \ldots, R$. To this aim, notice that:

$$\mathcal{G}_l = \sum_{r=1}^{R} \boldsymbol{\gamma}_{1,l}^{(r)} \circ \boldsymbol{\gamma}_{2,l}^{(r)} \circ \boldsymbol{\gamma}_{3,l}^{(r)} \circ \boldsymbol{\gamma}_{4,l}^{(r)} = \mathcal{G}_l^{(r)} + \mathcal{G}_l^{(-r)}\,, \tag{D.17}$$

where we have defined:

$$\mathcal{G}_l^{(r)} = \boldsymbol{\gamma}_{1,l}^{(r)} \circ \boldsymbol{\gamma}_{2,l}^{(r)} \circ \boldsymbol{\gamma}_{3,l}^{(r)} \circ \boldsymbol{\gamma}_{4,l}^{(r)} \tag{D.18a}$$

$$\mathcal{G}_l^{(-r)} = \sum_{\substack{v=1 \\ v \neq r}}^{R} \mathcal{G}_l^{(v)}\,. \tag{D.18b}$$

By exploiting the definitions of mode-n product and PARAFAC decomposition, we obtain:

$$\mathcal{G}_{l,t} = \mathcal{G}_l \times_4 \mathbf{z}_t = \sum_{r=1}^{R} \left(\boldsymbol{\gamma}_{1,l}^{(r)} \circ \boldsymbol{\gamma}_{2,l}^{(r)} \circ \boldsymbol{\gamma}_{3,l}^{(r)} \right) \langle \boldsymbol{\gamma}_{4,l}^{(r)}, \mathbf{z}_t \rangle = \sum_{r=1}^{R} \mathcal{G}_{l,t}^{(r)}\,. \tag{D.19}$$

Here $\langle \cdot, \cdot \rangle$ denotes the standard inner product in the Euclidean space $\mathbb{R}^n$. Since the latter is a scalar, we have that:

$$\overline{\mathbf{g}}_{l,t} = \operatorname{vec}\left(\mathcal{G}_{l,t}\right) = \operatorname{vec}\left(\mathcal{G}_l \times_4 \mathbf{z}_t\right) = \sum_{r=1}^{R} \operatorname{vec}\left(\mathcal{G}_{l,t}^{(r)}\right) = \sum_{r=1}^{R} \overline{\mathbf{g}}_{l,t}^{(r)}\,. \tag{D.20}$$

The vectorisation of a tensor can be expressed in the following way, which is a generalisation of a well known property holding for matrices: it consists in stacking in a column vector all the vectorised slices of the tensor. For the sake of clarity, let $\boldsymbol{\alpha}_1 \in \mathbb{R}^I$, $\boldsymbol{\alpha}_2 \in \mathbb{R}^J$ and $\boldsymbol{\alpha}_3 \in \mathbb{R}^K$ and let the tensor $\mathcal{A} = \boldsymbol{\alpha}_1 \circ \boldsymbol{\alpha}_2 \circ \boldsymbol{\alpha}_3$. Denote $\mathcal{A}_{::k} \in \mathbb{R}^{I \times J}$ the k-th frontal slice of the tensor $\mathcal{A}$. Then, by applying the properties of Kronecker product, $\otimes$, and of the vectorization operator, vec, we obtain[10]:

$$\begin{aligned} \operatorname{vec}(\mathcal{A}) = \operatorname{vec}(\boldsymbol{\alpha}_1 \circ \boldsymbol{\alpha}_2 \circ \boldsymbol{\alpha}_3) &= \left[\operatorname{vec}(\mathcal{A}_{::1})', \ldots, \operatorname{vec}(\mathcal{A}_{::K})'\right]' \\ &= \left[\operatorname{vec}(\boldsymbol{\alpha}_1 \circ \boldsymbol{\alpha}_2)' \alpha_{3,1}, \ldots, \operatorname{vec}(\boldsymbol{\alpha}_1 \circ \boldsymbol{\alpha}_2)' \alpha_{3,K}\right]' \end{aligned}$$

[10]The outer product and Kronecker products are two operators acting on:

$$\begin{aligned} \circ &: \mathbb{R}^{n_1} \times \ldots \times \mathbb{R}^{n_K} \quad \to \mathbb{R}^{n_1 \times \ldots \times n_K} \\ \otimes &: \mathbb{R}^{n_1 \times m_1} \times \mathbb{R}^{n_2 \times m_2} \quad \to \mathbb{R}^{n_1 n_2 \times m_1 m_2}\,. \end{aligned}$$

Notice that the Kronecker product is defined on the space of matrices (and vectors, as a particular case), while the outer product is defined on arrays of possible different number of dimensions (e.g. it is defined between two vectors, and returns a matrix, as well as between a vector and a matrix, yielding a third order tensor). In practice, in the particular case aring when dealing with two vectors $\mathbf{u} \in \mathbb{R}^n$ and $\mathbf{v} \in \mathbb{R}^m$, their outer product and Kronecker product are related and given by, respectively:

$$\begin{aligned} \mathbf{u} \circ \mathbf{v} &= \mathbf{u}\mathbf{v}' \in \mathbb{R}^{n \times m} \\ \mathbf{u} \otimes \mathbf{v} &= \operatorname{vec}\left(\mathbf{v}\mathbf{u}'\right) = \operatorname{vec}(\mathbf{v} \circ \mathbf{u}) \in \mathbb{R}^{nm}\,. \end{aligned}$$

For two matrices $\mathbf{A} \in \mathbb{R}^{m \times n}$ and $\mathbf{B} \in \mathbb{R}^{n \times k}$ it holds:

$$\operatorname{vec}(\mathbf{AB}) = (\mathbf{I}_k \otimes \mathbf{A}) \operatorname{vec}(\mathbf{B}) = (\mathbf{B}' \otimes \mathbf{I}_m) \operatorname{vec}(\mathbf{A}) \in \mathbb{R}^{mk \times 1}\,.$$

Moreover, if $n = 1$ then $\mathbf{B}$ is a row vector of length k, as a consequence $\mathbf{B}' = \operatorname{vec}(\mathbf{B}) \in \mathbb{R}^{k \times 1}$. See (Cichocki et al., 2009, p.31).

$$= \boldsymbol{\alpha}_3 \otimes \text{vec}\left(\boldsymbol{\alpha}_1 \circ \boldsymbol{\alpha}_2\right) = \boldsymbol{\alpha}_3 \otimes \text{vec}\left(\boldsymbol{\alpha}_1 \boldsymbol{\alpha}_2'\right) . \tag{D.21}$$

The use of the same property allows to rewrite eq. (D.21) in three equivalent ways, each one written as a product of a matrix and one of the vectors $\boldsymbol{\alpha}_1, \boldsymbol{\alpha}_2, \boldsymbol{\alpha}_3$, respectively. In fact, we have:

$$\text{vec}\left(\mathcal{A}\right) = \boldsymbol{\alpha}_3 \otimes \text{vec}\left(\boldsymbol{\alpha}_1 \boldsymbol{\alpha}_2'\right) = \boldsymbol{\alpha}_3 \otimes \left(\boldsymbol{\alpha}_2 \otimes \mathbf{I}_I\right) \text{vec}\left(\boldsymbol{\alpha}_1\right) = \left(\boldsymbol{\alpha}_3 \otimes \boldsymbol{\alpha}_2 \otimes \mathbf{I}_I\right) \boldsymbol{\alpha}_1 \tag{D.22}$$

$$\text{vec}\left(\mathcal{A}\right) = \boldsymbol{\alpha}_3 \otimes \text{vec}\left(\boldsymbol{\alpha}_1 \boldsymbol{\alpha}_2'\right) = \boldsymbol{\alpha}_3 \otimes \left[\left(\mathbf{I}_J \otimes \boldsymbol{\alpha}_1\right) \text{vec}\left(\boldsymbol{\alpha}_2'\right)\right] = \left(\boldsymbol{\alpha}_3 \otimes \mathbf{I}_J \otimes \boldsymbol{\alpha}_1\right) \boldsymbol{\alpha}_2 \tag{D.23}$$

$$\begin{aligned} \text{vec}\left(\mathcal{A}\right) &= \boldsymbol{\alpha}_3 \otimes \text{vec}\left(\boldsymbol{\alpha}_1 \boldsymbol{\alpha}_2'\right) = \text{vec}\left(\text{vec}\left(\boldsymbol{\alpha}_1 \boldsymbol{\alpha}_2'\right) \boldsymbol{\alpha}_3'\right) = \left(\mathbf{I}_K \otimes \text{vec}\left(\boldsymbol{\alpha}_1 \boldsymbol{\alpha}_2'\right)\right) \text{vec}\left(\boldsymbol{\alpha}_3'\right) \\ &= \left(\mathbf{I}_K \otimes \text{vec}\left(\boldsymbol{\alpha}_1 \boldsymbol{\alpha}_2'\right)\right) \boldsymbol{\alpha}_3 = \left(\mathbf{I}_K \otimes \boldsymbol{\alpha}_2 \otimes \boldsymbol{\alpha}_1\right) \boldsymbol{\alpha}_3 . \end{aligned} \tag{D.24}$$

The first line represents a product between the matrix $\boldsymbol{\alpha}_3 \otimes \boldsymbol{\alpha}_2 \otimes \mathbf{I}_I \in \mathbb{R}^{IJK \times I}$ and the vector $\boldsymbol{\alpha}_1$, the second is a product between the matrix $\boldsymbol{\alpha}_3 \otimes \mathbf{I}_J \otimes \boldsymbol{\alpha}_1 \in \mathbb{R}^{IJK \times J}$ and the vector $\boldsymbol{\alpha}_2$. Finally, the last row is a product between the matrix $\mathbf{I}_K \otimes \boldsymbol{\alpha}_2 \otimes \boldsymbol{\alpha}_1 \in \mathbb{R}^{IJK \times K}$ and the vector $\boldsymbol{\alpha}_3$.

Starting from eq. (D.20), we can apply for $\boldsymbol{\gamma}_{1,l}^{(r)}, \ldots, \boldsymbol{\gamma}_{3,l}^{(r)}$ the same argument as for $\boldsymbol{\alpha}_1, \ldots, \boldsymbol{\alpha}_3$, with the aim of manipulating the likelihood function and obtain three different expressions where the dependence on $\boldsymbol{\gamma}_{1,l}^{(r)}, \boldsymbol{\gamma}_{2,l}^{(r)}, \boldsymbol{\gamma}_{3,l}^{(r)}$, respectively, is made explicit. This will then be used later on for deriving the posterior full conditional distributions of the PARAFAC marginals. Thus, from eq. (D.20) we have:

$$\overline{\mathbf{g}}_{l,t}^{(r)} = \text{vec}\left(\mathcal{G}_{l,t}^{(r)}\right) = \langle \boldsymbol{\gamma}_{4,l}^{(r)}, \mathbf{z}_t \rangle \, \text{vec}\left(\boldsymbol{\gamma}_{1,l}^{(r)} \circ \boldsymbol{\gamma}_{2,l}^{(r)} \circ \boldsymbol{\gamma}_{3,l}^{(r)}\right) = \text{vec}\left(\boldsymbol{\gamma}_{1,l}^{(r)} \circ \boldsymbol{\gamma}_{2,l}^{(r)} \circ \boldsymbol{\gamma}_{3,l}^{(r)}\right) \mathbf{z}_t' \boldsymbol{\gamma}_{4,l}^{(r)} = \mathbf{A}_4 \boldsymbol{\gamma}_{4,l}^{(r)} , \tag{D.25}$$

where:

$$\mathbf{A}_4 = \text{vec}\left(\boldsymbol{\gamma}_{1,l}^{(r)} \circ \boldsymbol{\gamma}_{2,l}^{(r)} \circ \boldsymbol{\gamma}_{3,l}^{(r)}\right) \mathbf{z}_t' . \tag{D.26}$$

Exploiting eq. (D.22) we have:

$$\overline{\mathbf{g}}_{l,t}^{(r)} = \text{vec}\left(\mathcal{G}_{l,t}^{(r)}\right) = \langle \boldsymbol{\gamma}_{4,l}^{(r)}, \mathbf{z}_t \rangle \left(\boldsymbol{\gamma}_{3,l}^{(r)} \otimes \boldsymbol{\gamma}_{2,l}^{(r)} \otimes \mathbf{I}_I\right) \boldsymbol{\gamma}_{1,l}^{(r)} = \mathbf{A}_1 \boldsymbol{\gamma}_{1,l}^{(r)} , \tag{D.27}$$

with:

$$\mathbf{A}_1 = \langle \boldsymbol{\gamma}_{4,l}^{(r)}, \mathbf{z}_t \rangle \left(\boldsymbol{\gamma}_{3,l}^{(r)} \otimes \boldsymbol{\gamma}_{2,l}^{(r)} \otimes \mathbf{I}_I\right) . \tag{D.28}$$

Exploiting eq. (D.23) we have:

$$\overline{\mathbf{g}}_{l,t}^{(r)} = \text{vec}\left(\mathcal{G}_{l,t}^{(r)}\right) = \langle \boldsymbol{\gamma}_{4,l}^{(r)}, \mathbf{z}_t \rangle \left(\boldsymbol{\gamma}_{3,l}^{(r)} \otimes \mathbf{I}_J \otimes \boldsymbol{\gamma}_{1,l}^{(r)}\right) \boldsymbol{\gamma}_{2,l}^{(r)} = \mathbf{A}_2 \boldsymbol{\gamma}_{2,l}^{(r)} , \tag{D.29}$$

with:

$$\mathbf{A}_2 = \langle \boldsymbol{\gamma}_{4,l}^{(r)}, \mathbf{z}_t \rangle \left(\boldsymbol{\gamma}_{3,l}^{(r)} \otimes \mathbf{I}_J \otimes \boldsymbol{\gamma}_{1,l}^{(r)}\right) . \tag{D.30}$$

Finally, using eq. (D.24) we obtain:

$$\overline{\mathbf{g}}_{l,t}^{(r)} = \text{vec}\left(\mathcal{G}_{l,t}^{(r)}\right) = \langle \boldsymbol{\gamma}_{4,l}^{(r)}, \mathbf{z}_t \rangle \left(\mathbf{I}_K \otimes \boldsymbol{\gamma}_{2,l}^{(r)} \otimes \boldsymbol{\gamma}_{1,l}^{(r)}\right) \boldsymbol{\gamma}_{3,l}^{(r)} = \mathbf{A}_3 \boldsymbol{\gamma}_{3,l}^{(r)} , \tag{D.31}$$

with:

$$\mathbf{A}_3 = \langle \boldsymbol{\gamma}_{4,l}^{(r)}, \mathbf{z}_t \rangle \left(\mathbf{I}_K \otimes \boldsymbol{\gamma}_{2,l}^{(r)} \otimes \boldsymbol{\gamma}_{1,l}^{(r)}\right) . \tag{D.32}$$

By using the definition of $f(\mathcal{G}_l, \mathbf{z}_t, \mathcal{U}_t^{(l)}, \boldsymbol{\Omega}_t)$, eq. (D.20) and the notation of eq. (D.17) we can thus write:

$$\text{vec}\left(\mathcal{G}_l \times_4 \mathbf{z}_t\right) = \overline{\mathbf{g}}_{l,t}^{(r)} + \sum_{\substack{v=1 \\ v \neq r}}^{R} \overline{\mathbf{g}}_{l,t}^{(v)} = \overline{\mathbf{g}}_{l,t}^{(r)} + \overline{\mathbf{g}}_{l,t}^{(-r)} . \tag{D.33}$$

From eq. (D.16), by focusing on regime $l \in \{1, \dots, L\}$, we get:

$$
\begin{aligned}
&L(\boldsymbol{\mathcal{X}}, \mathcal{D}, \boldsymbol{\Omega}, \mathbf{s}|\boldsymbol{\theta}) \propto \\
&\propto \exp\left\{-\frac{1}{2}\left(\text{vec}\left(\mathcal{G}_l \times_4 \mathbf{z}_t\right) - \text{vec}\left(\mathcal{U}_t\right)\right)' \text{diag}\left(\text{vec}\left(\boldsymbol{\Omega}_t\right)\right)\left(\text{vec}\left(\mathcal{G}_l \times_4 \mathbf{z}_t\right) - \text{vec}\left(\mathcal{U}_t\right)\right)\right\} \\
&= \exp\left\{-\frac{1}{2}\left(\overline{\mathbf{g}}_{l,t}^{(r)} + \overline{\mathbf{g}}_{l,t}^{(-r)} - \mathbf{u}_t\right)' \overline{\overline{\boldsymbol{\Omega}}}_t \left(\overline{\mathbf{g}}_{l,t}^{(r)} + \overline{\mathbf{g}}_{l,t}^{(-r)} - \mathbf{u}_t\right)\right\}
\end{aligned} \tag{D.34}
$$

where, for reducing the burden of notation, we have defined:

$$
\mathbf{u}_t = \text{vec}\left(\mathcal{U}_t\right) \tag{D.35}
$$

$$
\overline{\overline{\boldsymbol{\Omega}}}_t = \text{diag}\left(\text{vec}\left(\boldsymbol{\Omega}_t\right)\right) . \tag{D.36}
$$

We can now single out a specific component $\mathcal{G}_l^{(r)}$ of the PARAFAC decomposition of the tensor $\mathcal{G}$, which is incorporated in $\overline{\mathbf{g}}_{l,t}^{(r)}$. In fact, we can manipulate the function in eq. (D.34) with the aim of finding a proportionality relation, as follows:

$$
\begin{aligned}
L(\boldsymbol{\mathcal{X}}, \mathcal{D}, \boldsymbol{\Omega}, \mathbf{s}|\boldsymbol{\theta}) \propto \prod_{t \in \mathcal{T}_l} \exp\Bigg\{-\frac{1}{2}\Bigg[&\overline{\mathbf{g}}_{l,t}^{(r)\prime} \overline{\overline{\boldsymbol{\Omega}}}_t \overline{\mathbf{g}}_{l,t}^{(r)} + \mathbf{g}_{l,t}^{(r)\prime} \overline{\overline{\boldsymbol{\Omega}}}_t (\overline{\mathbf{g}}_{l,t}^{(-r)} - \mathbf{u}_t) \\
&+ (\overline{\mathbf{g}}_{l,t}^{(-r)} - \mathbf{u}_t)' \overline{\overline{\boldsymbol{\Omega}}}_t \overline{\mathbf{g}}_{l,t}^{(r)} + (\overline{\mathbf{g}}_{l,t}^{(-r)} - \mathbf{u}_t)' \overline{\overline{\boldsymbol{\Omega}}}_t (\overline{\mathbf{g}}_{l,t}^{(-r)} - \mathbf{u}_t)\Bigg]\Bigg\} \\
\propto \prod_{t \in \mathcal{T}_l} \exp\left\{-\frac{1}{2}\left[\overline{\mathbf{g}}_{l,t}^{(r)\prime} \overline{\overline{\boldsymbol{\Omega}}}_t \overline{\mathbf{g}}_{l,t}^{(r)} - 2(\mathbf{u}_t - \overline{\mathbf{g}}_{l,t}^{(-r)})' \overline{\overline{\boldsymbol{\Omega}}}_t \overline{\mathbf{g}}_{l,t}^{(r)}\right]\right\} .
\end{aligned} \tag{D.37}
$$

D.6.1 Full conditional distribution of $\boldsymbol{\gamma}_{1,l}^{(r)}$

The full conditional distribution of $\boldsymbol{\gamma}_{1,l}^{(r)}$ is given by:

$$
p(\boldsymbol{\gamma}_{1,l}^{(r)}|\boldsymbol{\mathcal{X}}, \mathcal{D}, \boldsymbol{\Omega}, \mathbf{s}, \boldsymbol{\gamma}_{2,l}^{(r)}, \boldsymbol{\gamma}_{3,l}^{(r)}, \boldsymbol{\gamma}_{4,l}^{(r)}, \mathcal{G}_l^{(-r)}, w_{1,r}, \phi_r, \tau) \sim \mathcal{N}_I(\tilde{\boldsymbol{\zeta}}_{1,l}^{r}, \tilde{\boldsymbol{\Lambda}}_{1,l}^{r}) \tag{D.38}
$$

where:

$$
\tilde{\boldsymbol{\Lambda}}_{1,l}^{r} = \left[\left(\tau \phi_r w_{1,r} \mathbf{I}_I\right)^{-1} + \sum_{t \in \mathcal{T}_l} \left(\overline{\overline{\boldsymbol{\Sigma}}}_{1,l,t}^{(r)}\right)^{-1}\right]^{-1} \tag{D.39a}
$$

$$
\tilde{\boldsymbol{\zeta}}_{1,l}^{r} = \tilde{\boldsymbol{\Lambda}}_{1,l}^{r'} \left[\overline{\boldsymbol{\zeta}}_{1,l}^{r'} \left(\tau \phi_r w_{1,r} \mathbf{I}_I\right)^{-1} + \sum_{t \in \mathcal{T}_l} \overline{\boldsymbol{\mu}}_{1,l,t}^{(r)\prime} \left(\overline{\overline{\boldsymbol{\Sigma}}}_{1,l,t}^{(r)}\right)^{-1}\right]' . \tag{D.39b}
$$

By exploiting the rightmost term in the equality chain in eq. (D.27), we can simplify the two addenda in eq. (D.37) as:

$$
\begin{aligned}
\overline{\mathbf{g}}_{l,t}^{(r)\prime} \overline{\overline{\boldsymbol{\Omega}}}_t \overline{\mathbf{g}}_{l,t}^{(r)} &= \left(\mathbf{A}_1 \boldsymbol{\gamma}_{1,l}^{(r)}\right)' \overline{\overline{\boldsymbol{\Omega}}}_t \left(\mathbf{A}_1 \boldsymbol{\gamma}_{1,l}^{(r)}\right) \\
&= \langle \boldsymbol{\gamma}_{4,l}^{(r)}, \mathbf{z}_t \rangle \boldsymbol{\gamma}_{1,l}^{(r)\prime} \left(\boldsymbol{\gamma}_{3,l}^{(r)} \otimes \boldsymbol{\gamma}_{2,l}^{(r)} \otimes \mathbf{I}_I\right)' \overline{\overline{\boldsymbol{\Omega}}}_t \left(\boldsymbol{\gamma}_{3,l}^{(r)} \otimes \boldsymbol{\gamma}_{2,l}^{(r)} \otimes \mathbf{I}_I\right) \boldsymbol{\gamma}_{1,l}^{(r)} \langle \boldsymbol{\gamma}_{4,l}^{(r)}, \mathbf{z}_t \rangle \\
&= \boldsymbol{\gamma}_{1,l}^{(r)\prime} \left[\left(\boldsymbol{\gamma}_{3,l}^{(r)\prime} \otimes \boldsymbol{\gamma}_{2,l}^{(r)\prime} \otimes \mathbf{I}_I'\right) \overline{\overline{\boldsymbol{\Omega}}}_t \left(\boldsymbol{\gamma}_{3,l}^{(r)} \otimes \boldsymbol{\gamma}_{2,l}^{(r)} \otimes \mathbf{I}_I\right) (\langle \boldsymbol{\gamma}_{4,l}^{(r)}, \mathbf{z}_t \rangle)^2\right] \boldsymbol{\gamma}_{1,l}^{(r)}
\end{aligned}
$$

$$= \boldsymbol{\gamma}_{1,l}^{(r)\prime} \left(\overline{\overline{\boldsymbol{\Sigma}}}_{1,l,t}^{(r)} \right)^{-1} \boldsymbol{\gamma}_{1,l}^{(r)} . \tag{D.40}$$

and

$$\begin{aligned} -2(\mathbf{u}_t - \overline{\mathbf{g}}_{l,t}^{(-r)})' \overline{\overline{\boldsymbol{\Omega}}}_t \overline{\mathbf{g}}_{l,t}^{(r)} &= -2(\mathbf{u}_t - \overline{\mathbf{g}}_{l,t}^{(-r)})' \overline{\overline{\boldsymbol{\Omega}}}_t \left(\boldsymbol{\gamma}_{3,l}^{(r)} \otimes \boldsymbol{\gamma}_{2,l}^{(r)} \otimes \mathbf{I}_I \right) \boldsymbol{\gamma}_{1,l}^{(r)} \langle \boldsymbol{\gamma}_{4,l}^{(r)}, \mathbf{z}_t \rangle \\ &= -2\langle \boldsymbol{\gamma}_{4,l}^{(r)}, \mathbf{z}_t \rangle (\mathbf{u}_t - \overline{\mathbf{g}}_{l,t}^{(-r)})' \overline{\overline{\boldsymbol{\Omega}}}_t \left(\boldsymbol{\gamma}_{3,l}^{(r)} \otimes \boldsymbol{\gamma}_{2,l}^{(r)} \otimes \mathbf{I}_I \right) \boldsymbol{\gamma}_{1,l}^{(r)} \\ &= -2\overline{\boldsymbol{\mu}}_{1,l,t}^{(r)\prime} \left(\overline{\overline{\boldsymbol{\Sigma}}}_{1,l,t}^{(r)} \right)^{-1} \boldsymbol{\gamma}_{1,l}^{(r)} . \end{aligned} \tag{D.41}$$

Now, by applying Bayes' rule and plugging eq. (D.40) and eq. (D.41) into eq. (D.37) we get:

$$\begin{aligned} p(\boldsymbol{\gamma}_{1,l}^{(r)}|-) &\propto L(\boldsymbol{\mathcal{X}}, \mathcal{D}, \boldsymbol{\Omega}, \mathbf{s}|\boldsymbol{\theta}) \pi(\boldsymbol{\gamma}_{1,l}^{(r)}|\mathbf{w}_{1,:}, \boldsymbol{\phi}, \tau) \\ &\propto \prod_{t \in \mathcal{T}_l} \exp\left\{ -\frac{1}{2} \left[\boldsymbol{\gamma}_{1,l}^{(r)\prime} \left(\overline{\overline{\boldsymbol{\Sigma}}}_{1,l,t}^{(r)} \right)^{-1} \boldsymbol{\gamma}_{1,l}^{(r)} - 2\overline{\boldsymbol{\mu}}_{1,l,t}^{(r)\prime} \left(\overline{\overline{\boldsymbol{\Sigma}}}_{1,l,t}^{(r)} \right)^{-1} \boldsymbol{\gamma}_{1,l}^{(r)} \right] \right\} \\ &\cdot \exp\left\{ -\frac{1}{2} \left[\boldsymbol{\gamma}_{1,l}^{(r)\prime} \left(\overline{\boldsymbol{\Lambda}}_{1,l}^{r} \right)^{-1} \boldsymbol{\gamma}_{1,l}^{(r)} - 2\overline{\boldsymbol{\zeta}}_{1,l}^{r\prime} \left(\overline{\boldsymbol{\Lambda}}_{1,l}^{r} \right)^{-1} \boldsymbol{\gamma}_{1,l}^{(r)} \right] \right\} \\ &= \exp\Bigg\{ -\frac{1}{2} \Bigg[\sum_{t \in \mathcal{T}_l} \left(\boldsymbol{\gamma}_{1,l}^{(r)\prime} \left(\overline{\overline{\boldsymbol{\Sigma}}}_{1,l,t}^{(r)} \right)^{-1} \boldsymbol{\gamma}_{1,l}^{(r)} - 2\overline{\boldsymbol{\mu}}_{1,l,t}^{(r)\prime} \left(\overline{\overline{\boldsymbol{\Sigma}}}_{1,l,t}^{(r)} \right)^{-1} \boldsymbol{\gamma}_{1,l}^{(r)} \right) \\ &+ \left(\boldsymbol{\gamma}_{1,l}^{(r)\prime} \left(\overline{\boldsymbol{\Lambda}}_{1,l}^{r} \right)^{-1} \boldsymbol{\gamma}_{1,l}^{(r)} - 2\overline{\boldsymbol{\zeta}}_{1,l}^{r\prime} \left(\overline{\boldsymbol{\Lambda}}_{1,l}^{r} \right)^{-1} \boldsymbol{\gamma}_{1,l}^{(r)} \right) \Bigg] \Bigg\} \\ &= \exp\Bigg\{ -\frac{1}{2} \Bigg[\boldsymbol{\gamma}_{1,l}^{(r)\prime} \left(\sum_{t \in \mathcal{T}_l} \left(\overline{\overline{\boldsymbol{\Sigma}}}_{1,l,t}^{(r)} \right)^{-1} \right) \boldsymbol{\gamma}_{1,l}^{(r)} - 2 \left(\sum_{t \in \mathcal{T}_l} \overline{\boldsymbol{\mu}}_{1,l,t}^{(r)\prime} \left(\overline{\overline{\boldsymbol{\Sigma}}}_{1,l,t}^{(r)} \right)^{-1} \right) \boldsymbol{\gamma}_{1,l}^{(r)} \\ &+ \boldsymbol{\gamma}_{1,l}^{(r)\prime} \left(\overline{\boldsymbol{\Lambda}}_{1,l}^{r} \right)^{-1} \boldsymbol{\gamma}_{1,l}^{(r)} - 2\overline{\boldsymbol{\zeta}}_{1,l}^{r\prime} \left(\overline{\boldsymbol{\Lambda}}_{1,l}^{r} \right)^{-1} \boldsymbol{\gamma}_{1,l}^{(r)} \Bigg] \Bigg\} \\ &= \exp\Bigg\{ -\frac{1}{2} \Bigg[\boldsymbol{\gamma}_{1,l}^{(r)\prime} \left(\left(\overline{\boldsymbol{\Lambda}}_{1,l}^{r} \right)^{-1} + \sum_{t \in \mathcal{T}_l} \left(\overline{\overline{\boldsymbol{\Sigma}}}_{1,l,t}^{(r)} \right)^{-1} \right) \boldsymbol{\gamma}_{1,l}^{(r)} \\ &- 2 \left(\overline{\boldsymbol{\zeta}}_{1,l}^{r\prime} \left(\overline{\boldsymbol{\Lambda}}_{1,l}^{r} \right)^{-1} + \sum_{t \in \mathcal{T}_l} \overline{\boldsymbol{\mu}}_{1,l,t}^{(r)\prime} \left(\overline{\overline{\boldsymbol{\Sigma}}}_{1,l,t}^{(r)} \right)^{-1} \right) \boldsymbol{\gamma}_{1,l}^{(r)} \Bigg] \Bigg\} . \end{aligned} \tag{D.42}$$

This is the kernel of a multivariate normal distribution with parameters:

$$\tilde{\boldsymbol{\Lambda}}_{1,l}^{r} = \left[\left(\tau \phi_r w_{1,r} \mathbf{I}_I \right)^{-1} + \sum_{t \in \mathcal{T}_l} \left(\overline{\overline{\boldsymbol{\Sigma}}}_{1,l,t}^{(r)} \right)^{-1} \right]^{-1} \tag{D.43a}$$

$$\tilde{\boldsymbol{\zeta}}_{1,l}^{r} = \tilde{\boldsymbol{\Lambda}}_{1,l}^{r\prime} \left[\overline{\boldsymbol{\zeta}}_{1,l}^{r\prime} \left(\tau \phi_r w_{1,r} \mathbf{I}_I \right)^{-1} + \sum_{t \in \mathcal{T}_l} \overline{\boldsymbol{\mu}}_{1,l,t}^{(r)\prime} \left(\overline{\overline{\boldsymbol{\Sigma}}}_{1,l,t}^{(r)} \right)^{-1} \right]' . \tag{D.43b}$$

D.6.2 Full conditional distribution of $\boldsymbol{\gamma}_{2,l}^{(r)}$

The full conditional distribution of $\boldsymbol{\gamma}_{2,l}^{(r)}$ is given by:

$$p(\boldsymbol{\gamma}_{2,l}^{(r)}|\boldsymbol{\mathcal{X}}, \mathcal{D}, \boldsymbol{\Omega}, \mathbf{s}, \boldsymbol{\gamma}_{1,l}^{(r)}, \boldsymbol{\gamma}_{3,l}^{(r)}, \boldsymbol{\gamma}_{4,l}^{(r)}, \mathcal{G}_l^{(-r)}, w_{2,r}, \phi_r, \tau) \sim \mathcal{N}_J(\tilde{\boldsymbol{\zeta}}_{2,l}^{r}, \tilde{\boldsymbol{\Lambda}}_{2,l}^{r}) \tag{D.44}$$

where:

$$\tilde{\mathbf{\Lambda}}_{2,l}^{\,r} = \left[\left(\tau\phi_r w_{2,r}\mathbf{I}_J\right)^{-1} + \sum_{t\in\mathcal{T}_l} \left(\overline{\overline{\mathbf{\Sigma}}}_{2,l,t}^{(r)}\right)^{-1} \right]^{-1} \tag{D.45a}$$

$$\tilde{\boldsymbol{\zeta}}_{2,l}^{r} = \tilde{\mathbf{\Lambda}}_{2,l}^{\,r'} \left[\overline{\boldsymbol{\zeta}}_{2,l}^{r'} \left(\tau\phi_r w_{2,r}\mathbf{I}_J\right)^{-1} + \sum_{t\in\mathcal{T}_l} \overline{\boldsymbol{\mu}}_{2,l,t}^{(r)\prime} \left(\overline{\overline{\mathbf{\Sigma}}}_{2,l,t}^{(r)}\right)^{-1} \right]' . \tag{D.45b}$$

By exploiting the central term in the equality chain in eq. (D.29), we can simplify the two addenda in eq. (D.37) as:

$$\begin{aligned}
\overline{\mathbf{g}}_{l,t}^{(r)\prime}\overline{\overline{\mathbf{\Omega}}}_t\overline{\mathbf{g}}_{l,t}^{(r)} &= \left(\mathbf{A}_2\boldsymbol{\gamma}_{2,l}^{(r)}\right)'\overline{\overline{\mathbf{\Omega}}}_t\left(\mathbf{A}_2\boldsymbol{\gamma}_{2,l}^{(r)}\right) \\
&= \langle\boldsymbol{\gamma}_{4,l}^{(r)},\mathbf{z}_t\rangle\boldsymbol{\gamma}_{2,l}^{(r)\prime}\left(\boldsymbol{\gamma}_{3,l}^{(r)}\otimes\mathbf{I}_J\otimes\boldsymbol{\gamma}_{1,l}^{(r)}\right)'\overline{\overline{\mathbf{\Omega}}}_t\left(\boldsymbol{\gamma}_{3,l}^{(r)}\otimes\mathbf{I}_J\otimes\boldsymbol{\gamma}_{1,l}^{(r)}\right)\boldsymbol{\gamma}_{2,l}^{(r)}\langle\boldsymbol{\gamma}_{4,l}^{(r)},\mathbf{z}_t\rangle \\
&= \boldsymbol{\gamma}_{2,l}^{(r)\prime}\left[\left(\boldsymbol{\gamma}_{3,l}^{(r)\prime}\otimes\mathbf{I}_J'\otimes\boldsymbol{\gamma}_{1,l}^{(r)\prime}\right)\overline{\overline{\mathbf{\Omega}}}_t\left(\boldsymbol{\gamma}_{3,l}^{(r)}\otimes\mathbf{I}_J\otimes\boldsymbol{\gamma}_{1,l}^{(r)}\right)\left(\langle\boldsymbol{\gamma}_{4,l}^{(r)},\mathbf{z}_t\rangle\right)^2\right]\boldsymbol{\gamma}_{2,l}^{(r)} \\
&= \boldsymbol{\gamma}_{2,l}^{(r)\prime}\left(\overline{\overline{\mathbf{\Sigma}}}_{2,l,t}^{(r)}\right)^{-1}\boldsymbol{\gamma}_{2,l}^{(r)} .
\end{aligned} \tag{D.46}$$

and

$$\begin{aligned}
-2(\mathbf{u}_t-\overline{\mathbf{g}}_{l,t}^{(-r)})'\overline{\overline{\mathbf{\Omega}}}_t\overline{\mathbf{g}}_{l,t}^{(r)} &= -2(\mathbf{u}_t-\mathbf{g}_{l,t}^{(-r)})'\overline{\overline{\mathbf{\Omega}}}_t\langle\boldsymbol{\gamma}_{4,l}^{(r)},\mathbf{z}_t\rangle\left(\boldsymbol{\gamma}_{3,l}^{(r)}\otimes\mathbf{I}_J\otimes\boldsymbol{\gamma}_{1,l}^{(r)}\right)\boldsymbol{\gamma}_{2,l}^{(r)} \\
&= -2\langle\boldsymbol{\gamma}_{4,l}^{(r)},\mathbf{z}_t\rangle(\mathbf{u}_t-\overline{\mathbf{g}}_{l,t}^{(-r)})'\overline{\overline{\mathbf{\Omega}}}_t\left(\boldsymbol{\gamma}_{3,l}^{(r)}\otimes\mathbf{I}_J\otimes\boldsymbol{\gamma}_{1,l}^{(r)}\right)\boldsymbol{\gamma}_{2,l}^{(r)} \\
&= -2\overline{\boldsymbol{\mu}}_{2,l,t}^{(r)\prime}\left(\overline{\overline{\mathbf{\Sigma}}}_{2,l,t}^{(r)}\right)^{-1}\boldsymbol{\gamma}_{2,l}^{(r)} .
\end{aligned} \tag{D.47}$$

Now, by applying Bayes' rule and plugging eq. (D.46) and eq. (D.47) into eq. (D.37) we get:

$$\begin{aligned}
p(\boldsymbol{\gamma}_{2,l}^{(r)}|-) &\propto L(\boldsymbol{\mathcal{X}},\mathcal{D},\mathbf{\Omega},\mathbf{s}|\boldsymbol{\theta})\pi(\boldsymbol{\gamma}_{2,l}^{(r)}|\mathbf{w}_{2,:},\boldsymbol{\phi},\tau) \\
&\propto \prod_{t\in\mathcal{T}_l}\exp\left\{-\frac{1}{2}\left[\boldsymbol{\gamma}_{2,l}^{(r)\prime}\left(\overline{\overline{\mathbf{\Sigma}}}_{2,l,t}^{(r)}\right)^{-1}\boldsymbol{\gamma}_{2,l}^{(r)} - 2\overline{\boldsymbol{\mu}}_{2,l,t}^{(r)\prime}\left(\overline{\overline{\mathbf{\Sigma}}}_{2,l,t}^{(r)}\right)^{-1}\boldsymbol{\gamma}_{2,l}^{(r)}\right]\right\} \\
&\cdot\exp\left\{-\frac{1}{2}\left[\boldsymbol{\gamma}_{2,l}^{(r)\prime}\left(\overline{\mathbf{\Lambda}}_{2,l}^{r}\right)^{-1}\boldsymbol{\gamma}_{2,l}^{(r)} - 2\overline{\boldsymbol{\zeta}}_{2,l}^{r\prime}\left(\overline{\mathbf{\Lambda}}_{2,l}^{r}\right)^{-1}\boldsymbol{\gamma}_{2,l}^{(r)}\right]\right\} \\
&= \exp\Bigg\{-\frac{1}{2}\Bigg[\sum_{t\in\mathcal{T}_l}\left(\boldsymbol{\gamma}_{2,l}^{(r)\prime}\left(\overline{\overline{\mathbf{\Sigma}}}_{2,l,t}^{(r)}\right)^{-1}\boldsymbol{\gamma}_{2,l}^{(r)} - 2\overline{\boldsymbol{\mu}}_{2,l,t}^{(r)\prime}\left(\overline{\overline{\mathbf{\Sigma}}}_{2,l,t}^{(r)}\right)^{-1}\boldsymbol{\gamma}_{2,l}^{(r)}\right) \\
&+ \left(\boldsymbol{\gamma}_{2,l}^{(r)\prime}\left(\overline{\mathbf{\Lambda}}_{2,l}^{r}\right)^{-1}\boldsymbol{\gamma}_{2,l}^{(r)} - 2\overline{\boldsymbol{\zeta}}_{2,l}^{r\prime}\left(\overline{\mathbf{\Lambda}}_{2,l}^{r}\right)^{-1}\boldsymbol{\gamma}_{2,l}^{(r)}\right)\Bigg]\Bigg\} \\
&= \exp\Bigg\{-\frac{1}{2}\Bigg[\boldsymbol{\gamma}_{2,l}^{(r)\prime}\left(\sum_{t\in\mathcal{T}_l}\left(\overline{\overline{\mathbf{\Sigma}}}_{2,l,t}^{(r)}\right)^{-1}\right)\boldsymbol{\gamma}_{2,l}^{(r)} - 2\left(\sum_{t\in\mathcal{T}_l}\overline{\boldsymbol{\mu}}_{2,l,t}^{(r)\prime}\left(\overline{\overline{\mathbf{\Sigma}}}_{2,l,t}^{(r)}\right)^{-1}\right)\boldsymbol{\gamma}_{2,l}^{(r)} \\
&+ \boldsymbol{\gamma}_{2,l}^{(r)\prime}\left(\overline{\mathbf{\Lambda}}_{2,l}^{r}\right)^{-1}\boldsymbol{\gamma}_{2,l}^{(r)} - 2\overline{\boldsymbol{\zeta}}_{2,l}^{r\prime}\left(\overline{\mathbf{\Lambda}}_{2,l}^{r}\right)^{-1}\boldsymbol{\gamma}_{2,l}^{(r)}\Bigg]\Bigg\} \\
&= \exp\Bigg\{-\frac{1}{2}\Bigg[\boldsymbol{\gamma}_{2,l}^{(r)\prime}\left(\left(\overline{\mathbf{\Lambda}}_{2,l}^{r}\right)^{-1} + \sum_{t\in\mathcal{T}_l}\left(\overline{\overline{\mathbf{\Sigma}}}_{2,l,t}^{(r)}\right)^{-1}\right)\boldsymbol{\gamma}_{2,l}^{(r)}
\end{aligned}$$

$$- 2 \left(\overline{\boldsymbol{\zeta}}_{2,l}^{r'} \left(\overline{\boldsymbol{\Lambda}}_{2,l}^{r} \right)^{-1} + \sum_{t \in \mathcal{T}_l} \overline{\boldsymbol{\mu}}_{2,l,t}^{(r)'} \left(\overline{\overline{\boldsymbol{\Sigma}}}_{2,l,t}^{(r)} \right)^{-1} \right) \boldsymbol{\gamma}_{2,l}^{(r)} \Bigg] \Bigg\} . \tag{D.48}$$

This is the kernel of a multivariate normal distribution with parameters:

$$\tilde{\boldsymbol{\Lambda}}_{2,l}^{r} = \left[\left(\tau \phi_r w_{2,r} \mathbf{I}_J \right)^{-1} + \sum_{t \in \mathcal{T}_l} \left(\overline{\overline{\boldsymbol{\Sigma}}}_{2,l,t}^{(r)} \right)^{-1} \right]^{-1} \tag{D.49a}$$

$$\tilde{\boldsymbol{\zeta}}_{2,l}^{r} = \tilde{\boldsymbol{\Lambda}}_{2,l}^{r'} \left[\overline{\boldsymbol{\zeta}}_{2,l}^{r'} \left(\tau \phi_r w_{2,r} \mathbf{I}_J \right)^{-1} + \sum_{t \in \mathcal{T}_l} \overline{\boldsymbol{\mu}}_{2,l,t}^{(r)'} \left(\overline{\overline{\boldsymbol{\Sigma}}}_{2,l,t}^{(r)} \right)^{-1} \right]' . \tag{D.49b}$$

D.6.3 Full conditional distribution of $\boldsymbol{\gamma}_{3,l}^{(r)}$

The full conditional distribution of $\boldsymbol{\gamma}_{3,l}^{(r)}$ is given by:

$$p(\boldsymbol{\gamma}_{3,l}^{(r)} | \boldsymbol{\mathcal{X}}, \mathcal{D}, \boldsymbol{\Omega}, \mathbf{s}, \boldsymbol{\gamma}_{1,l}^{(r)}, \boldsymbol{\gamma}_{2,l}^{(r)}, \boldsymbol{\gamma}_{4,l}^{(r)}, \mathcal{G}_l^{(-r)}, w_{3,r}, \phi_r, \tau) \sim \mathcal{N}_K(\tilde{\boldsymbol{\zeta}}_{3,l}^{r}, \tilde{\boldsymbol{\Lambda}}_{3,l}^{r}) \tag{D.50}$$

where:

$$\tilde{\boldsymbol{\Lambda}}_{3,l}^{r} = \left[\left(\tau \phi_r w_{3,r} \mathbf{I}_K \right)^{-1} + \sum_{t \in \mathcal{T}_l} \left(\overline{\overline{\boldsymbol{\Sigma}}}_{3,l,t}^{(r)} \right)^{-1} \right]^{-1} \tag{D.51a}$$

$$\tilde{\boldsymbol{\zeta}}_{3,l}^{r} = \tilde{\boldsymbol{\Lambda}}_{3,l}^{r'} \left[\overline{\boldsymbol{\zeta}}_{3,l}^{r'} \left(\tau \phi_r w_{3,r} \mathbf{I}_K \right)^{-1} + \sum_{t \in \mathcal{T}_l} \overline{\boldsymbol{\mu}}_{3,l,t}^{(r)'} \left(\overline{\overline{\boldsymbol{\Sigma}}}_{3,l,t}^{(r)} \right)^{-1} \right]' . \tag{D.51b}$$

By exploiting the rightmost term in the equality chain in eq. (D.31), we can simplify the two addenda in eq. (D.37) as:

$$\begin{aligned}
\overline{\mathbf{g}}_{l,t}^{(r)'} \overline{\overline{\boldsymbol{\Omega}}}_t \overline{\mathbf{g}}_{l,t}^{(r)} &= \left(\mathbf{A}_3 \boldsymbol{\gamma}_{3,l}^{(r)} \right)' \overline{\overline{\boldsymbol{\Omega}}}_t \left(\mathbf{A}_3 \boldsymbol{\gamma}_{3,l}^{(r)} \right) \\
&= \langle \boldsymbol{\gamma}_{4,l}^{(r)}, \mathbf{z}_t \rangle \boldsymbol{\gamma}_{3,l}^{(r)'} \left(\mathbf{I}_K \otimes \boldsymbol{\gamma}_{2,l}^{(r)} \otimes \boldsymbol{\gamma}_{1,l}^{(r)} \right)' \overline{\overline{\boldsymbol{\Omega}}}_t \left(\mathbf{I}_K \otimes \boldsymbol{\gamma}_{2,l}^{(r)} \otimes \boldsymbol{\gamma}_{1,l}^{(r)} \right) \boldsymbol{\gamma}_{3,l}^{(r)} \langle \boldsymbol{\gamma}_{4,l}^{(r)}, \mathbf{z}_t \rangle \\
&= \boldsymbol{\gamma}_{3,l}^{(r)'} \left[\left(\mathbf{I}_K' \otimes \boldsymbol{\gamma}_{2,l}^{(r)'} \otimes \boldsymbol{\gamma}_{1,l}^{(r)'} \right) \overline{\overline{\boldsymbol{\Omega}}}_t \left(\mathbf{I}_K \otimes \boldsymbol{\gamma}_{2,l}^{(r)} \otimes \boldsymbol{\gamma}_{1,l}^{(r)} \right) \left(\langle \boldsymbol{\gamma}_{4,l}^{(r)}, \mathbf{z}_t \rangle \right)^2 \right] \boldsymbol{\gamma}_{3,l}^{(r)} \\
&= \boldsymbol{\gamma}_{3,l}^{(r)'} \left(\overline{\overline{\boldsymbol{\Sigma}}}_{3,l,t}^{(r)} \right)^{-1} \boldsymbol{\gamma}_{3,l}^{(r)} .
\end{aligned} \tag{D.52}$$

and

$$\begin{aligned}
-2(\mathbf{u}_t - \overline{\mathbf{g}}_{l,t}^{(-r)})' \overline{\overline{\boldsymbol{\Omega}}}_t \overline{\mathbf{g}}_{l,t}^{(r)} &= -2(\mathbf{u}_t - \overline{\mathbf{g}}_{l,t}^{(-r)})' \overline{\overline{\boldsymbol{\Omega}}}_t \left(\mathbf{I}_K \otimes \boldsymbol{\gamma}_{2,l}^{(r)} \otimes \boldsymbol{\gamma}_{1,l}^{(r)} \right) \boldsymbol{\gamma}_{3,l}^{(r)} \langle \boldsymbol{\gamma}_{4,l}^{(r)}, \mathbf{z}_t \rangle \\
&= -2 \langle \boldsymbol{\gamma}_{4,l}^{(r)}, \mathbf{z}_t \rangle (\mathbf{u}_t - \overline{\mathbf{g}}_{l,t}^{(-r)})' \overline{\overline{\boldsymbol{\Omega}}}_t \left(\mathbf{I}_K \otimes \boldsymbol{\gamma}_{2,l}^{(r)} \otimes \boldsymbol{\gamma}_{1,l}^{(r)} \right) \boldsymbol{\gamma}_{3,l}^{(r)} \\
&= -2 \overline{\boldsymbol{\mu}}_{3,l,t}^{(r)'} \left(\overline{\overline{\boldsymbol{\Sigma}}}_{3,l,t}^{(r)} \right)^{-1} \boldsymbol{\gamma}_{3,l}^{(r)} .
\end{aligned} \tag{D.53}$$

Now, by applying Bayes' rule and plugging eq. (D.52) and eq. (D.53) into eq. (D.37) we get:

$$p(\boldsymbol{\gamma}_{3,l}^{(r)} | -) \propto L(\boldsymbol{\mathcal{X}}, \mathcal{D}, \boldsymbol{\Omega}, \mathbf{s} | \boldsymbol{\theta}) \pi(\boldsymbol{\gamma}_{3,l}^{(r)} | \mathbf{w}_{3,:}, \boldsymbol{\phi}, \tau)$$

$$
\begin{aligned}
&\propto \prod_{t\in\mathcal{T}_l} \exp\left\{-\frac{1}{2}\left[\boldsymbol{\gamma}_{3,l}^{(r)\prime}\left(\overline{\overline{\boldsymbol{\Sigma}}}_{3,l,t}^{(r)}\right)^{-1}\boldsymbol{\gamma}_{3,l}^{(r)} - 2\overline{\boldsymbol{\mu}}_{3,l,t}^{(r)\prime}\left(\overline{\overline{\boldsymbol{\Sigma}}}_{3,l,t}^{(r)}\right)^{-1}\boldsymbol{\gamma}_{3,l}^{(r)}\right]\right\} \\
&\cdot \exp\left\{-\frac{1}{2}\left[\boldsymbol{\gamma}_{3,l}^{(r)\prime}\left(\overline{\boldsymbol{\Lambda}}_{3,l}^{r}\right)^{-1}\boldsymbol{\gamma}_{3,l}^{(r)} - 2\overline{\boldsymbol{\zeta}}_{3,l}^{r\prime}\left(\overline{\boldsymbol{\Lambda}}_{3,l}^{r}\right)^{-1}\boldsymbol{\gamma}_{3,l}^{(r)}\right]\right\} \\
&= \exp\Bigg\{-\frac{1}{2}\Bigg[\sum_{t\in\mathcal{T}_l}\left(\boldsymbol{\gamma}_{3,l}^{(r)\prime}\left(\overline{\overline{\boldsymbol{\Sigma}}}_{3,l,t}^{(r)}\right)^{-1}\boldsymbol{\gamma}_{3,l}^{(r)} - 2\overline{\boldsymbol{\mu}}_{3,l,t}^{(r)\prime}\left(\overline{\overline{\boldsymbol{\Sigma}}}_{3,l,t}^{(r)}\right)^{-1}\boldsymbol{\gamma}_{3,l}^{(r)}\right) \\
&+ \left(\boldsymbol{\gamma}_{3,l}^{(r)\prime}\left(\overline{\boldsymbol{\Lambda}}_{3,l}^{r}\right)^{-1}\boldsymbol{\gamma}_{3,l}^{(r)} - 2\overline{\boldsymbol{\zeta}}_{3,l}^{r\prime}\left(\overline{\boldsymbol{\Lambda}}_{3,l}^{r}\right)^{-1}\boldsymbol{\gamma}_{3,l}^{(r)}\right)\Bigg]\Bigg\} \\
&= \exp\Bigg\{-\frac{1}{2}\Bigg[\boldsymbol{\gamma}_{3,l}^{(r)\prime}\left(\sum_{t\in\mathcal{T}_l}\left(\overline{\overline{\boldsymbol{\Sigma}}}_{3,l,t}^{(r)}\right)^{-1}\right)\boldsymbol{\gamma}_{3,l}^{(r)} - 2\left(\sum_{t\in\mathcal{T}_l}\overline{\boldsymbol{\mu}}_{3,l,t}^{(r)\prime}\left(\overline{\overline{\boldsymbol{\Sigma}}}_{3,l,t}^{(r)}\right)^{-1}\right)\boldsymbol{\gamma}_{3,l}^{(r)} \\
&+ \boldsymbol{\gamma}_{3,l}^{(r)\prime}\left(\overline{\boldsymbol{\Lambda}}_{3,l}^{r}\right)^{-1}\boldsymbol{\gamma}_{3,l}^{(r)} - 2\overline{\boldsymbol{\zeta}}_{3,l}^{r\prime}\left(\overline{\boldsymbol{\Lambda}}_{3,l}^{r}\right)^{-1}\boldsymbol{\gamma}_{3,l}^{(r)}\Bigg]\Bigg\} \\
&= \exp\Bigg\{-\frac{1}{2}\Bigg[\boldsymbol{\gamma}_{3,l}^{(r)\prime}\left(\left(\overline{\boldsymbol{\Lambda}}_{3,l}^{r}\right)^{-1} + \sum_{t\in\mathcal{T}_l}\left(\overline{\overline{\boldsymbol{\Sigma}}}_{3,l,t}^{(r)}\right)^{-1}\right)\boldsymbol{\gamma}_{3,l}^{(r)} \\
&- 2\left(\overline{\boldsymbol{\zeta}}_{3,l}^{r\prime}\left(\overline{\boldsymbol{\Lambda}}_{3,l}^{r}\right)^{-1} + \sum_{t\in\mathcal{T}_l}\overline{\boldsymbol{\mu}}_{3,l,t}^{(r)\prime}\left(\overline{\overline{\boldsymbol{\Sigma}}}_{3,l,t}^{(r)}\right)^{-1}\right)\boldsymbol{\gamma}_{3,l}^{(r)}\Bigg]\Bigg\}. \qquad \text{(D.54)}
\end{aligned}
$$

This is the kernel of a multivariate normal distribution with parameters:

$$
\tilde{\boldsymbol{\Lambda}}_{3,l}^{r} = \left[\left(\tau\phi_r w_{3,r}\mathbf{I}_K\right)^{-1} + \sum_{t\in\mathcal{T}_l}\left(\overline{\overline{\boldsymbol{\Sigma}}}_{3,l,t}^{(r)}\right)^{-1}\right]^{-1} \qquad \text{(D.55a)}
$$

$$
\tilde{\boldsymbol{\zeta}}_{3,l}^{r} = \tilde{\boldsymbol{\Lambda}}_{3,l}^{r\prime}\left[\overline{\boldsymbol{\zeta}}_{3,l}^{r\prime}\left(\tau\phi_r w_{3,r}\mathbf{I}_K\right)^{-1} + \sum_{t\in\mathcal{T}_l}\overline{\boldsymbol{\mu}}_{3,l,t}^{(r)\prime}\left(\overline{\overline{\boldsymbol{\Sigma}}}_{3,l,t}^{(r)}\right)^{-1}\right]^{\prime}. \qquad \text{(D.55b)}
$$

D.6.4 Full conditional distribution of $\boldsymbol{\gamma}_{4,l}^{(r)}$

The full conditional distribution of $\boldsymbol{\gamma}_{4,l}^{(r)}$ is given by:

$$
p(\boldsymbol{\gamma}_{4,l}^{(r)}|\boldsymbol{\mathcal{X}},\mathcal{D},\boldsymbol{\Omega},\mathbf{s},\boldsymbol{\gamma}_{1,l}^{(r)},\boldsymbol{\gamma}_{2,l}^{(r)},\boldsymbol{\gamma}_{3,l}^{(r)},\mathcal{G}_l^{(-r)},w_{4,r},\phi_r,\tau) \sim \mathcal{N}_Q(\tilde{\boldsymbol{\zeta}}_{4,l}^{r},\tilde{\boldsymbol{\Lambda}}_{4,l}^{r}) \qquad \text{(D.56)}
$$

where:

$$
\tilde{\boldsymbol{\Lambda}}_{4,l}^{r} = \left[\left(\tau\phi_r w_{4,r}\mathbf{I}_Q\right)^{-1} + \sum_{t\in\mathcal{T}_l}\left(\overline{\overline{\boldsymbol{\Sigma}}}_{4,l,t}^{(r)}\right)^{-1}\right]^{-1} \qquad \text{(D.57a)}
$$

$$
\tilde{\boldsymbol{\zeta}}_{4,l}^{r} = \tilde{\boldsymbol{\Lambda}}_{4,l}^{r\prime}\left[\overline{\boldsymbol{\zeta}}_{4,l}^{r\prime}\left(\tau\phi_r w_{4,r}\mathbf{I}_Q\right)^{-1} + \sum_{t\in\mathcal{T}_l}\overline{\boldsymbol{\mu}}_{4,l,t}^{(r)\prime}\left(\overline{\overline{\boldsymbol{\Sigma}}}_{4,l,t}^{(r)}\right)^{-1}\right]^{\prime}. \qquad \text{(D.57b)}
$$

By exploiting the central term in the equality chain in eq. (D.25), we can simplify the two addenda in eq. (D.37) as:

$$
\overline{\mathbf{g}}_{l,t}^{(r)\prime}\overline{\overline{\boldsymbol{\Omega}}}_t\overline{\mathbf{g}}_{l,t}^{(r)} = \left(\mathbf{A}_4\boldsymbol{\gamma}_{4,l}^{(r)}\right)^{\prime}\overline{\overline{\boldsymbol{\Omega}}}_t\left(\mathbf{A}_4\boldsymbol{\gamma}_{4,l}^{(r)}\right)
$$

$$= \boldsymbol{\gamma}_{4,l}^{(r)\prime} \mathbf{z}_t \operatorname{vec}\left(\boldsymbol{\gamma}_{1,l}^{(r)} \circ \boldsymbol{\gamma}_{2,l}^{(r)} \circ \boldsymbol{\gamma}_{3,l}^{(r)}\right) \overline{\overline{\boldsymbol{\Omega}}}_t \operatorname{vec}\left(\boldsymbol{\gamma}_{1,l}^{(r)} \circ \boldsymbol{\gamma}_{2,l}^{(r)} \circ \boldsymbol{\gamma}_{3,l}^{(r)}\right) \mathbf{z}_t' \boldsymbol{\gamma}_{4,l}^{(r)}$$
$$= \boldsymbol{\gamma}_{4,l}^{(r)\prime} \left(\overline{\overline{\boldsymbol{\Sigma}}}_{4,l,t}^{(r)}\right)^{-1} \boldsymbol{\gamma}_{4,l}^{(r)} . \tag{D.58}$$

and

$$-2(\mathbf{u}_t - \overline{\mathbf{g}}_{l,t}^{(-r)})' \overline{\overline{\boldsymbol{\Omega}}}_t \overline{\mathbf{g}}_{l,t}^{(r)} = -2(\mathbf{u}_t - \overline{\mathbf{g}}_{l,t}^{(-r)})' \overline{\overline{\boldsymbol{\Omega}}}_t \operatorname{vec}\left(\boldsymbol{\gamma}_{1,l}^{(r)} \circ \boldsymbol{\gamma}_{2,l}^{(r)} \circ \boldsymbol{\gamma}_{3,l}^{(r)}\right) \mathbf{z}_t' \boldsymbol{\gamma}_{4,l}^{(r)}$$
$$= -2\overline{\boldsymbol{\mu}}_{4,l,t}^{(r)\prime} \left(\overline{\overline{\boldsymbol{\Sigma}}}_{4,l,t}^{(r)}\right)^{-1} \boldsymbol{\gamma}_{4,l}^{(r)} . \tag{D.59}$$

Now, by applying Bayes' rule and plugging eq. (D.58) and eq. (D.59) into eq. (D.37) we get:

$$\begin{aligned}
p(\boldsymbol{\gamma}_{4,l}^{(r)}|-) &\propto L(\boldsymbol{\mathcal{X}}, \mathcal{D}, \boldsymbol{\Omega}, \mathbf{s}|\boldsymbol{\theta}) \pi(\boldsymbol{\gamma}_{4,l}^{(r)}|\mathbf{w}_{4,:}, \boldsymbol{\phi}, \tau) \\
&\propto \prod_{t \in \mathcal{T}_l} \exp\left\{-\frac{1}{2}\left[\boldsymbol{\gamma}_{4,l}^{(r)\prime} \left(\overline{\overline{\boldsymbol{\Sigma}}}_{4,l,t}^{(r)}\right)^{-1} \boldsymbol{\gamma}_{4,l}^{(r)} - 2\overline{\boldsymbol{\mu}}_{4,l,t}^{(r)\prime} \left(\overline{\overline{\boldsymbol{\Sigma}}}_{4,l,t}^{(r)}\right)^{-1} \boldsymbol{\gamma}_{4,l}^{(r)}\right]\right\} \\
&\cdot \exp\left\{-\frac{1}{2}\left[\boldsymbol{\gamma}_{4,l}^{(r)\prime} \left(\overline{\boldsymbol{\Lambda}}_{4,l}^{r}\right)^{-1} \boldsymbol{\gamma}_{4,l}^{(r)} - 2\overline{\boldsymbol{\zeta}}_{4,l}^{r\prime} \left(\overline{\boldsymbol{\Lambda}}_{4,l}^{r}\right)^{-1} \boldsymbol{\gamma}_{4,l}^{(r)}\right]\right\} \\
&= \exp\Bigg\{-\frac{1}{2}\Bigg[\sum_{t \in \mathcal{T}_l}\left(\boldsymbol{\gamma}_{3,l}^{(r)\prime} \left(\overline{\overline{\boldsymbol{\Sigma}}}_{4,l,t}^{(r)}\right)^{-1} \boldsymbol{\gamma}_{4,l}^{(r)} - 2\overline{\boldsymbol{\mu}}_{4,l,t}^{(r)\prime} \left(\overline{\overline{\boldsymbol{\Sigma}}}_{4,l,t}^{(r)}\right)^{-1} \boldsymbol{\gamma}_{4,l}^{(r)}\right) \\
&+ \left(\boldsymbol{\gamma}_{4,l}^{(r)\prime} \left(\overline{\boldsymbol{\Lambda}}_{4,l}^{r}\right)^{-1} \boldsymbol{\gamma}_{4,l}^{(r)} - 2\overline{\boldsymbol{\zeta}}_{4,l}^{r\prime} \left(\overline{\boldsymbol{\Lambda}}_{4,l}^{r}\right)^{-1} \boldsymbol{\gamma}_{4,l}^{(r)}\right)\Bigg]\Bigg\} \\
&= \exp\Bigg\{-\frac{1}{2}\Bigg[\boldsymbol{\gamma}_{4,l}^{(r)\prime}\left(\sum_{t \in \mathcal{T}_l}\left(\overline{\overline{\boldsymbol{\Sigma}}}_{4,l,t}^{(r)}\right)^{-1}\right)\boldsymbol{\gamma}_{4,l}^{(r)} - 2\left(\sum_{t \in \mathcal{T}_l}\overline{\boldsymbol{\mu}}_{4,l,t}^{(r)\prime}\left(\overline{\overline{\boldsymbol{\Sigma}}}_{4,l,t}^{(r)}\right)^{-1}\right)\boldsymbol{\gamma}_{4,l}^{(r)} \\
&+ \boldsymbol{\gamma}_{4,l}^{(r)\prime}\left(\overline{\boldsymbol{\Lambda}}_{4,l}^{r}\right)^{-1}\boldsymbol{\gamma}_{4,l}^{(r)} - 2\overline{\boldsymbol{\zeta}}_{4,l}^{r\prime}\left(\overline{\boldsymbol{\Lambda}}_{4,l}^{r}\right)^{-1}\boldsymbol{\gamma}_{4,l}^{(r)}\Bigg]\Bigg\} \\
&= \exp\Bigg\{-\frac{1}{2}\Bigg[\boldsymbol{\gamma}_{4,l}^{(r)\prime}\left(\left(\overline{\boldsymbol{\Lambda}}_{4,l}^{r}\right)^{-1} + \sum_{t \in \mathcal{T}_l}\left(\overline{\overline{\boldsymbol{\Sigma}}}_{4,l,t}^{(r)}\right)^{-1}\right)\boldsymbol{\gamma}_{4,l}^{(r)} \\
&- 2\left(\overline{\boldsymbol{\zeta}}_{4,l}^{r\prime}\left(\overline{\boldsymbol{\Lambda}}_{4,l}^{r}\right)^{-1} + \sum_{t \in \mathcal{T}_l}\overline{\boldsymbol{\mu}}_{4,l,t}^{(r)\prime}\left(\overline{\overline{\boldsymbol{\Sigma}}}_{4,l,t}^{(r)}\right)^{-1}\right)\boldsymbol{\gamma}_{4,l}^{(r)}\Bigg]\Bigg\} .
\end{aligned} \tag{D.60}$$

This is the kernel of a multivariate normal distribution with parameters:

$$\tilde{\boldsymbol{\Lambda}}_{4,l}^{r} = \left[\left(\tau\phi_r w_{4,r}\mathbf{I}_Q\right)^{-1} + \sum_{t \in \mathcal{T}_l}\left(\overline{\overline{\boldsymbol{\Sigma}}}_{4,l,t}^{(r)}\right)^{-1}\right]^{-1} \tag{D.61a}$$

$$\tilde{\boldsymbol{\zeta}}_{4,l}^{r} = \tilde{\boldsymbol{\Lambda}}_{4,l}^{r\prime}\left[\overline{\boldsymbol{\zeta}}_{4,l}^{r\prime}\left(\tau\phi_r w_{4,r}\mathbf{I}_Q\right)^{-1} + \sum_{t \in \mathcal{T}_l}\overline{\boldsymbol{\mu}}_{4,l,t}^{(r)\prime}\left(\overline{\overline{\boldsymbol{\Sigma}}}_{4,l,t}^{(r)}\right)^{-1}\right]' . \tag{D.61b}$$

D.7 Full conditional distribution of $\omega_{ijk,t}$

The full conditional distribution for the latent variable $\omega_{ijk,t}$ for every $i = 1, \ldots, I$, $j = 1, \ldots, J$, $k = 1, \ldots, K$ and $t = 1, \ldots, T$:

$$p(\omega_{ijk,t}|x_{ijk,t}, s_t, \mathcal{G}_{s_t}) \sim PG(1,\, \mathbf{z}_t'\mathbf{g}_{ijk,s_t}) . \tag{D.62}$$

To shorten the notation, define $\psi_{ijk,t} = \mathbf{z}_t' \mathbf{g}_{ijk,s_t}$. The full conditional is derived by integrating out the latent allocation variable $d_{ijk,t}$, as follows:

$$
\begin{aligned}
&p(\omega_{ijk,t}|x_{ijk,t}, s_t, \mathcal{G}_{s_t}) \\
&= \int_D \int_\rho p(\omega_{ijk,t}, d_{ijk,t}|x_{ijk,t}, s_t, \mathcal{G}_{s_t}, \rho_{s_t}) p(\rho_{s_t}) \, \mathrm{d}\rho_{s_t} \mathrm{d}d_{ijk,t} \\
&= \int_D \int_\rho \frac{p(x_{ijk,t}, d_{ij,t}|\omega_{ijk,t}, s_t, \mathcal{G}_{s_t}, \rho_{s_t}) p(\omega_{ijk,t}) p(\rho_{s_t})}{\int_\Omega p(x_{ijk,t}, \omega_{ijk,t}, d_{ijk,t}|s_t, \mathcal{G}_{s_t}, \rho_{s_t}) \, \mathrm{d}\omega_{ijk,t}} \, \mathrm{d}\rho_{s_t} \mathrm{d}d_{ijk,t} \\
&= \int_D \int_\rho \frac{p(x_{ijk,t}, \omega_{ijk,t}, d_{ijk,t}|s_t, \mathcal{G}_{s_t}, \rho_{s_t})}{p(x_{ijk,t}, d_{ijk,t}|s_t, \mathcal{G}_{s_t}, \rho_{s_t})} p(\rho_{s_t}) \, \mathrm{d}\rho_{s_t} \mathrm{d}d_{ijk,t} \\
&= \int_D \int_\rho \frac{\left(\rho_{s_t} \delta_{\{0\}}(x_{ijk,t})\right)^{d_{ijk,t}} \left(\frac{1-\rho_{s_t}}{2}\right)^{d_{ijk,t}} \exp\left\{-\frac{\omega_{ijk,t}}{2}\psi_{ijk,t}^2 + \kappa_{ijk,t}\psi_{ijk,t}\right\} p(\omega_{ijk,t}) p(\rho_{s_t})}{\left(\rho_{s_t} \delta_{\{0\}}(x_{ijk,t})\right)^{d_{ijk,t}} \left(\frac{1-\rho_{s_t}}{2}\right)^{d_{ijk,t}} \left(\exp\{\psi_{ijk,t}x_{ijk,t}\}/(1+\exp\{\psi_{ijk,t}\})\right)^{1-d_{ijk,t}}} \, \mathrm{d}\rho_{s_t} \mathrm{d}d_{ijk,t} \\
&= \int_D \int_\rho \exp\{\kappa_{ijk,t}^{(s_t)} \psi_{ijk,t}\} \frac{\exp\{\psi_{ijk,t}x_{ijk,t}(1-d_{ijk,t})\}}{(1+\exp\{\psi_{ijk,t}\})^{1-d_{ijk,t}}} \exp\left\{-\frac{\omega_{ijk,t}}{2}\psi_{ijk,t}^2\right\} p(\omega_{ijk,t}) p(\rho_{s_t}) \, \mathrm{d}\rho_{s_t} \mathrm{d}d_{ijk,t} \\
&= \int_D \int_\rho \left[\frac{1+\exp\{\psi_{ijk,t}\}}{\exp\{\psi_{ijk,t}x_{ijk,t}\}} \cdot \frac{\exp\{\psi_{ijk,t}x_{ijk,t}\}}{\exp\{\psi_{ijk,t}/2\}}\right]^{1-d_{ijk,t}} \left[\exp\{-\psi_{ijk,t}^2 \omega_{ijk,t}/2\} p(\omega_{ijk,t})\right] p(\rho_{s_t}) \, \mathrm{d}\rho_{s_t} \mathrm{d}d_{ijk,t} \\
&= \left(1 + \frac{1+\exp\{\psi_{ijk,t}\}}{\exp\{\psi_{ijk,t}/2\}}\right) \left[\exp\{-\psi_{ijk,t}^2 \omega_{ijk,t}/2\} p(\omega_{ijk,t})\right] \\
&\propto \exp\{-\psi_{ijk,t}^2 \omega_{ijk,t}/2\} p(\omega_{ijk,t}) \,. \qquad \text{(D.63)}
\end{aligned}
$$

Since $p(\omega_{ijk,t}) \sim PG(1,0)$, by Theorem 1 in Polson et al. (2013) the result follows.

D.8 Full conditional distribution of $d_{ijk,t}$

The full conditional posterior probabilities for the latent allocation variables $d_{ijk,t}$, which select the component of the mixture in eq. (3), for each $t = 1, \ldots, T$ and for every $i = 1, \ldots, I$, $j = 1, \ldots, J$ and $k = 1, \ldots, K$, are given by:

$$
p(d_{ijk,t} = 1|\boldsymbol{\mathcal{X}}, \mathbf{s}, \mathcal{G}_{s_t}, \boldsymbol{\rho}_{s_t}) = \frac{\tilde{p}(d_{ijk,t} = 1|\boldsymbol{\mathcal{X}}, \mathbf{s}, \mathcal{G}_{s_t}, \boldsymbol{\rho}_{s_t})}{\tilde{p}(d_{ijk,t} = 1|\boldsymbol{\mathcal{X}}, \mathbf{s}, \mathcal{G}_{s_t}, \boldsymbol{\rho}_{s_t}) + \tilde{p}(d_{ijk,t} = 0|\boldsymbol{\mathcal{X}}, \mathbf{s}, \mathcal{G}_{s_t}, \boldsymbol{\rho}_{s_t})} \qquad \text{(D.64a)}
$$

$$
p(d_{ij,t} = 0|\boldsymbol{\mathcal{X}}, \mathbf{s}, \mathcal{G}_{s_t}, \boldsymbol{\rho}_{s_t}) = \frac{\tilde{p}(d_{ijk,t} = 0|\boldsymbol{\mathcal{X}}, \mathbf{s}, \mathcal{G}_{s_t}, \boldsymbol{\rho}_{s_t})}{\tilde{p}(d_{ijk,t} = 1|\boldsymbol{\mathcal{X}}, \mathbf{s}, \mathcal{G}_{s_t}, \boldsymbol{\rho}_{s_t}) + \tilde{p}(d_{ijk,t} = 0|\boldsymbol{\mathcal{X}}, \mathbf{s}, \mathcal{G}_{s_t}, \boldsymbol{\rho}_{s_t})} \,. \qquad \text{(D.64b)}
$$

The unnormalised posterior probabilities are given by:

$$
\tilde{p}(d_{ijk,t} = 1|\boldsymbol{\mathcal{X}}, \mathbf{s}, \mathcal{G}_{s_t}, \boldsymbol{\rho}_{s_t}) = \rho_{s_t} \delta_{\{0\}}(x_{ijk,t}) \qquad \text{(D.65a)}
$$

$$
\tilde{p}(d_{ijk,t} = 0|\boldsymbol{\mathcal{X}}, \mathbf{s}, \mathcal{G}_{s_t}, \boldsymbol{\rho}_{s_t}) = (1-\rho_{s_t}) \frac{\exp\left\{(\mathbf{z}_t' \mathbf{g}_{ijk,s_t}) x_{ijk,t}\right\}}{1+\exp\{\mathbf{z}_t' \mathbf{g}_{ijk,s_t}\}} \,. \qquad \text{(D.65b)}
$$

We have obtained the result starting from eq. (12) after having integrated out the latent variables $\boldsymbol{\Omega}$, as follows:

$$
\begin{aligned}
\tilde{p}(d_{ijk,t}|\boldsymbol{\mathcal{X}}, \mathbf{s}, \mathcal{G}_{s_t}, \boldsymbol{\rho}_{s_t}) &\propto p(\boldsymbol{\mathcal{X}}, \mathbf{s}|\mathcal{G}_{s_t}, \boldsymbol{\rho}_{s_t}, d_{ijk,t}) \pi(d_{ijk,t}) \\
&= \rho_{s_t}^{d_{ijk,t}} \delta_{\{0\}}(x_{ijk,t})^{d_{ijk,t}} (1-\rho_{s_t})^{1-d_{ijk,t}} \frac{(\exp\{\mathbf{z}_t' \mathbf{g}_{ijk,s_t}\})^{x_{ijk,t}(1-d_{ijk,t})}}{(1+\exp\{\mathbf{z}_t' \mathbf{g}_{ijk,s_t}\})^{(1-d_{ijk,t})}} \\
&= \left[\rho_{s_t} \delta_{\{0\}}(x_{ijk,t})\right]^{d_{ijk,t}} \left[(1-\rho_{s_t}) \frac{(\exp\{\mathbf{z}_t' \mathbf{g}_{ijk,s_t}\})^{x_{ijk,t}}}{1+\exp\{\mathbf{z}_t' \mathbf{g}_{ijk,s_t}\}}\right]^{1-d_{ijk,t}} . \qquad \text{(D.66)}
\end{aligned}
$$

D.9 Full conditional distribution of ρ_l

For each regime $l = 1, \ldots, L$, the full conditional distribution for the mixing probability ρ_l of the observation model in eq (2) is given by:

$$p(\rho_l|\boldsymbol{\mathcal{X}}, \mathcal{D}, \mathbf{s}) = p(\rho_l|\mathcal{D}, \mathbf{s}) \sim \mathcal{B}e(\tilde{a}_l, \tilde{b}_l)\,, \tag{D.67}$$

with:

$$\tilde{a}_l = N_1^l + \overline{a}_l^\rho \tag{D.68a}$$

$$\tilde{b}_l = N_0^l + \overline{b}_l^\rho\,. \tag{D.68b}$$

We get this result starting from eq. (12) and integrating out the latent variables $\boldsymbol{\Omega}$, as follows:

$$\begin{aligned}
p(\rho_l|\boldsymbol{\mathcal{X}}, \mathcal{D}, \mathbf{s}) &\propto \pi(\rho_l) \int_G L(\boldsymbol{\mathcal{X}}, \mathcal{D}, \mathbf{s}|\rho_l, \mathcal{G}_l) p(\mathcal{G}_l)\, \mathrm{d}\mathcal{G}_l \\
&\propto \left[\int_G \prod_{t\in\mathcal{T}_l} \prod_{i=1}^{I} \prod_{j=1}^{J} \prod_{k=1}^{K} \rho_l^{d_{ijk,t}} \cdot \left[\delta_{\{0\}}(x_{ijk,t})\right]^{d_{ijk,t}} \cdot (1-\rho_l)^{1-d_{ijk,t}} \right. \\
&\left. \cdot \frac{\left(\exp\{\mathbf{z}_t'\mathbf{g}_{ijk,l}\}\right)^{x_{ijk,t}(1-d_{ijk,t})}}{\left(1+\exp\{\mathbf{z}_t'\mathbf{g}_{ijk,l}\}\right)^{(1-d_{ijk,t})}}\, \mathrm{d}\mathcal{G}_l \right] \cdot \rho_l^{\overline{a}_l^\rho - 1}(1-\rho_l)^{\overline{b}_l^\rho - 1} \\
&\propto \left[\prod_{t\in\mathcal{T}_l} \prod_{i=1}^{I} \prod_{j=1}^{J} \prod_{k=1}^{K} \rho_l^{d_{ijk,t}} (1-\rho_l)^{1-d_{ijk,t}} \right] \rho_l^{\overline{a}_l^\rho - 1}(1-\rho_l)^{\overline{b}_l^\rho - 1} \\
&= \rho_l^{N_1^l}(1-\rho_l)^{N_0^l} \rho_l^{\overline{a}_l^\rho - 1}(1-\rho_l)^{\overline{b}_l^\rho - 1} \\
&= \rho_l^{N_1^l + \overline{a}_l^\rho - 1}(1-\rho_l)^{N_0^l + \overline{b}_l^\rho - 1}\,,
\end{aligned} \tag{D.69}$$

where we have defined the counting variables, for every $l = 1, \ldots, L$:

$$N_1^l = \sum_{t\in\mathcal{T}_l} \sum_{i=1}^{I} \sum_{j=1}^{J} \sum_{k=1}^{K} \mathbb{1}\{d_{ijk,t} = 1\} \tag{D.70a}$$

$$N_0^l = \sum_{t\in\mathcal{T}_l} \sum_{i=1}^{I} \sum_{j=1}^{J} \sum_{k=1}^{K} \mathbb{1}\{d_{ijk,t} = 0\}\,. \tag{D.70b}$$

D.10 Full conditional distribution of $\boldsymbol{\mu}_l$

The full conditional distribution for the intercept term of the second equation of the model is given by:

$$p(\boldsymbol{\mu}_l|\mathbf{y}, \mathbf{s}, \boldsymbol{\Sigma}_l) \sim \mathcal{N}_M(\tilde{\boldsymbol{\mu}}_l, \tilde{\boldsymbol{\Upsilon}}_l)\,, \tag{D.71}$$

with:

$$\tilde{\boldsymbol{\mu}}_l = \tilde{\boldsymbol{\Upsilon}}_l' \left(\overline{\boldsymbol{\mu}}_l' \overline{\boldsymbol{\Upsilon}}_l^{-1} + \sum_{t\in\mathcal{T}_l} \boldsymbol{y}_t' \boldsymbol{\Sigma}_l^{-1} \right)'\,, \tag{D.72a}$$

$$\tilde{\boldsymbol{\Upsilon}}_l = \left[T_l \boldsymbol{\Sigma}_l^{-1} + \overline{\boldsymbol{\Upsilon}}_l^{-1} \right]^{-1}\,, \tag{D.72b}$$

for each regime $l = 1, \ldots, L$. We have derived the updated hyperparameters from:

$$p(\boldsymbol{\mu}_l|\mathbf{y}, \mathbf{s}, \boldsymbol{\Sigma}_l) \propto \pi(\boldsymbol{\mu}_l) p(\mathbf{y}|\mathbf{s}, \boldsymbol{\Sigma}_l, \boldsymbol{\mu}_l)$$

$$\propto \exp\left\{-\frac{1}{2}(\boldsymbol{\mu}_l-\overline{\boldsymbol{\mu}}_l)'\overline{\boldsymbol{\Upsilon}}_l^{-1}(\boldsymbol{\mu}_l-\overline{\boldsymbol{\mu}}_l)\right\}\prod_{t\in\mathcal{T}_l}\exp\left\{-\frac{1}{2}(\mathbf{y}_t-\boldsymbol{\mu}_l)'\boldsymbol{\Sigma}_l^{-1}(\mathbf{y}_t-\boldsymbol{\mu}_l)\right\}$$

$$\propto \exp\left\{-\frac{1}{2}\left[\boldsymbol{\mu}_l'\overline{\boldsymbol{\Upsilon}}_l^{-1}\boldsymbol{\mu}_l-2\overline{\boldsymbol{\mu}}_l'\overline{\boldsymbol{\Upsilon}}_l^{-1}\boldsymbol{\mu}_l+\sum_{t\in\mathcal{T}_l}\boldsymbol{\mu}_l'\boldsymbol{\Sigma}_l^{-1}\boldsymbol{\mu}_l-2\mathbf{y}_t'\boldsymbol{\Sigma}_l^{-1}\boldsymbol{\mu}_l\right]\right\}$$

$$\propto \exp\left\{-\frac{1}{2}\left[\boldsymbol{\mu}_l'\left(T_l\boldsymbol{\Sigma}_l^{-1}+\overline{\boldsymbol{\Upsilon}}_l^{-1}\right)\boldsymbol{\mu}_l-2\left(\sum_{t\in\mathcal{T}_l}\mathbf{y}_t'\boldsymbol{\Sigma}_l^{-1}+\overline{\boldsymbol{\mu}}_l'\overline{\boldsymbol{\Upsilon}}_l^{-1}\right)\boldsymbol{\mu}_l\right]\right\}. \quad \text{(D.73)}$$

D.11 Full conditional distribution of $\boldsymbol{\Sigma}_l$

The full conditional distribution for the covariance of the error term of the second equation of the model is given by:

$$p(\boldsymbol{\Sigma}_l|\mathbf{y},\mathbf{s},\boldsymbol{\mu}_l)\sim\mathcal{IW}_M(\tilde{\nu}_l,\tilde{\boldsymbol{\Psi}}_l)\,, \quad \text{(D.74)}$$

with:

$$\tilde{\boldsymbol{\nu}}_l=\overline{\nu}_l+T_l\,, \quad \text{(D.75a)}$$

$$\tilde{\boldsymbol{\Psi}}_l=\overline{\Psi}_l+\sum_{t\in\mathcal{T}_l}(\mathbf{y}_t-\boldsymbol{\mu}_l)(\mathbf{y}_t-\boldsymbol{\mu}_l)'\,, \quad \text{(D.75b)}$$

for each regime $l=1,\ldots,L$. We have derived the updated hyperparameters from:

$$\begin{aligned}
p(\boldsymbol{\Sigma}_l|\mathbf{y},\mathbf{s},\boldsymbol{\mu}_l)&\propto\pi(\boldsymbol{\Sigma}_l)p(\mathbf{y}|\mathbf{s},\boldsymbol{\mu}_l,\boldsymbol{\Sigma}_l)\\
&\propto|\boldsymbol{\Sigma}_l|^{-\frac{\overline{\nu}_l+m-1}{2}}\exp\left\{-\frac{1}{2}\operatorname{tr}\left(\overline{\boldsymbol{\Psi}}_l\boldsymbol{\Sigma}_l^{-1}\right)\right\}\prod_{t\in\mathcal{T}_l}|\boldsymbol{\Sigma}_l|^{-1/2}\exp\left\{-\frac{1}{2}(\mathbf{y}_t-\boldsymbol{\mu}_l)'\boldsymbol{\Sigma}_l^{-1}(\mathbf{y}_t-\boldsymbol{\mu}_l)\right\}\\
&=|\boldsymbol{\Sigma}_l|^{-\frac{\overline{\nu}_l+m-1+T_l}{2}}\exp\left\{-\frac{1}{2}\left[\operatorname{tr}\left(\overline{\boldsymbol{\Psi}}_l\boldsymbol{\Sigma}_l^{-1}\right)+\sum_{t\in\mathcal{T}_l}(\mathbf{y}_t-\boldsymbol{\mu}_l)'\boldsymbol{\Sigma}_l^{-1}(\mathbf{y}_t-\boldsymbol{\mu}_l)\right]\right\}\\
&=|\boldsymbol{\Sigma}_l|^{-\frac{\overline{\nu}_l+m-1+T_l}{2}}\exp\left\{-\frac{1}{2}\left[\operatorname{tr}\left(\overline{\boldsymbol{\Psi}}_l\boldsymbol{\Sigma}_l^{-1}\right)+\operatorname{tr}\left(\sum_{t\in\mathcal{T}_l}(\mathbf{y}_t-\boldsymbol{\mu}_l)(\mathbf{y}_t-\boldsymbol{\mu}_l)'\boldsymbol{\Sigma}_l^{-1}\right)\right]\right\}\\
&=|\boldsymbol{\Sigma}_l|^{-\frac{\overline{\nu}_l+m-1+T_l}{2}}\exp\left\{-\frac{1}{2}\left[\operatorname{tr}\left(\left(\overline{\boldsymbol{\Psi}}_l+\sum_{t\in\mathcal{T}_l}(\mathbf{y}_t-\boldsymbol{\mu}_l)(\mathbf{y}_t-\boldsymbol{\mu}_l)'\right)\boldsymbol{\Sigma}_l^{-1}\right)\right]\right\},
\end{aligned} \quad \text{(D.76)}$$

where we have used the property of linearity of the trace operator.

D.12 Full conditional distribution of $\boldsymbol{\xi}_{l,:}$

The full conditional distributionof each row $l=1,\ldots,L$ of the transition matrix of the hidden Markov chain, under the assumption that the initial distribution of the state s_t is independent from the transition matrix $\boldsymbol{\Xi}$, that is $p(s_0|\boldsymbol{\Xi})=p(s_0)$, is given by:

$$p(\boldsymbol{\xi}_{l,:}|\mathbf{s})\sim\mathcal{D}ir(\tilde{\mathbf{c}})\,, \quad \text{(D.77)}$$

where:

$$\tilde{\mathbf{c}} = \left(\bar{c}_1 + N_{l,1}(\mathbf{s}), \ldots, \bar{c}_L + N_{l,L}(\mathbf{s})\right) . \tag{D.78}$$

It can be derived from:

$$\begin{aligned} p(\boldsymbol{\xi}_{l,:}|\mathbf{s}) &\propto \pi(\boldsymbol{\xi}_{l,:}) p(\mathbf{s}|\boldsymbol{\xi}_{l,:}) \\ &\propto \prod_{k=1}^{L} \xi_{l,k}^{\bar{c}_k - 1} \prod_{g=1}^{L} \prod_{k=1}^{L} \xi_{g,k}^{N_{g,k}(\mathbf{s})} p(s_0|\boldsymbol{\Xi}) \\ &\propto \prod_{k=1}^{L} \xi_{l,k}^{\bar{c}_k - 1} \prod_{k=1}^{L} \xi_{l,k}^{N_{l,k}(\mathbf{s})} p(s_0|\boldsymbol{\Xi}) \\ &= \prod_{k=1}^{L} \xi_{l,k}^{\bar{c}_k + N_{l,k}(\mathbf{s}) - 1} p(s_0|\boldsymbol{\Xi}) . \end{aligned} \tag{D.79}$$

Concerning the notation, we denoted the collection of hidden states up to time t by $\mathbf{s}^t = (s_0, \ldots, s_t)$ and we used $N_{i,j}(\mathbf{s}) = \sum_t \mathbb{1}(s_{t-1} = i)\mathbb{1}(s_t = j)$ for counting the number of transitions from state i to state j up to time T. Under the assumption $p(s_0|\boldsymbol{\Xi}) = p(s_0)$, we obtain the full conditional posterior in eq. (D.77). By contrast, if the initial distribution of s_0 depends on the transition matrix (for example, when it coincides with the ergodic distribution $\boldsymbol{\eta}^*(\boldsymbol{\Xi})$), we have:

$$p(\boldsymbol{\xi}_{l,:}|\mathbf{s}) \propto g_l(\boldsymbol{\xi}_{l,:}) \boldsymbol{\eta}^*(\boldsymbol{\Xi}) , \tag{D.80}$$

where $g_l(\boldsymbol{\xi}_{l,:})$ is the kernel of the Dirichlet distribution in eq. (D.79). We can sample from it via a Metropolis Hastings step, either for a single or for multiple rows of the transition matrix, using $g_l(\boldsymbol{\xi}_{l,:})$ as proposal for row l. See Frühwirth-Schnatter (2006) for further details.

D.13 Full conditional distribution of s_t

For sampling the trajectory $\mathbf{s} = (s_1, \ldots, s_T)$, we can adopt two approaches: (i) update s_t for each $t = 1, \ldots, T$ using a single-move Gibbs sampler step. This implies sampling each state s_t from its posterior distribution conditioning on all the other states. (ii) update the whole path $\mathbf{s}$ from the full joint conditional distribution in a multi-move Gibbs sampler step, also called the Forward-Filtering-Backward-Sampling (FFBS) algorithm (see Frühwirth-Schnatter (2006)).

Define $\mathbf{s}_{-t} = (s_0, \ldots, s_{t-1}, s_{t+1}, \ldots, s_T)'$. Since the hidden chain is assumed to be first order Markov, we can derive the full conditional distribution for the each state s_t:

$$p(s_t|\mathbf{s}_{-t}, \boldsymbol{\mathcal{X}}, \mathbf{y}, \mathcal{D}, \boldsymbol{\Omega}, \mathcal{G}, \boldsymbol{\mu}, \boldsymbol{\Sigma}, \boldsymbol{\Xi}, \boldsymbol{\rho}, \mathbf{W}, \boldsymbol{\phi}, \tau) = p(s_t|s_{t-1}, s_{t+1}, \mathcal{X}_t, \mathbf{y}_t, \mathcal{D}, \mathcal{G}, \boldsymbol{\mu}, \boldsymbol{\Sigma}, \boldsymbol{\Xi}, \boldsymbol{\rho}) . \tag{D.81}$$

Staring from the complete data likelihood in eq. (12) for a given time t and integrating out the latent variables $(\mathcal{D}, \boldsymbol{\Omega}_t)$, we obtain the unnormalized posterior probability of state l at time t for $l \in \{1, \ldots, L\}$:

$$p(s_t = l|s_{t-1} = u,\, s_{t+1} = v,\, \mathcal{X}_t, \mathbf{y}_t, \boldsymbol{\rho}, \mathcal{G}, \boldsymbol{\mu}, \boldsymbol{\Sigma}, \boldsymbol{\Xi}) \propto q_{l,uv}^t , \tag{D.82}$$

where $q_{l,uv}^t$ is given by:

$$\begin{aligned} q_{l,uv}^t = &\prod_{i=1}^{I} \prod_{j=1}^{J} \left[(1 - \rho_l) \frac{\exp\{\mathbf{z}_t' \mathbf{g}_{ijk,l}\}}{1 + \exp\{\mathbf{z}_t' \mathbf{g}_{ijk,l}\}} \right]^{x_{ij,t}} \left[\rho_l + (1 - \rho_l) \frac{1}{1 + \exp\{\mathbf{z}_t' \mathbf{g}_{ijk,l}\}} \right]^{1 - x_{ij,t}} \\ &\cdot |\boldsymbol{\Sigma}_l|^{-1/2} \exp\left\{ -\frac{1}{2} (\mathbf{y}_t - \boldsymbol{\mu}_l)' \boldsymbol{\Sigma}_l^{-1} (\mathbf{y}_t - \boldsymbol{\mu}_l) \right\} \end{aligned}$$

$$\cdot \left(\prod_{g=1}^{L} \xi_{g,l}^{\mathbb{1}\{s_{t-1}=u\}} \right) \left(\prod_{k=1}^{L} \xi_{l,k}^{\mathbb{1}\{s_{t+1}=v\}} \right) . \tag{D.83}$$

By normalizing one gets:

$$p(s_t = l | s_{t-1} = u,\, s_{t+1} = v,\, \mathcal{X}_t, \mathbf{y}_t, \boldsymbol{\rho}, \mathcal{G}, \boldsymbol{\mu}, \boldsymbol{\Sigma}, \boldsymbol{\Xi}) = \frac{q_{l,uv}^t}{\sum_{k=1}^{L} q_{k,uv}^t} \qquad \forall\, l\,. \tag{D.84}$$

Combining together all possible L values of the state variable, we can recognise that the posterior distribution of the state latent variable at time t follows a categorical distribution with probability vector $\tilde{\mathbf{p}}_{uv}^t = (\tilde{p}_{1,uv}^t, \ldots, \tilde{p}_{L,uv}^t)'$:

$$p(s_t | s_{t-1} = u,\, s_{t+1} = v,\, \mathcal{X}_t, \mathbf{y}_t, \boldsymbol{\rho}, \mathcal{G}, \boldsymbol{\mu}, \boldsymbol{\Sigma}, \boldsymbol{\Xi}) \propto \prod_{l=1}^{L} (q_{l,uv}^t)^{\mathbb{1}\{s_t=l\}}\,. \tag{D.85}$$

If we consider conditioning on (s_{t-1}, s_{t+1}) instead of on the specific couple $(s_{t-1} = u,\, s_{t+1} = v)$, we get an unnormalised posterior probability (denoted q_l^t) similar to eq. (D.84), but without the indicator variables. The result in eq. (D.85) thus translates in:

$$p(s_t = l | s_{t-1}, s_{t+1}, \mathcal{X}_t, \mathbf{y}_t, \mathcal{G}, \boldsymbol{\rho}, \boldsymbol{\mu}, \boldsymbol{\Sigma}, \boldsymbol{\Xi}) = \frac{q_l^t}{\sum_{k=1}^{L} q_k^t} \propto q_l^t \qquad \forall\, l \tag{D.86}$$

$$p(s_t | s_{t-1}, s_{t+1}, \mathcal{X}_t, \mathbf{y}_t, \mathcal{G}, \boldsymbol{\rho}, \boldsymbol{\mu}, \boldsymbol{\Sigma}, \boldsymbol{\Xi}) \propto \prod_{l=1}^{L} (q_l^t)^{\mathbb{1}\{s_t=l\}}\,. \tag{D.87}$$

By contrast, the multi-move Gibbs sampler consists in sampling the path from the joint full conditional distribution $p(\mathbf{s}|-)$. It is based on the factorisation of the full joint conditional distribution as the product of the entries of the transition matrix $\boldsymbol{\Xi}$ and the filtered probabilities. Since the observations $(\mathcal{X}_t, \mathbf{y}_t)$ depend only on the contemporaneous value of the hidden chain s_t, filtering the state probabilities is feasible. Staring from the complete data likelihood in eq. (12), we integrate the latent variables $(\mathcal{D}, \boldsymbol{\Omega})$ and sample the trajectory from the full joint conditional distribution:

$$p(\mathbf{s}|\boldsymbol{\mathcal{X}}, \mathbf{y}, \mathcal{G}, \boldsymbol{\rho}, \boldsymbol{\mu}, \boldsymbol{\Sigma}, \boldsymbol{\Xi}) \propto p(\boldsymbol{\mathcal{X}}, \mathbf{y}, \mathbf{s}|\mathcal{G}, \boldsymbol{\rho}, \boldsymbol{\mu}, \boldsymbol{\Sigma}) = p(\boldsymbol{\mathcal{X}}, \mathbf{y}|\mathbf{s}, \mathcal{G}, \boldsymbol{\rho}, \boldsymbol{\mu}, \boldsymbol{\Sigma}) p(\mathbf{s}|\boldsymbol{\Xi})\,. \tag{D.88}$$

Consequently, at each iteration of the Gibbs sampler we firstly compute the filtered state probabilities using $p(\boldsymbol{\mathcal{X}}, \mathbf{y}|\mathbf{s}, \mathcal{G}, \boldsymbol{\mu}, \boldsymbol{\Sigma})$ as likelihood function. Define $\mathcal{X}^{t-1} = \{\mathcal{X}_1, \ldots, \mathcal{X}_{t-1}\}$ and $\mathbf{y}^{t-1} = \{\mathbf{y}_1, \ldots, \mathbf{y}_{t-1}\}$. Since the two observation processes are independent from each other as well as from their own past conditionally on the current state, the predictive probability correspond to the conditional distribution of the observations given the state:

$$\begin{aligned} p(\mathcal{X}_t, \mathbf{y}_t | s_t = l, \mathcal{X}^{t-1}, \mathbf{y}^{t-1}, \mathcal{G}, \boldsymbol{\rho}, \boldsymbol{\mu}, \boldsymbol{\Sigma}) &= p(\mathcal{X}_t, \mathbf{y}_t | s_t = l, \mathcal{G}, \boldsymbol{\rho}, \boldsymbol{\mu}, \boldsymbol{\Sigma}) \\ &= p(\mathbf{y}_t | s_t = l, \boldsymbol{\mu}_l, \boldsymbol{\Sigma}_l) \cdot p(\mathcal{X}_t | s_t = l, \rho_l, \mathcal{G}_l) \qquad \text{(D.89a)} \\ &= p(\mathbf{y}_t | s_t = l, \boldsymbol{\mu}_l, \boldsymbol{\Sigma}_l) \cdot \prod_{i=1}^{I} \prod_{j=i}^{J} \prod_{k=1}^{K} p(x_{ijk,t} | s_t = l, \rho_l, \mathcal{G}_l)\,. \end{aligned}$$

(D.89b)

From eq. (C.5), we have that the logarithm of the predictive probability is:

$$\log p(\mathcal{X}_t, \mathbf{y}_t | s_t = l, \mathcal{X}^{t-1}, \mathbf{y}^{t-1}, \mathcal{G}, \boldsymbol{\rho}, \boldsymbol{\mu}, \boldsymbol{\Sigma}) =$$

$$= \log p(\mathbf{y}_t|s_t = l, \boldsymbol{\mu}_l, \boldsymbol{\Sigma}_l) + \sum_{i=1}^{I}\sum_{j=1}^{J}\sum_{k=1}^{K} \log p(x_{ijk,t}|s_t = l, \rho_l, \mathcal{G}_l) \tag{D.90}$$

where:

$$p(\mathbf{y}_t|s_t = l, \boldsymbol{\mu}_l, \boldsymbol{\Sigma}_l) = (2\pi)^{-m/2} |\boldsymbol{\Sigma}_l|^{-1/2} \exp\left\{-\frac{1}{2}(\mathbf{y}_y - \boldsymbol{\mu}_l)'\boldsymbol{\Sigma}_l^{-1}(\mathbf{y}_t - \boldsymbol{\mu}_l)\right\} \tag{D.91}$$

$$p(x_{ijk,t} = 1|s_t = l, \rho_l, \mathcal{G}_l) = (1 - \rho_l)\frac{\exp\{\mathbf{z}_t'\mathbf{g}_{ijk,l}\}}{1 + \exp\{\mathbf{z}_t'\mathbf{g}_{ijk,l}\}} \tag{D.92}$$

$$p(x_{ijk,t} = 0|s_t = l, \rho_l, \mathcal{G}_l) = \rho_l + (1 - \rho_l)\frac{1}{1 + \exp\{\mathbf{z}_t'\mathbf{g}_{ijk,l}\}}\,. \tag{D.93}$$

E Computation for Pooled case

The complete data likelihood from (C.13) reads:

$$L(\boldsymbol{\mathcal{X}}|\boldsymbol{\theta}) = \prod_{t\in\mathcal{T}_l}\prod_{i=1}^{I}\prod_{j=1}^{J}\prod_{k=1}^{K} \rho_l^{d_{ijk,t}} \cdot \left(0^{x_{ijk,t}}1^{1-x_{ijk,t}}\right)^{d_{ijk,t}} \cdot \left(\frac{1-\rho_l}{2}\right)^{1-d_{ijk,t}}$$
$$\cdot \exp\left\{-\frac{\omega_{ijk,t}}{2}(\mathbf{z}_t'\mathbf{g}_{ijk,l})^2 + \kappa_{ijk,t}(\mathbf{z}_t'\mathbf{g}_{ijk,l})\right\} p(\omega_{ijk,t})\,. \tag{E.1}$$

In the pooling case, we are assuming that the tensor of coefficients in each regime $l = 1, \ldots, L$ is given by:

$$\mathcal{G}_l = g_l \cdot \mathcal{I}\,, \tag{E.2}$$

where $\mathcal{I}$ is a $I \times J \times Q \times K$ tensor made of ones and $g_l \in \mathbb{R}$, for each $l = 1, \ldots, L$. Therefore $\mathbf{g}_{ijk,l} = g_l\boldsymbol{\iota}_Q$, where $\boldsymbol{\iota}_Q$ is a column vector of ones of length Q. We can rewrite the complete data likelihood as:

$$L(\boldsymbol{\mathcal{X}}|\boldsymbol{\theta}) \propto \prod_{t\in\mathcal{T}_l}\prod_{i=1}^{I}\prod_{j=1}^{J}\prod_{k=1}^{K} \exp\left\{-\frac{\omega_{ijk,t}}{2}(\mathbf{z}_t'g_l\boldsymbol{\iota}_Q)^2 + \kappa_{ijk,t}(\mathbf{z}_t'g_l\boldsymbol{\iota}_Q)\right\}$$
$$= \prod_{t\in\mathcal{T}_l}\prod_{i=1}^{I}\prod_{j=1}^{J}\prod_{k=1}^{K} \exp\left\{-\frac{\omega_{ijk,t}}{2}(g_l S_t^z)^2 + \kappa_{ijk,t}(g_l S_t^z)\right\}\,, \tag{E.3}$$

where $S_t^z = \mathbf{z}_t'\boldsymbol{\iota}_Q = \sum_{q=1}^{Q} z_{q,t}$. Then:

$$L(\boldsymbol{\mathcal{X}}|\boldsymbol{\theta}) \propto \exp\left\{-\frac{1}{2}\sum_{t\in\mathcal{T}_l}\sum_{i,j,k} g_l^2(S_t^z)^2\omega_{ijk,t} - 2g_l S_t^z\kappa_{ijk,t}\right\}\,, \tag{E.4}$$

It is assumed that g_l, for each $l = 1, \ldots, L$, has prior distribution:

$$g_l|\tau, w_l \sim \mathcal{N}(0, \tau w_l)\,. \tag{E.5}$$

This yields the posterior distribution:

$$p(g_l|\boldsymbol{\Omega}_t, \tau, w_l) \propto \exp\left\{-\frac{1}{2}\sum_{t\in\mathcal{T}_l}\sum_{i,j,k} g_l^2(S_t^z)^2\omega_{ijk,t} - 2g_l S_t^z\kappa_{ijk,t}\right\} \exp\left\{-\frac{1}{2}\frac{g_l^2}{\tau w_l}\right\}$$

$$= \exp\left\{-\frac{1}{2}\left[\frac{g_l^2}{\tau w_l} + \sum_{t\in\mathcal{T}_l}\sum_{i,j,k} g_l^2 (S_t^z)^2 \omega_{ijk,t} - 2g_l S_t^z \kappa_{ijk,t}\right]\right\}$$

$$= \exp\left\{-\frac{1}{2}\left[g_l^2\left(\frac{1}{\tau w_l} + \sum_{t\in\mathcal{T}_l}\sum_{i,j,k}(S_t^z)^2\omega_{ijk,t}\right) - 2g_l\left(\sum_{t\in\mathcal{T}_l}\sum_{i,j,k} S_t^z\kappa_{ijk,t}\right)\right]\right\}. \tag{E.6}$$

Therefore, for each $l = 1, \ldots, L$:

$$\pi(g_l|\mathbf{\Omega}_t, \tau, w_l) \sim \mathcal{N}(m_l, s_l^2)\,, \tag{E.7}$$

with:

$$s_l^2 = \left(\frac{1}{\tau w_l} + \sum_{t\in\mathcal{T}_l}\sum_{i,j,k}(S_t^z)^2\omega_{ijk,t}\right)^{-1} \tag{E.8}$$

$$m_l = \left(\sum_{t\in\mathcal{T}_l}\sum_{i,j,k} S_t^z\kappa_{ijk,t}\right)\cdot s_l^{-2}\,. \tag{E.9}$$

Assume the prior distributions:

$$\pi(\tau) \sim \mathcal{G}a(\overline{a}^\tau, \overline{b}^\tau) \tag{E.10}$$

$$\pi(w_l|\lambda_l) \sim \mathcal{E}xp(\lambda_l^2/2) \tag{E.11}$$

$$\pi(\lambda_l) \sim \mathcal{G}a(a_\lambda^l, b_\lambda^l)\,, \tag{E.12}$$

then the posterior distributions of the variance hyperparameters τ, w_l, λ_l are obtained as follows.

The posterior distribution of τ is given by:

$$\begin{aligned} p(\tau|\mathbf{g},\mathbf{w}) &\propto \pi(\tau)p(\mathbf{g}|\mathbf{w},\tau) \\ &\propto \tau^{\overline{a}^\tau - 1}\exp\left\{-\overline{b}^\tau\tau\right\}\prod_{l=1}^{L}\exp\left\{-\frac{g_l^2}{2\tau w_l}\right\} \\ &= \tau^{\overline{a}^\tau - 1}\exp\left\{-\frac{1}{2}\left[2\overline{b}^\tau\tau + \sum_{l=1}^{L}\frac{g_l^2}{w_l}\frac{1}{\tau}\right]\right\} \\ &\sim \text{GiG}\left(\overline{a}^\tau - 1, 2\overline{b}^\tau, \sum_{l=1}^{L}\frac{g_l^2}{w_l}\right). \end{aligned} \tag{E.13}$$

The posterior distribution of w_l, for each $l = 1, \ldots, L$, is given by:

$$\begin{aligned} p(w_l|g_l,\tau,\lambda_l) &\propto \pi(w_l|\lambda_l)p(g_l|w_l,\tau) \\ &\propto \frac{\lambda_l^2}{2}\exp\left\{-\frac{\lambda_l^2}{2}w_l\right\}\exp\left\{-\frac{g_l^2}{2\tau w_l}\right\} \\ &= \exp\left\{-\frac{1}{2}\left[\lambda_l^2 w_l + \frac{g_l^2}{\tau}\frac{1}{w_l}\right]\right\} \end{aligned}$$

$$\sim \text{GiG}\left(1, \lambda_l^2, \frac{g_l^2}{\tau}\right) . \tag{E.14}$$

The posterior distribution of λ_l (integrating out w_l), for each $l = 1, \ldots, L$, is given by:

$$\begin{aligned} p(\lambda_l|\tau, g_l) &\propto \pi(\lambda_l) \int p(g_l|\tau, w_l) p(w_l|\lambda_l)\, \mathrm{d}w_l \\ &\propto \pi(\lambda_l) p(g_l|\tau, \lambda_l) \\ &\propto \lambda_l^{a_\lambda^l - 1} \exp\left\{-b_\lambda^l \lambda_l\right\} \frac{\sqrt{\tau}}{2\lambda_l} \exp\left\{-\frac{|g_l|\sqrt{\tau}}{\lambda_l}\right\} \\ &\propto \lambda_l^{a_\lambda^l - 2} \exp\left\{-\frac{1}{2}\left[2b_\lambda^l \lambda_l + |g_l|\sqrt{\tau}\frac{1}{\lambda_l}\right]\right\} \\ &\sim \text{GiG}\left(a_\lambda^l - 1, 2b_\lambda^l, |g_l|\sqrt{\tau}\right) . \end{aligned} \tag{E.15}$$

F Additional Simulations' Output

F.1 Size 100,100,3,2

Setup: $I = J = 100$, $Q = 3$, $M = 2$.
We run the Gibbs sampler for $N = 500$ iterations and the outcome is plotted from Fig. **??** to (**??**).

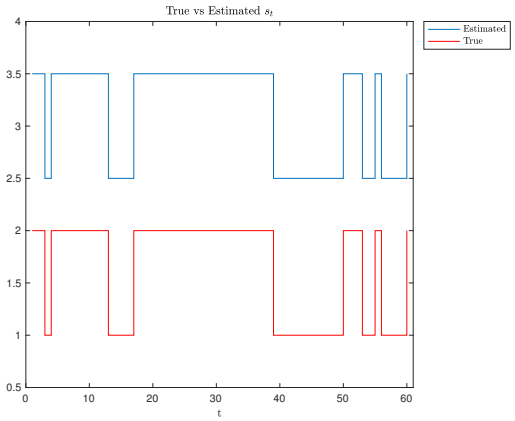

Figure 20: Hidden Markov chain: true (blue) versus estimated (red).

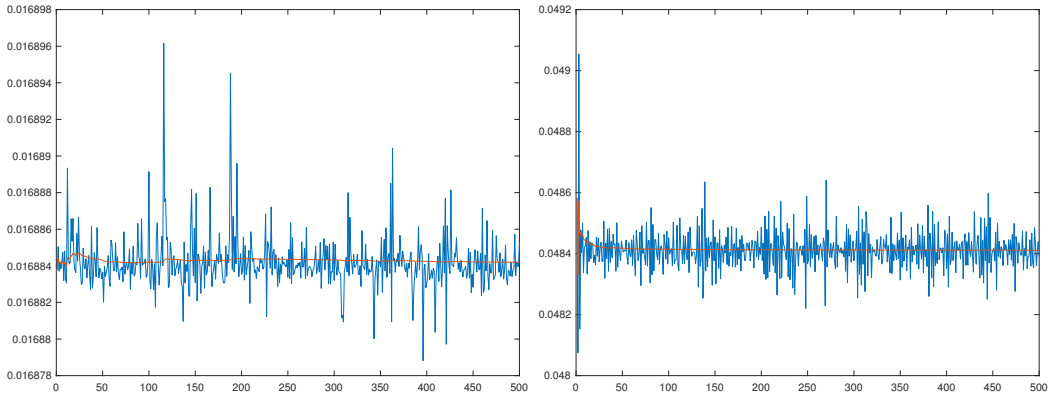

(a) Regime 1. (b) Regime 2.

Figure 21: Frobenious norm (blue line) and its progressive mean (red line) of the difference between the true tensor $\mathcal{G}_l^*$ and the MCMC samples of the tensor $\hat{\mathcal{G}}_l$.

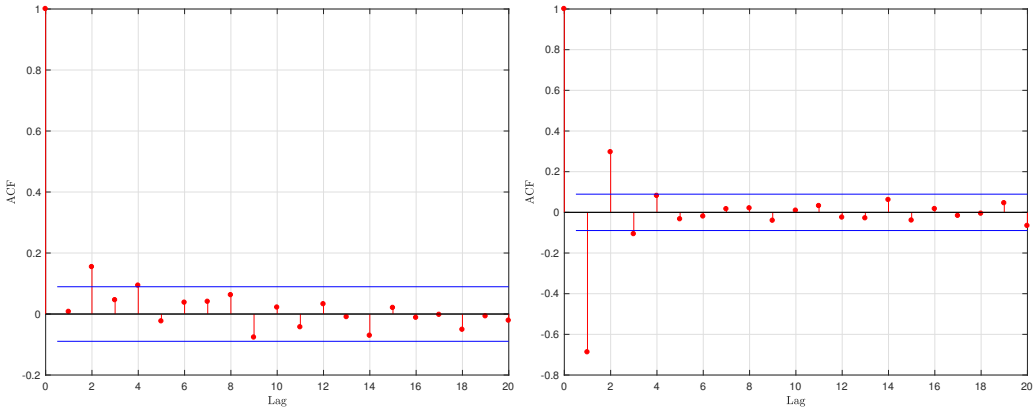

(a) Regime 1. (b) Regime 2.

Figure 22: ACF of Frobenious norm of the difference between the true tensor $\mathcal{G}_l^*$ and the MCMC samples of the tensor $\hat{\mathcal{G}}_l$.

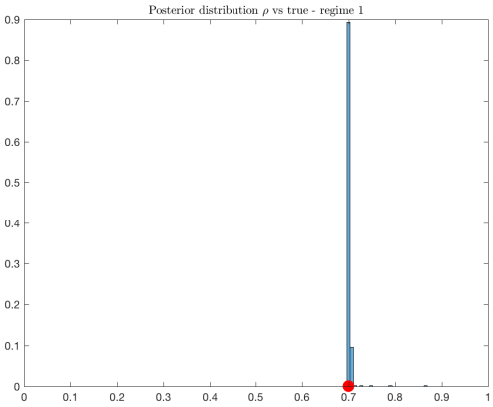

(a) Regime 1.

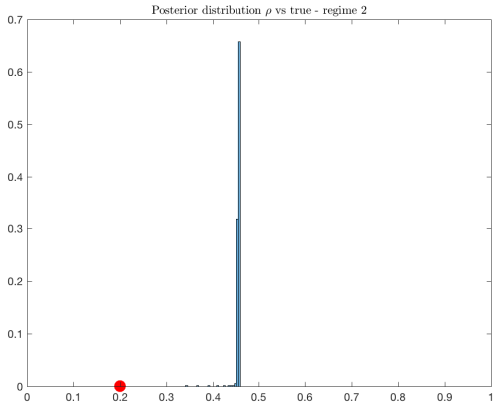

(b) Regime 2.

Figure 23: Posterior distribution of the mixing probability parameter ρ_l (blue) and the true value of the parameter (red).

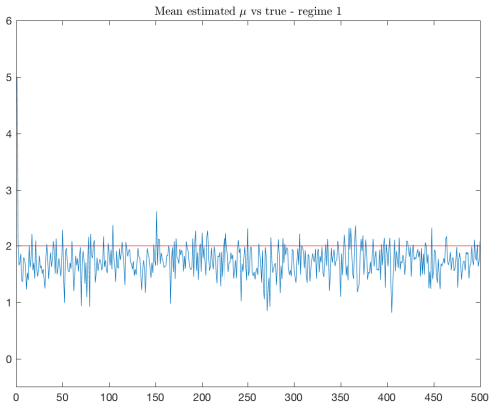

(a) Regime 1.

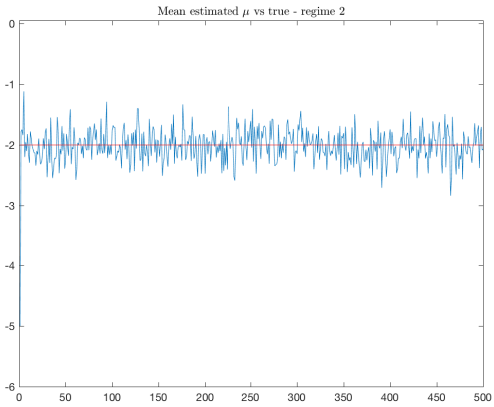

(b) Regime 2.

Figure 24: Frobenious norm of the MCMC samples (blue line) and true value (red line) of the parameter $\hat{\boldsymbol{\mu}}_l$.

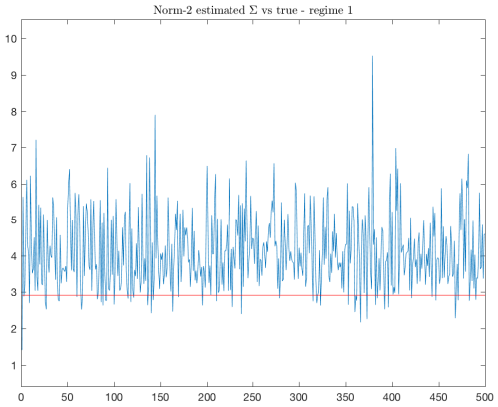

(a) Regime 1.

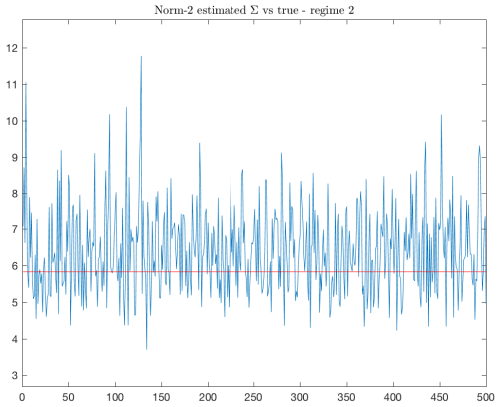

(b) Regime 2.

Figure 25: Frobenious norm of the MCMC samples (blue line) and true value (red line) of the parameter $\hat{\mathbf{\Sigma}}_l$.

F.2 Size 150,150,3,2

Setup: $I = J = 150$, $Q = 3$, $M = 2$.
We run the Gibbs sampler for $N = 500$ iterations and the outcome is plotted from Fig. **??** to (**??**).

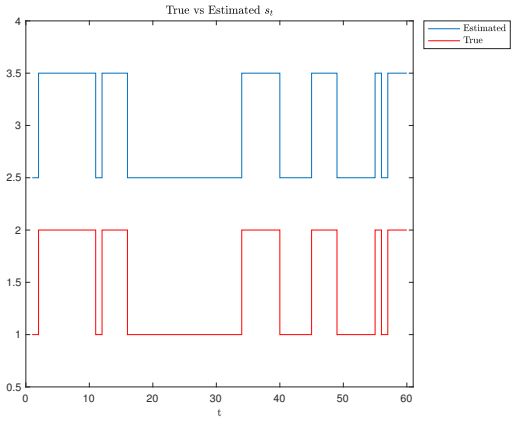

Figure 26: Hidden Markov chain: true (blue) versus estimated (red).

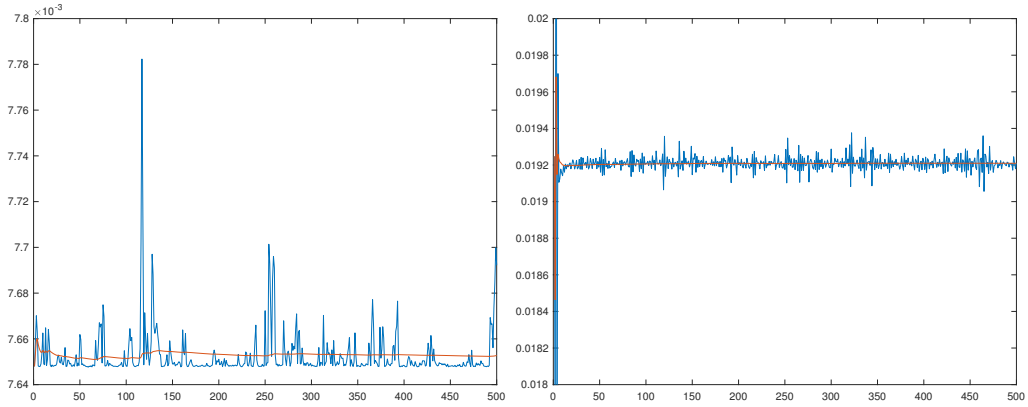

(a) Regime $l = 1$. (b) Regime $l = 2$.

Figure 27: Frobenious norm (blue line) and its progressive mean (red line) of the difference between the true tensor $\mathcal{G}_l^*$ and the MCMC samples of the tensor $\hat{\mathcal{G}}_l$.

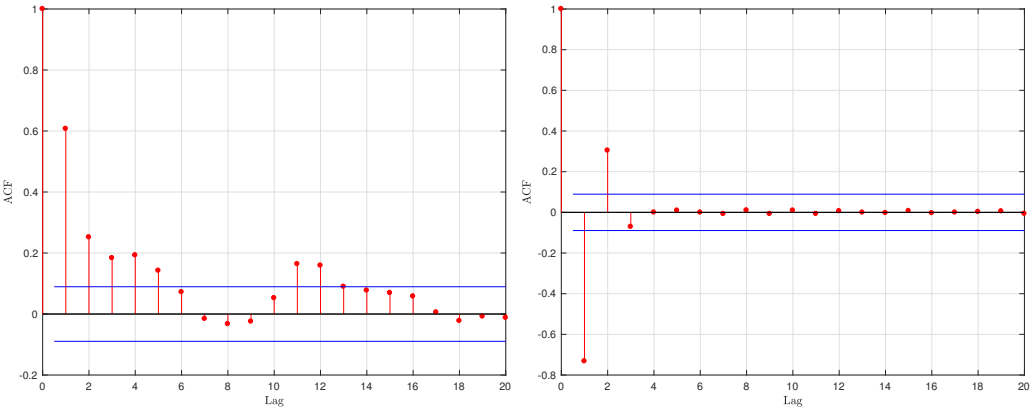

(a) Regime 1. (b) Regime 2.

Figure 28: ACF of Frobenious norm of the difference between the true tensor $\mathcal{G}_l^*$ and the MCMC samples of the tensor $\hat{\mathcal{G}}_l$.

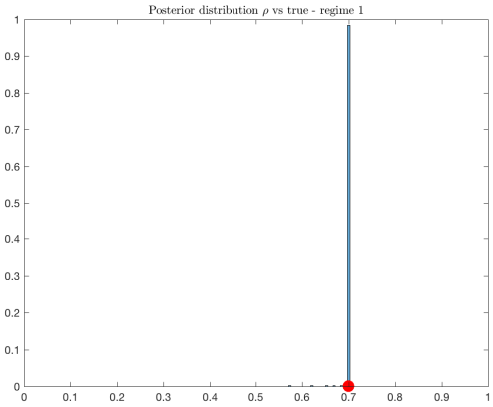

(a) Regime 1.

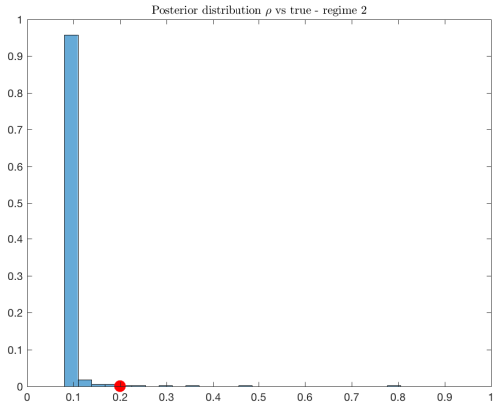

(b) Regime 2.

Figure 29: Posterior distribution of the mixing probability parameter ρ_l (blue) and the true value of the parameter (red).

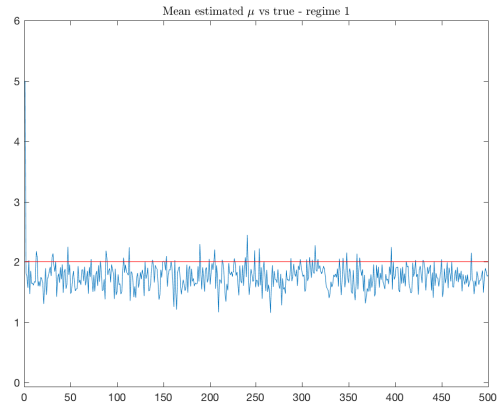

(a) Regime 1.

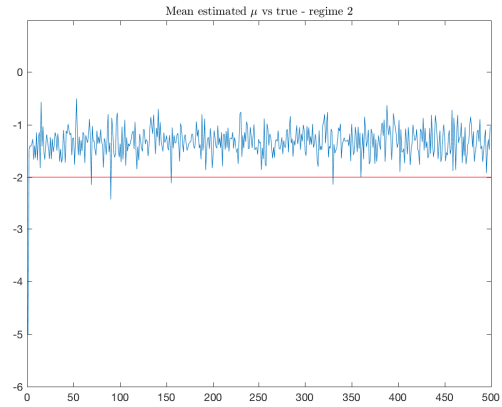

(b) Regime 2.

Figure 30: Frobenious norm of the MCMC samples (blue line) and true value (red line) of the parameter $\hat{\boldsymbol{\mu}}_l$.

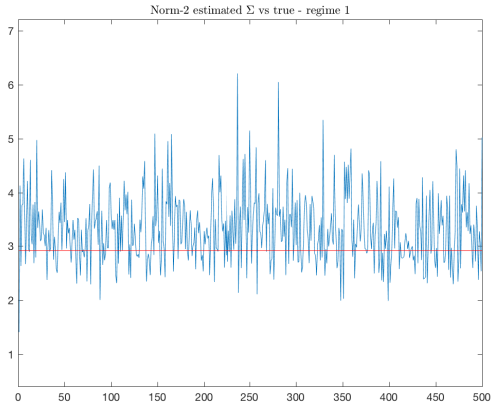

(a) Regime 1.

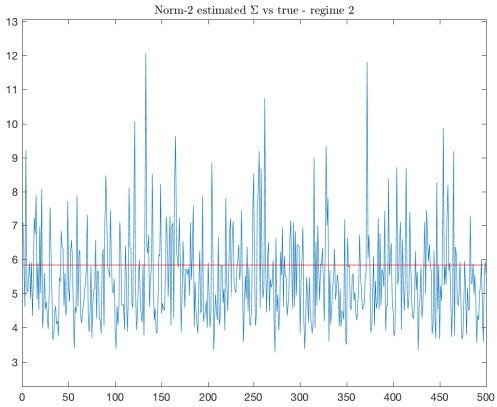

(b) Regime 2.

Figure 31: Frobenious norm of the MCMC samples (blue line) and true value (red line) of the parameter $\hat{\mathbf{\Sigma}}_l$.

F.3 Size 200,200,3,2

Setup: $I = J = 200$, $Q = 3$, $M = 2$.
We run the Gibbs sampler for $N = 200$ iterations and the outcome is plotted from Fig. **??** to (38(d)).

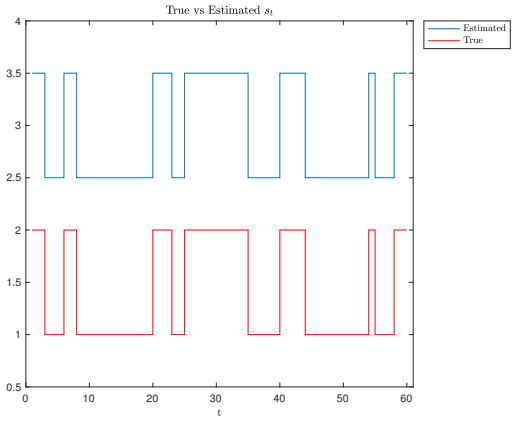

Figure 32: Hidden Markov chain: true (blue) versus estimated (red).

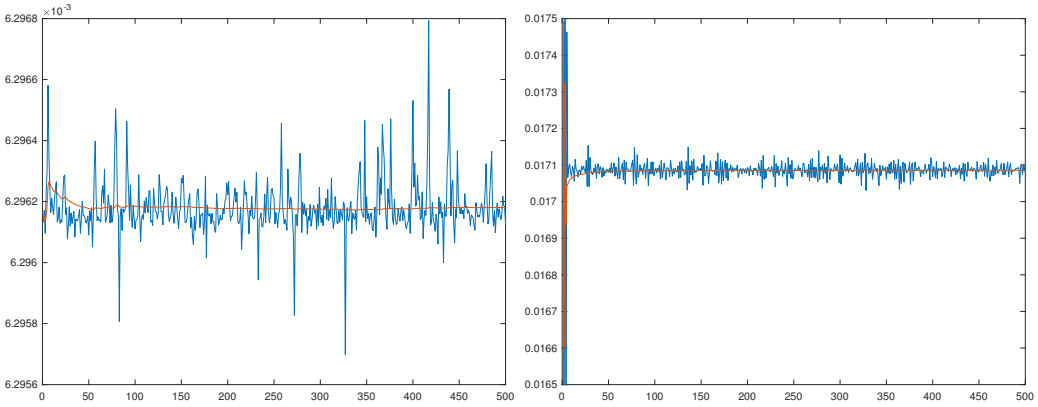

(a) Regime 1. (b) Regime 2.

Figure 33: Frobenious norm (blue line) and its progressive mean (red line) of the difference between the true tensor $\mathcal{G}_l^*$ and the MCMC samples of the tensor $\hat{\mathcal{G}}_l$.

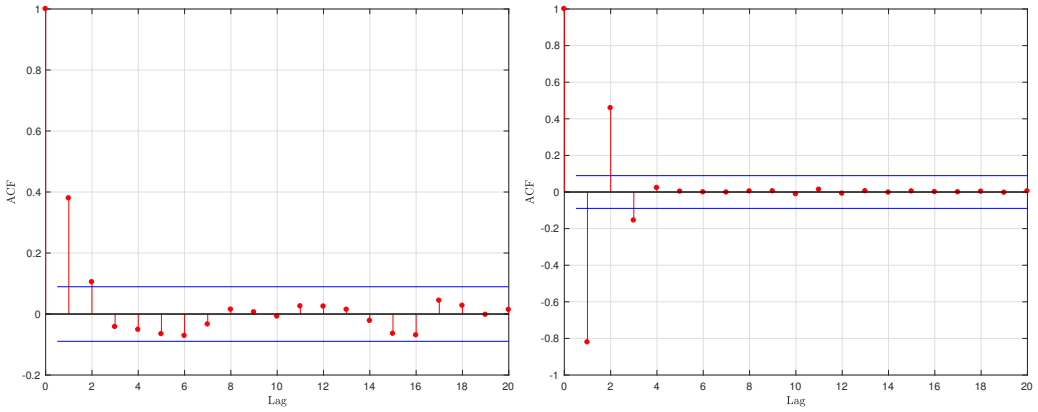

(a) Regime 1. (b) Regime 2.

Figure 34: ACF of Frobenious norm of the difference between the true tensor $\mathcal{G}_l^*$ and the MCMC samples of the tensor $\hat{\mathcal{G}}_l$.

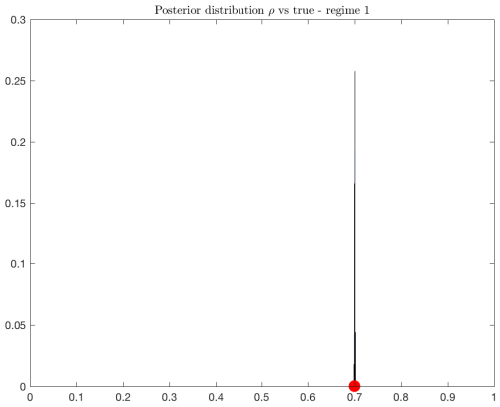

(a) Regime 1.

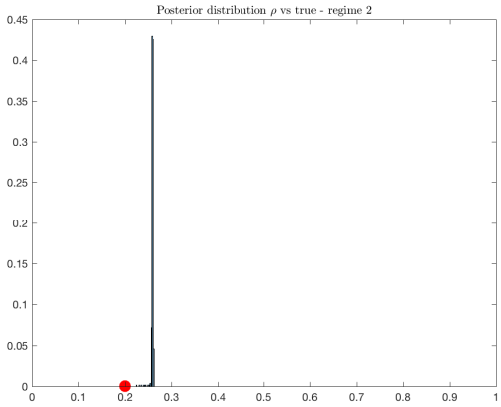

(b) Regime 2.

Figure 35: Posterior distribution of the mixing probability parameter ρ_l (blue) and the true value of the parameter (red).

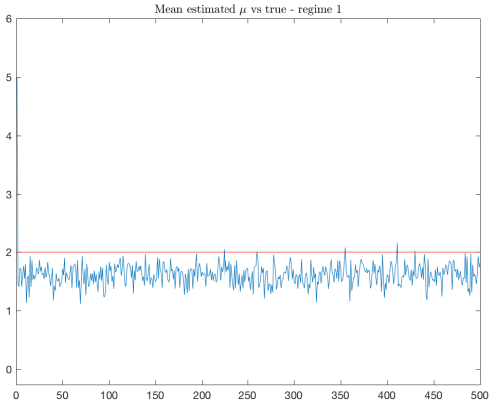

(a) Regime 1.

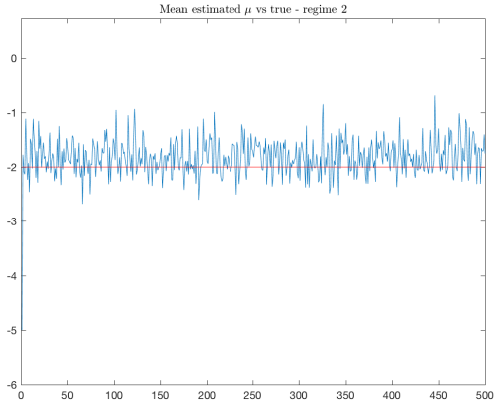

(b) Regime 2.

Figure 36: Frobenious norm of the MCMC samples (blue line) and true value (red line) of the parameter $\hat{\boldsymbol{\mu}}_l$.

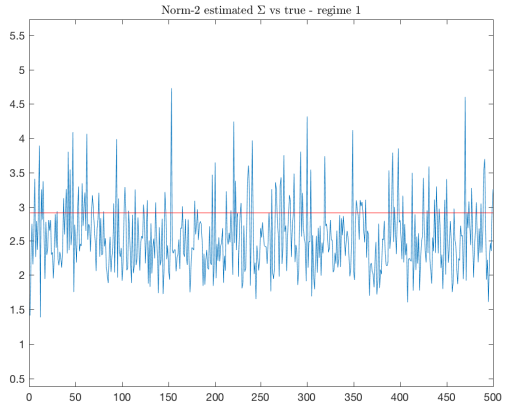

(a) Regime 1.

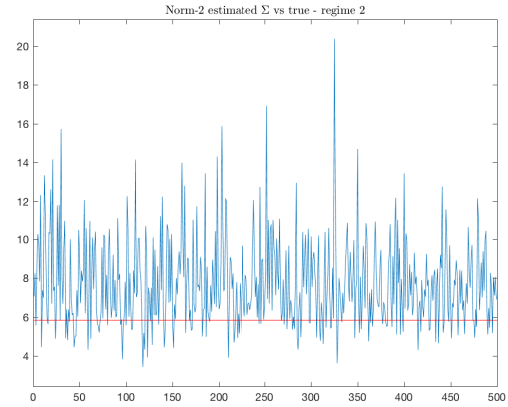

(b) Regime 2.

Figure 37: Frobenious norm of the MCMC samples (blue line) and true value (red line) of the parameter $\hat{\mathbf{\Sigma}}_l$.

G Additional Application's Output

In this section we report some additional plots concerning the Gibbs sampler's output for the estimation of the hyper-parameters in the application described in Section 6.

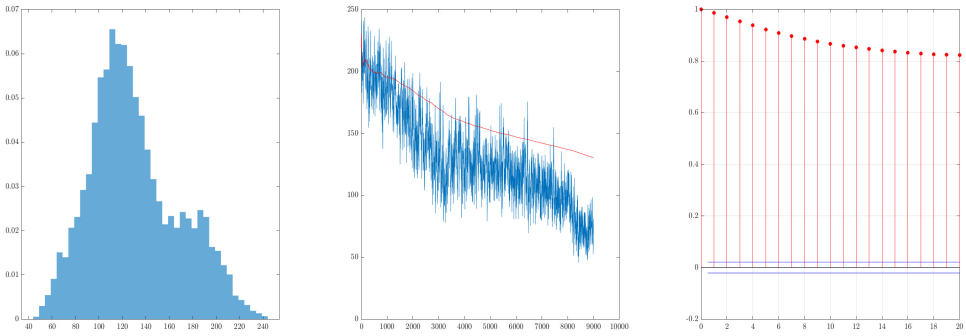

Figure 38: Posterior distribution (*left*), MCMC output (*middle*) and auto-correlation function (*right*) of the global variance parameter τ.

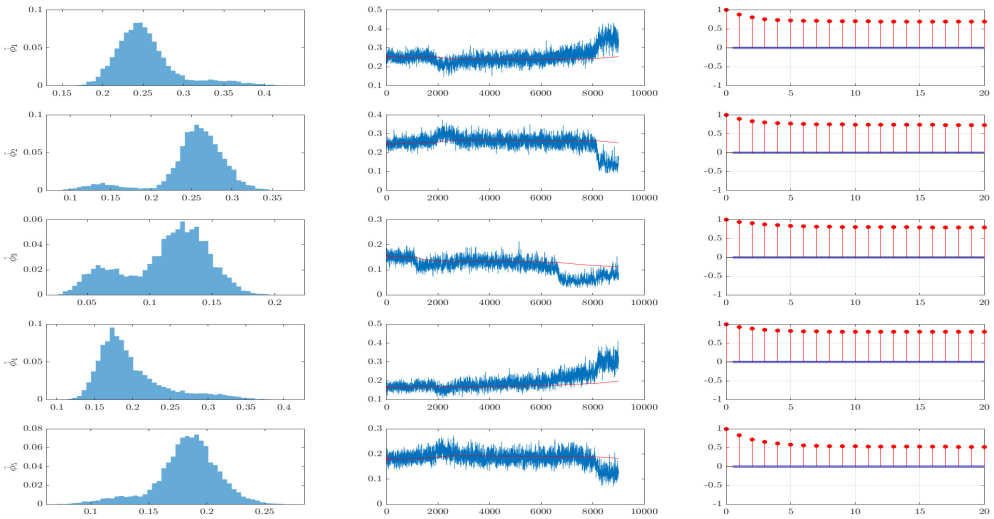

Figure 39: Posterior distribution (*left* plots), MCMC output (*middle* plots) and autocorrelation functions (*right* plots) of the level-specific variance parameters $\boldsymbol{\phi}$. Each row corresponds to a different value of $r = 1, \ldots, R$.

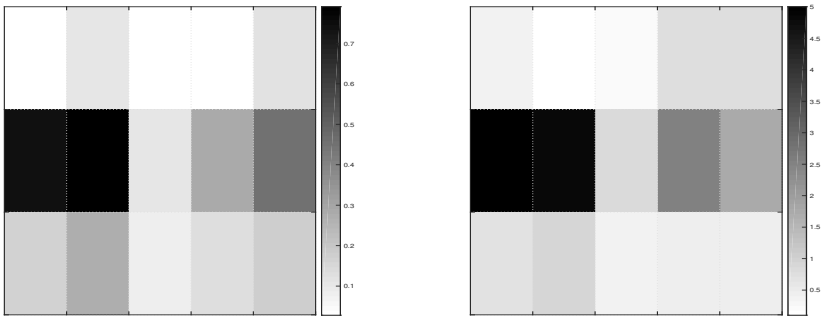

Figure 40: Posterior mean of the variance each marginal of the tensor of coefficients, in state 1 (*left*) and state 2 (*right*). The cell (h, r) of each matrix, for $h = 1, \ldots, 3$ and $r = 1, \ldots, R$, corresponds to the estimated variance $\hat{\tau}\hat{\phi}_r\hat{w}_{h,r,l}$ of the marginal $\boldsymbol{\gamma}_{h,l}^{(r)}$.

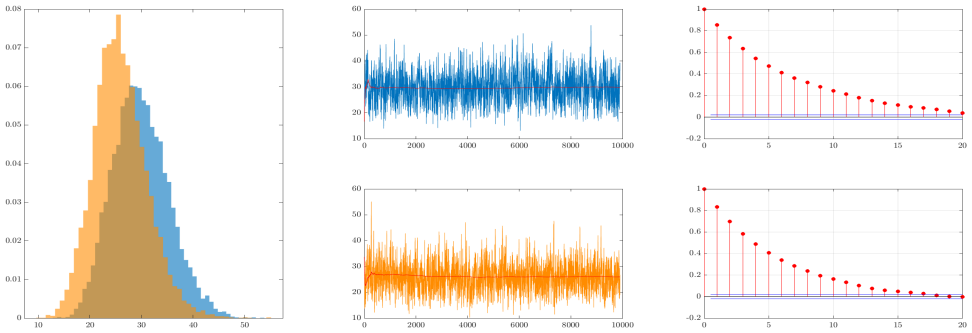

Figure 41: Posterior distribution (*left* plot), MCMC output (*middle* plots) and autocorrelation functions (*right* plots) of the local variance hyper-parameters $\boldsymbol{\lambda}$. Regime 1 (*blue*) and regime 2 (*orange*).

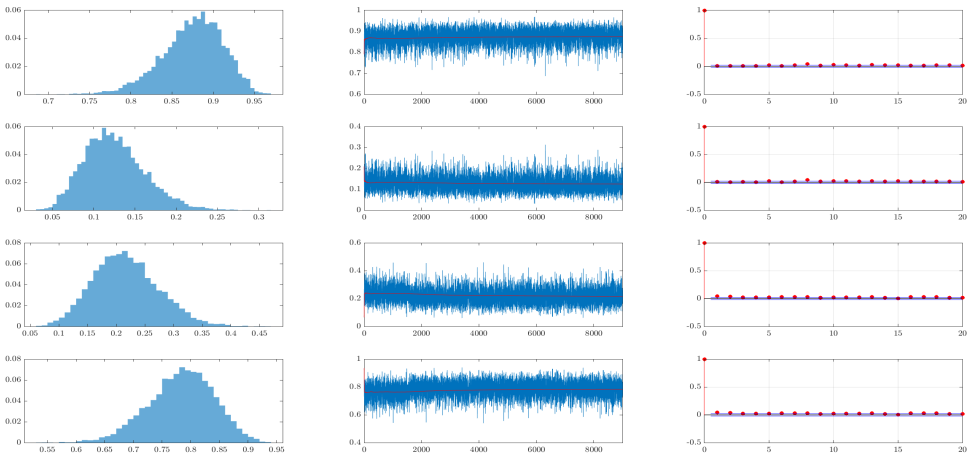

Figure 42: Posterior distribution (*left* plots), MCMC output (*middle* plots) and autocorrelation functions (*right* plots) of the transition probabilities of the hidden Markov chain $\boldsymbol{\Xi}$, in the order (*top to bottom*): $\xi_{1,1}, \xi_{1,2}, \xi_{2,1}, \xi_{2,2}$.

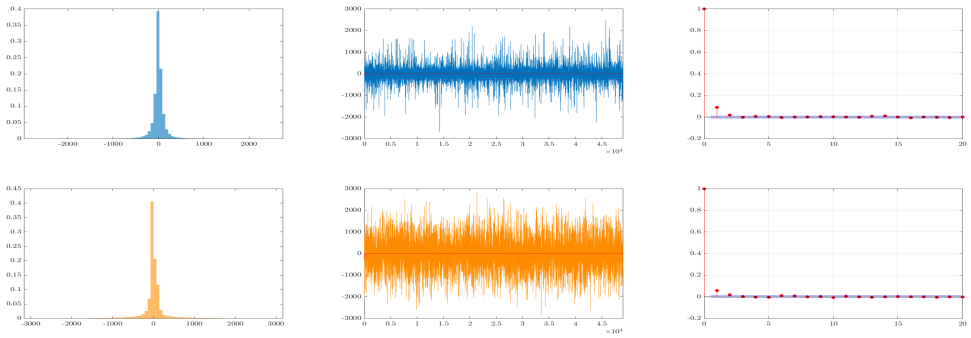

Figure 43: Posterior distribution (*left* plots), MCMC output (*middle* plots) and autocorrelation functions (*right* plots) of the common coefficient g_l in the pooled model. Regime 1 (*blue*) and regime 2 (*orange*).